The Dissertation Committee for Christina May Shoemaker

certifies that this is the approved version of the following dissertation:

Elucidating the molecular network underlying

temperature-dependent sex determination

in the red-eared slider turtle, *Trachemys scripta*

Committee:

_____

David P Crews, Supervisor

_____

James Bull

_____

John Wallingford

_____

Jeffrey Gross

_____

Tom Juenger

Elucidating the molecular network underlying temperature-dependent sex determination in the red-eared slider turtle, *Trachemys scripta*

by

Christina May Shoemaker, B.A.

Dissertation

Presented to the Faculty of the Graduate School of

The University of Texas at Austin

in Partial Fulfillment

of the Requirements

for the Degree of

Doctor of Philosophy

The University of Texas at Austin

May 2009

Dedication

To my family.

Leah,

Mops, Pops, Leslie,

Griffin and Lucy.

Your love and support mean more
than any degree.

Acknowledgements

First and foremost, my deepest thanks goes out to my advisor, **David Crews**, and my dissertation committee, **John Wallingford**, **Jeff Gross**, **Tom Juenger** and **Jim Bull**. Scientists proceed only by standing on the shoulders of giants who came before, and my work is no exception. Your input, support, guidance, and critiques through the years were of paramount importance to the success of this work, and there are no words other than Thank You.

To the legion of undergraduates who tirelessly helped with turtle research along the way: **Joanna Queen, Kristen Berkstresser, Kyle Jackson, Ryohei Yatsu, Jason Chandrapal, Lia Ortiz, Mary Madaleil, Sarah Withycombe, James Kan**.

To **Raymond S. Porter**, without whom this work would not have been possible, nor would I ever have danced to Cajun music next to the swamp in Henderson.

To **Mary Ramsey**, my turtle teammate, who understands what it means to be in the basement during Turtle Season!

To Crews lab members past and present: **Brian Dias, Nicholas Sanderson, Kimberly Hillsman, Yuiko Matsumoto, Vicky Huang, Lauren Munchrath**. Safety First!

To the legion of scientists whose generosity of time, supplies, equipment and advice was invaluable…
John Wallingford for the kind gift of pCS plasmids, sample antibodies, and frog embryos, **Jeff Gross** for immunocytochemistry reagents and supplies, **Tom Juenger** and **Nate Marti** for statistical assistance and support, **Norma Moreno-Mendoza** and **Horacio Merchant-Larios** for assistance setting up the *in vitro* culture technique, **Molly Cummings** and **Dave Parichy** for generosity in utilizing their microscope equipment, **Robbie Bayly** for assistance with electroporation techniques and GFP plasmid, **Rebecca Brady** for assistance and advice with Western blotting, **Chanjae Lee** for conceptual subcloning advice, **Ian Quigley** for the scotch, sodas & an infinite number of couch chalk talks, **James Skipper** for assistance early in the conception of the turtle projects, **Pascal Bernard** for the kind gift of *Wnt4* primers

To our financial support. This work was funded by a **National Science Foundation** grant awarded to David Crews and several Graduate Research/Travel Fellowships from **The University of Texas at Austin** awarded to Christina Shoemaker.

Elucidating the molecular network underlying temperature-dependent sex determination in the red-eared slider turtle, *Trachemys scripta*

Christina May Shoemaker, Ph.D.

The University of Texas at Austin, 2009

Supervisor: David Crews

Components of the molecular pathway underlying gonadogenesis in organisms with temperature-dependent sex determination (TSD) have been retained from genetic sex determination. Furthermore, although much of this network has been conserved, new functions for these genes have evolved in this different mode of sex determination. We find that the transcription factors *Sox9* and *Dmrt1* and the hormone *Mis* are involved in the formation of a testis and/or the repression of an ovary at a male-producing temperature. While *Mis* expression may be maintained by *Sox9*, the initial upregulation of *Mis* in the developing testis is most likely modulated by some other upstream factor. *Dmrt1* appears to play an upstream role in testis sex determination. We provide evidence that the transcription factor *Dax1* and the signaling molecule *Wnt4*, cloned for the first time in an organism with TSD, play roles in gonadogenesis in both sexes. Finally, we show that the transcription factor *FoxL2* and the signaling molecule *Rspo1* are involved in the formation of an ovary and/or the repression of a testis at a female-producing temperature. In the first investigation of *Rspo1* in any organism exhibiting TSD, we demonstrate it is involved upstream in ovarian sex determination.

Complementary to descriptive studies, we optimize a whole organ culture system in which gonad explants develop *in vitro* for up to three weeks. We show that expression of the sex-determining network in isolated gonads mimics *in ovo* patterns, revealing an endogenous temperature-sensing mechanism that does not require other embryonic tissues. Ectopic

expression of *Sox9* reveals a possible positive feedback regulation of *Dmrt1*. The use of this culture system opens the door to functional manipulation of the gonad at the molecular level and is suitable for a myriad of future studies. This work makes strides in elucidating the molecular network underlying gonadogenesis in an organism exhibiting TSD, and invites investigation of the evolution of gene function. The data lend insight into the changing roles of molecules in sex determination across diverse taxa, and into the evolution of developmental pathways in general.

Table of Contents

Glossary of Terms xi

List of Tables and Figures xii

Chapter One: Temperature-dependent sex determination 1
- Species with TSD: who to study? 2
- The red-eared slider turtle, *Trachemys scripta* 4
- Generation of a differentiated gonad in organisms with TSD 4
- The molecular network underlying sex determination and gonad differentiation in organisms with GSD 5
- Investigation of these candidate genes in organisms exhibiting temperature-dependent sex determination 11
- Examining the molecular network underlying gonadogenesis in an organism with temperature-dependent sex determination 13

Chapter Two: Expression of *Sox9*, *Mis* and *Dmrt1* in the gonad of a species with temperature-dependent sex determination 17
- **Methods** 18
- **Results and Discussion** 20
  - *Sox9* expression is dimorphic near the beginning of the temperature-sensitive period 20
  - Dimorphic *Mis* expression occurs later in the temperature-sensitive period 21
  - *Dmrt1* expression is consistent with a possible upstream role in *T. scripta* 22
  - Tissue-specific quantitative real-time PCR 23
  - Exploring functional roles of genes in a non-model system 24

Chapter Three: Response of candidate sex-determining genes to changes in temperature reveals their involvement in the molecular network underlying temperature-dependent sex determination 29
- **Methods** 30
- **Results** 33
  - Examining a new stage of development 34
  - *FoxL2* expression becomes ovarian-specific at the end of the temperature-sensitive period 34
  - *Wnt4* is widely expressed throughout the gonad, mesonephros and metanephros 35
  - *Dax1* is expressed throughout the gonad, Müllerian and Wolffian ducts 36
  - *Rspo1* expression implicates its involvement in ovarian development 37
  - Testis-specific genes show a rapid response to temperature shifts 37

Discussion 39
FoxL2 expression is consistent with a role in ovarian development 39
Expression of *Wnt4* is conserved across GSD and TSD vertebrates and is consistent with a role in both ovary and testis development, as well as duct and kidney formation 40
Dax1 expression is consistent with a role in gonad and adrenal development 42
Rspo1 expression is consistent with a conserved, upstream role in ovarian sex determination 44
Response to temperature suggests an early role for *Dmrt1*, and a later role for *Mis*, in testicular development 44

Chapter Four: Whole organ *in vitro* culture allows functional manipulation of the genetic network underlying temperature-dependent sex determination 61
Methods 62
Results 67
Rate of development changes throughout embryonic incubation 67
Estrogenic phenol red strongly regulates gene expression patterns in the gonad 68
Morphological development of gonads *in ovo* and *in vitro* 69
Temperature regulates the molecular network underlying gonadogenesis in ovo and in vitro 70
Sox9 expression *in ovo* shows a strong, sustained temperature-sensitive response 71
Gonadal *Sox9* expression *in vitro* mimics patterns observed *in ovo* 72
Gonadal *Dmrt1* expression *in ovo* reveals an immediate, sustained response to temperature 73
Dmrt1 expression in gonads *in vitro* mimics *in ovo* patterns 74
Gonadal *Mis* expression *in ovo* reveals a strong, immediate temperature-response 74
Expression of *Mis in vitro* is strongly sexually dimorphic and responsive to temperature 75
In ovo FoxL2 expression reveals a response to changes in temperature 76
FoxL2 in vitro expression is strongly temperature-sensitive, and similar to *in ovo* patterns 76
Individual variation within shifted gonads 77
Misexpression studies 77
Discussion 78
Temperature-sensitive period is a time of rapid overall development 78
Expression of the molecular network underlying gonadogenesis is altered by estrogen-mimicking compounds 79
Mis, Dmrt1 and *FoxL2* exhibit previously undetected sustained responses to changes in temperature during in ovo development 81
Sox9 localization early in the temperature-sensitive period is not sexually dimorphic 82
Gonads cultured *in vitro* exhibit gene expression patterns strongly similar to *in ovo* development 83
In vitro gonads allow functional manipulation of the sex-determining molecular network 85

Evidence *Sox9* may not regulate *Mis* in the slider turtle gonad....86
Evidence that *Dmrt1* does not directly sense temperature in the slider turtle....87

Chapter Five: Analysis of candidate genes involved in temperature-dependent sex determination....107
Testicular development....108
Interacting pathways....113
Ovarian development....114
Analyzing function in a non-traditional model system....115

References....120

Vita....133

Glossary of Terms

AKG, adrenal-kidney-gonad
DAX1, DSS-AHC critical region on the X chromosome
DMRT1, doublesex mab3 related transcription factor 1
ESD, environmental sex determination
FGF9, fibroblast growth factor 9
FOXL2, forkhead box protein L2
FPT, female-producing temperature
GAM, gonad-adrenal-mesonephros
GSD, genotypic sex determination
ISH, in situ hybridization
MIS, Müllerian-inhibiting substance
MIS-R2, Mis receptor type II
MPT, male-producing temperature
PP1, protein phosphatase type I
qPCR, quantitative real-time PCR
RSPO1, R-spondin 1
RT-PCR, reverse transcriptase polymerase chain reaction
SF1, Steroidogenic factor 1
SOX8, SRY-like HMG-box containing transcription factor 8
SOX9, SRY-like HMG-box containing transcription factor 9
SRY, sex-determining region of the Y chromosome
TSD, temperature-dependent sex determination
TSP, temperature-sensitive period
WNT4, wingless integration site family member 4
WT1, Wilms tumor 1

List of Tables and Figures

Table 1. Organisms historically used in studies examining the molecular network underlying temperature-dependent sex determination.....15

Figure 1. Genetic events underlying gonad determination and differentiation in GSD mammals and TSD reptiles.....16

Figure 2. Developmental expression of *Sox9* in embryonic gonads of the red-eared slider turtle measured by *in situ* hybridization and qPCR.....26

Figure 3. Developmental expression of *Mis* in embryonic gonads of the red-eared slider turtle measured by *in situ* hybridization and qPCR.....27

Figure 4. Developmental expression of *Dmrt1* in embryonic gonads of the red-eared slider turtle measured by *in situ* hybridization and qPCR.....28

Figure 5. Morphological development of *Trachemys scripta* during the temperature-sensitive period.....48

Figure 6. Expression of *FoxL2*, *Wnt4* and *Dax1* in the turtle adrenal-kidney-gonad (AKG) complex by *in situ* hybridization.....49

Figure 7. Expression of *FoxL2*, *Wnt4* and *Dax1* in the turtle gonad by qPCR.....51

Figure 8. Expression of *Dmrt1*, *Mis* and *Sox9* in the turtle gonad by qPCR.....52

Figure 9. Expression of Rspo1 mRNA in the gonads of the slider turtle during the temperature-sensitive period by qPCR.....53

Figure 10. Nucleotide sequence and deduced translation of partial *Wnt4* in *Trachemys scripta*.54

Figure 11. Alignment of vertebrate WNT4 sequences.....55

Figure 12. Nucleotide sequence and deduced translation of partial *Dax1* in *Trachemys scripta*.56

Figure 13. Alignment of vertebrate DAX1 sequences.....57

Table 2. Two-factor ANOVA tested effects of temperature, stage or temperature by stage interaction within each gene.....58

Table 3. Significant post-hoc pair-wise comparisons within stage between temperatures after correction by Tukey's HSD.....59

Table 4. Significant post-hoc pair-wise comparisons of *Dax1* expression within FPT between stages after correction by Tukey's HSD. 60

Figure 14. Experimental design. 89

Figure 15. Developmental rate variation at different incubation temperatures. 90

Figure 16. Effect of phenol red in culture medium on gonadal gene expression. 91

Figure 17. Morphological characteristics of gonad development *in ovo* and *in vitro*. 92

Figure 18. Gonadal expression of *Sox9* in individual turtle gonads *in ovo* and *in vitro*. 93

Figure 19. Gonadal expression of *Dmrt1*, *Mis*, and *FoxL2* in individual turtle gonads *in ovo* and *in vitro*. 94

Figure 20. Individual variation in gene expression levels during *in vitro* gonad development. ... 95

Figure 21. Misexpression of *Sox9* in gonads developing *in vitro* at female-producting temperatures. 96

Table 5. Data from staging embryos used in analyzing rates of development in Figure 15. 97

Table 6. Type 3 Tests of Fixed Effects 98

Table 7. Differences of Least Squares Means, adjusted by Tukey-Kramer 99

Figure 22. Expression of various candidate sex-determining genes in gonads of the slider turtle, *Trachemys scripta*. 118

Figure 23. Simplified model of molecular network underlying sex determination in both mammal and slider turtle. 119

CHAPTER ONE

Temperature-dependent sex determination

Vertebrates exhibit a dazzling array of sex-determining mechanisms that can generally be classified as belonging to one of two categories: genotypic sex determination (GSD) and environmental sex determination (ESD). Gonochoristic vertebrate species exhibiting genotypic sex determination utilize a heritable genetic element that initially directs the gonad down one of two sexual trajectories. In contrast, the sex-determining factor in organisms with ESD is derived from the physical or biotic environment (Bull 1980, Crews 1993). All studied crocodilians, tuataras, many turtles and some lizard species exhibit a particular mode of ESD known as temperature-dependent sex determination (TSD), in which the incubation temperature of the developing embryo directs sexual fate. First documented by Charnier (Charnier 1966), species with TSD are sensitive to the action of temperature during a specific window of development known as the temperature-sensitive period (TSP) (for review see Bull 1980). It is thought that species with TSD commonly lack heteromorphic sex chromosomes, although there is evidence of the co-existence of GSD and TSD mechanisms within particular lizard species (Radder et al. 2008), as occurs in some fish (Conover & Kynard 1981, Godwin et al. 2009).

Downstream of the action of either a genetic or an environmental sex-determining trigger lies a complex network of molecular interactions and cellular behaviors leading to the formation of an ovary or a testis. This has best been studied in mammals and birds, lending much insight into both the process of gonadogenesis in GSD organisms as well as points of therapeutic intervention in a variety of human sexual development disorders (for review see DiNapoli & Capel 2008, Wilhelm et al. 2007, Blecher & Erickson 2007, Cederroth et al. 2007, Brennan & Capel 2004). Although gonadogenesis has been extensively studied in vertebrates with GSD, investigations at the molecular level in nontraditional model organisms with temperature-

dependent sex determination are a relatively new area of research. As information concerning the genetic players of GSD has blossomed, investigators have become curious if these networks are conserved in other types of sex-determining mechanisms. Studies investigating the molecules underlying TSD began appearing in the mid-1990's and have since become a field of their own (for review see Morrish & Sinclair 2002, Place & Lance 2004, Yao & Capel 2005). It is an important line of research because a comparative approach informs our understanding of the evolution of signaling pathways, molecular function and interactions, and cellular behaviors across diverse taxa.

It is useful to emphasize that all development occurs within a contextual environment, whether it be at the level of neighboring cells, adjacent tissues, or external surroundings. This is a particularly informative trait in organisms with TSD. Simply by shifting the incubation temperature of the egg during the temperature-sensitive period, one can re-set embryonic gonadal development midway through gonadogenesis. Thus, we can cause full sex-reversal by changing the embryonic environment. This ability offers a unique opportunity to study the molecular mechanisms of environmental influence on development.

Species with TSD: who to study?

The study of nontraditional model systems in developmental biology is both a blessing and a curse: we choose to examine them for their insights into the differences between taxa, but this often results in new stumbling blocks. Working with these non-model critters is less well-developed at a technological/experimental level than that with more traditional organisms, and applied techniques must be re-optimized for each particular species. Furthermore, for many TSD organisms, seasonal breeding and relatively slow rates of development inherently mean that experiments must often be optimized and completed over several seasons. Not only does this draw out the time needed for conclusive results to be gathered, it also begets complexity in the interpretation of data collected from multiple clutches, mothers, months within a season, and even years. Thus, it becomes important to ask which organisms initially make the most sense to utilize in studying the genetics underlying TSD.

Species with TSD are highly variable in their patterns of temperature-sensitivity. For many turtle species, low incubation temperatures during development lead to all males (male-producing temperature or MPT), whereas higher incubation temperatures lead to all females (female-producing temperature or FPT) (Bull & Vogt 1979, Ewert & Nelson 1991, Wibbels et al. 1991, Merchant-Larios et al. 1997, for review see Ewert et al. 2004). In contrast, crocodiles and some turtle and lizard species exhibit a different mode of TSD in which extreme cool and warm temperatures produce females, while intermediate temperatures lead to males (for review see Ewert et al. 2004, Deeming 2004, Harlow 2004). Studies in the laboratory of either pattern reveals transitional and fluctuating incubation temperatures produce clutches of eggs with varying sex ratios, and intersex embryos are uncommon. While some conservation across sex-determining mechanisms clearly exists in the function of molecules involved in gonadogenesis (McLaren 1988), it is also probable that divergence has occurred between GSD and the varying patterns of TSD. This is particularly true in terms of the initial triggers underlying sex determination, and investigating the temperature-sensing mechanism may unearth different molecular explanations for different TSD patterns. Furthermore, divergence within molecular function may extend to the downstream network involved in sex determination and commitment, and possibly even within gonad differentiation.

The species currently being utilized in studies investigating the genetics of TSD are listed in Table 1, along with particular details of their TSD patterns. We chose to conduct our studies in the red-eared slider turtle, *Trachemys scripta*. To select a model organism to examine the molecular network underlying TSD, several factors were considered, including whether species were amenable to laboratory study due to size and availability, have previously garnered the most data, or were predicted to be most evolutionarily informative. Selection in this manner of a few key species by researchers within the field as a whole would result in a more rapid accumulation of data and a clearer understanding of the TSD molecular network. It must be noted that understanding other aspects of TSD, including ecological, behavioral and evolutionary questions (for review see Valenzuela & Lance 2004), clearly do not fall within the same parameters as molecular studies, and should and do cover a much broader range of taxa.

***The red-eared slider turtle,* Trachemys scripta**

We chose to conduct this research using the red-eared slider turtle, *Trachemys scripta*, a fresh-water turtle species that exhibits temperature-dependent sex determination. The slider turtle is naturally found living in the swamps of Texas and Louisiana and therefore large numbers of eggs are readily available and relatively inexpensive to obtain. Furthermore, a complete staging series was recently conducted, allowing a reliable method of tracking embryonic morphological development (Greenbaum 2002). Research in this species has been ongoing in several laboratories (e.g., Crews, Capel, Wibbels), providing a foundation for the work that is stronger than in the case of other species (e.g., *Chrysemys picta, Chelydra serpentina*, see Table 1).

The red-eared slider turtle is sensitive to the effect of temperature during the middle third of embryonic development, and after this window closes, the gonad becomes committed to an ovarian or testicular fate (Bull et al. 1990, Wibbels et al. 1991). The timing of this window in *T. scripta* lasts from approximately stage 14 (Greenbaum staging series) through stage 19 at a female-producing temperature (FPT) and through stage 20 at a male-producing temperature (MPT) (Wibbels et al. 1991, Greenbaum 2002). Cooler incubation temperatures (25 - 27°C) produce all male hatchlings and warmer temperatures (31 - 35°C) result in all female hatchlings, with varying sex ratios produced by temperatures in between (Wibbels et al. 1991). Shifting eggs during the temperature-sensitive period (TSP) from one end of the temperature spectrum to the other (i.e., from 26°C to 31°C or vice versa) redirects gonadal development, resulting in 100% sex reversal (Crews et al. 1994, Crews 1996, Crews 2003).

Generation of a differentiated gonad in organisms with TSD

In the deceptively simple statement "sex is determined" lies a range of meaning. Plausible interpretations include that the cells of the gonad have begun expressing sex-specific markers, that some individual embryos at this point are no longer sex-reversible, or that all embryos at this point are no longer sex-reversible. This confusion is problematic, and thus a possible way of distinguishing between critical events in the timeline of gonadogenesis in organisms with TSD is presented in Figure 1 in the text contained in the center gray bar. Initially, during the formation of the urogenital ridge and the bipotential gonad, individuals of TSD species are equipotential in

their ability to become male or female. Temperature acts on this bipotential gonad, perhaps cumulatively, via target temperature-sensing molecule(s), and thus molecular differentiation begins as the temperature-sensitive period opens. Molecular differentiation continues as sex-specific pathways begin to be expressed, directing the gonad towards its eventual sexual fate. As molecular differentiation continues, sex is eventually "determined", or fated, such that if nothing perturbs the system, the gonad will continue in the developmental trajectory it has begun. At this point, gonads at different temperatures are no longer equal, but the TSP window remains open and sex is still reversible. Next, morphological differentiation begins as cells adopt different fates and reorganize, forming new, sex-specific structures within the gonad. Thus, molecular differentiation precedes morphological differentiation. Subsequently, the TSP window closes, at which point sex is "committed" and is irreversible. Sex-specific morphological differentiation continues and eventually results in a fully formed gonad. Clearly, deviations from this generalized timeline exist within some reptiles, such as in the Olive Ridley sea turtle, *Lepidochelys olivacea*, in which the TSP ends at MPT before morphological differentiation is observable (Merchant-Larios et al. 1997).

An important distinction arises from this theoretical framework. Most notably in organisms with TSD, sex determination does not equal final commitment to a sex. As studies elucidate the molecular network underlying TSD progress and gene function, scientists must take care when specifying particular steps of the pathway.

The molecular network underlying sex determination and gonad differentiation in organisms with GSD

The development of a vertebrate gonad can be thought of in two phases: the initial construction of an organ from which a variety of outcomes are possible, and the subsequent narrowing of these possibilities into one particular fate. Specifically, this translates to a) the formation of an equipotent urogenital ridge and its successor, the bipotential gonad, and b) the determination of sex and the subsequent molecular and morphological differentiation that results in a fully formed testis or ovary. The introduction of the molecular network that follows is broken down into these processes, with candidate genes being placed within a certain phase or sex-specific trajectory

based on information from GSD species. However, the roles of these gene products in TSD remain unclear and is the focus of our research. The level of convergence that exists across phyla in the function of these molecular players remains to be determined.

i. Formation of the bipotential gonad

In mammals, the formation of the urogenital ridge and subsequent bipotential gonad from underlying mesonephric and coelomic epithelial tissues utilizes several factors, including *Sf1*, *Wt1*, *Emx2*, *Lhx9*, and *M33* (for review see Wilhelm et al. 2007, Brennan & Capel 2004). Only two of these, *Sf1* and *Wt1*, have been examined thus far in organisms with TSD. *Steroidogenic factor 1* (*Sf1*, also known as *Ad4BP* and *Nr5a1*) is an orphan nuclear receptor that regulates transcription of many downstream genes, including several steroidogenic enzymes (for review see Sadovsky & Dorn 2000). In early gonadogenesis, it appears to modulate cell proliferation and prevent apoptosis in the forming bipotential gonad in both sexes (Luo et al. 1994). It also plays several later testis-specific roles: in concert with *Sry* (*Sex-determining region of the Y chromosome*) it appears to upregulate a specific enhancer element of *Sox9* (*Sry-like HMG-box containing transcription factor 9*) (26), and in conjunction with *Sox9* directly upregulates *Mis* (*Müllerian-inhibiting substance*) (Shen et al. 1994, Giuili et al. 1997, De Santa Barbara et al. 1998, Arango et al. 1999).

Wilms tumor 1 (*Wt1*), a nuclear zinc-finger transcription factor, is also expressed throughout the mammalian urogenital ridge in both sexes and appears to prevent apoptosis in the forming bipotential gonad (Armstrong et al. 1993, Kreidberg et al. 1993, Roberts 2005, Hartkamp & Roberts 2008). Two spliceoforms of *Wt1*, distinguishable by only three amino acids, play different roles in gonadogenesis: Wt1(+KTS) appears to lead to the initial upregulation of *Sry* (Hammes et al. 2001, Matsuzawa-Watanabe et al. 2003), while Wt1(-KTS) may directly upregulate *Sf1* (Nachtigal et al. 1998, Wilhelm & Englert 2002, Klattig et al. 2007). Thus, in mammals, *Sf1* and *Wt1* both play an early non-sex-specific function in bipotential gonad formation as well as later testis-specific roles, and are good candidates to examine for function across sex-determining mechanisms.

ii. Testis-determining pathway

The formation of a testis from its bipotential gonad precursor is a complex process involving many molecular and cellular interactions that has been intensely studied in vertebrates with GSD (see DiNapoli & Capel 2008, Wilhelm et al. 2007, Brennan & Capel 2004, Fleming & Vilain 2004). Five particular genes involved in testis determination and differentiation in mammals have also been studied in organisms with TSD, and are discussed here, namely *Sox9*, *Sox8*, *Fibroblast growth factor 9 (Fgf9)*, *Mis* and *Doublesex mab3 related transcription factor 1(Dmrt1)*.

Excitingly, the search for the direct target of mammalian sex-determining factor *Sry* has finally been solved. A long-standing postulation was recently verified by Sekido and Lovell-Badge, namely that *Sry*, in concert with *Sf1*, binds to a promoter element of the gene *Sox9* (Sekido & Lovell-Badge 2008). Analysis of human patients with campomelic dysplasia, roughly two thirds of whom develop as XY females, revealed the importance of the *Sry*-related gene *Sox9* in the molecular sex-determining cascade (Foster et al. 1994). Extensive studies in the mouse have since shown *Sox9* to be both necessary and sufficient to cause the determination and differentiation of a testis (Vidal et al. 2001). Loss of *Sox9* causes male-to-female sex reversal in both humans (Wagner et al. 1994, Foster et al. 1994) and mice (Chaboissier et al. 2004, Barrionuevo et al. 2006), while transgenic XX mice containing a copy of *Sox9* develop testes (Bishop et al. 2000, Vidal et al. 2001). The closely related *Sox8* appears to reinforce the function of *Sox9*, but is not able to replace it (Chaboissier et al. 2004). While *Sry*/*Sf1* action initiates pre-Sertoli cell *Sox9* expression, *Fgf9* is required to maintain its expression and is thought to contribute to Sertoli cell differentiation (Colvin et al. 2001, Schmahl et al. 2004, Kim et al. 2006). Loss of *Fgf9* leads to male-to-female sex reversal in some individuals, and it has been shown to play an antagonistic role together with *Sox9* in apposition to the *Wnt4* signaling pathway (Kim et al. 2006).

In both humans and mice, SOX9 interacts directly with SF1 (*Steroidogenic factor 1*) to upregulate the expression of *Müllerian-inhibiting substance* (*Mis* or *anti-Müllerian hormone*, *Amh*) (de Santa Barbara et al. 1998, Arango et al. 1999). *Mis*, a member of the transforming

growth factor-β (TGF-β) superfamily, is an early factor secreted by differentiated Sertoli cells in the testis. Via the specific receptor *MisRII*, MIS causes the regression of the Müllerian ducts, anlagen which otherwise develop into the uterus, cervix and fallopian tubes in females (Behringer et al. 1990, Josso et al. 2006). The regulatory relationship between *Sox9* and *Mis* in mammals has not been strictly conserved across phyla or mechanisms of sex determination. In the chicken, *Gallus gallus*, another vertebrate with GSD, sexually dimorphic expression of *Mis* in the gonad precedes *Sox9*, and the relationship between the two has yet to be fully characterized (Oreal et al. 1998, Smith et al. 1999a).

Continued evidence of molecular conservation between sex-determining mechanisms across phyla came with the discovery of *Dmrt1* (*Doublesex mab3 related transcription factor 1*). It is one of the few genes found to have homologs involved in sex differentiation across widely diverse taxa, including *Drosophila*, *C. elegans*, and vertebrates, including human, mouse, turtles, birds, alligator, fish and lizards (Shen & Hodgkin 1998, Burtis & Baker 1989, Raymond et al. 1998, Smith et al. 1999b, Kettlewell et al. 2000, Nanda et al. 2002, Matsuda et al. 2002, Sreenivasulu et al. 2002). After sex has been determined in the mammalian testis, *Dmrt1* function is critical to vertebrate testis differentiation (Veitia et al. 1997, Raymond et al. 2000). Loss of *Dmrt1* is thought to be responsible for the male-to-female sex reversal seen in XY humans with chromosome 9 deletions (Flejter et al. 1998), and *Dmrt1* has since been studied in a variety of vertebrates. While it seems to play a downstream role in testis differentiation in mammals (Raymond et al. 2000), it has been proposed to be a master sex-determining gene in both chicken and medaka (Nanda et al. 2002, Matsuda et al. 2002, Kobayashi et al. 2004, Smith & Sinclair 2004), although further studies are needed to confirm this role (e.g., Zhao et al. 2007).

iii. Intersecting pathways

Several factors have been shown to play complex roles in the development of both the mammalian testis and the ovary, including *Dax1* and *Wnt4*. Differing functions of the same molecule can be regulated by the timing and localization of expression, the presence/absence of other co-regulators, and the presence/absence of activators/repressors of the molecules themselves.

The nuclear receptor *Dax1* (*Dosage-sensitive sex-reversal, Adrenal hypoplasia congenital on the X chromosome 1*, also known as *Nr0b1* and *Ahch*) is a novel orphan member of the nuclear hormone receptor superfamily and plays a role in both mammalian sex determination and adrenal function (see Niakan & McCabe 2005). The otherwise highly conserved DNA-binding domain has been replaced in *Dax1* by a protein binding domain thought to bind other nuclear receptors (see Wilhelm et al. 2007). Understanding its role in gonadogenesis in mammals has been complicated over the past decade. *Dax1* was originally thought to have an ovarian-determining function during development (Bardoni et al. 1994, Swain et al. 1996). Undisrupted embryonic gonadogenesis but abnormal postnatal formation of follicles in *Dax1-/-* XX mice indicate a role for *Dax1* later in the adult ovary as well (Yu et al. 1998). However, the early ovary- and late testis-specific expression pattern of *Dax1* in the mouse suggested a complex role in the development of the gonad in both sexes (Ikeda et al. 1996), and it is now understood to be critical to testicular development as well (Ikeda et al. 2001, Meeks et al. 2003a, 2003b). In testicular development, *Dax1* may control availability of estrogens by regulating *aromatase* transcription (Wang et al. 2001, Meeks et al. 2003a, 2003b). Thus, it has been suggested to operate at multiple time points within both sexes as a "common" regulator of gonad development with several functions (for review see Ludbrook & Harley 2004).

Wnt4 (*Wingless-type MMTV integration site family member 4*) signaling has also been implicated in the development of the mammalian reproductive system in both sexes (for review see Bernard & Harley 2007). It has been shown to both mediate the initial formation of the Müllerian ducts and regulate the migration of steroidogenic mesonephric cells into the developing gonad (Vainio et al. 1999, Jeays-Ward et al. 2003). However, it also seems to play several sex-specific roles during gonadogenesis as well. In the ovary, *Wnt4* acts via *Follistatin* to prevent the formation of a testis-specific coelomic blood vessel (Yao et al. 2004a). Furthermore, antagonistic action and/or competition to reach threshold levels between *Wnt4* and *Sox9/Fgf9* may tip the balance between female and male development (Kim et al. 2006). In the testis, gonadal expression of *Sox9*, *Mis*, *Dhh* and *Sf1* is decreased in *Wnt4* -/- XY mice and can be rescued by ectopic Wnt4, suggesting an active role for *Wnt4* in testicular development as well (Jeays-Ward et al. 2004). Finally, studies in mouse suggest that *Dax1* may be upregulated by

Wnt4 signaling, further complicating the story of these two factors (Jordan et al. 2001, Mizusaki et al. 2003).

iv. Ovary-determining pathway

Ovarian development is characterized by a proliferation of cells in the cortical region of the gonad concurrent with medullary regression. Within the thickened cortex, granulosa cells organize to surround germ cells while steroidogenic thecal cells remain interstitial between developing follicles (for review see Yao 2005). One of the few ovarian-specific factors is *FoxL2* (*Forkhead box protein L2*), a single-exon transcription factor with a conserved winged-helix forkhead domain, mutations in which cause ovarian failure in humans with BPES Type I disease (Crisponi et al. 2001, Udar et al. 2003). *FoxL2* is expressed in the developing ovary of mouse and chick embryos (Loffler et al. 2003, Govoroun et al. 2004), and is involved in postnatal mammalian granulosa cell differentiation (Schmidt et al. 2004). Furthermore, *FoxL2 -/-* XX adult mice exhibit marked upregulation of several testis-specific markers, including *Sox9*, *Dhh*, and *Fgf9*, indicating that *FoxL2* repression of testis-determining genes may occur well past mammalian embryonic sex determination (Ottolenghi et al. 2005). Recent studies have shown that double *FoxL2*/*Wnt4* knockout mice exhibit female-to-male sex reversal, and have identified *FoxL2* promoter elements that may be mechanistically responsible for this reversal (Ottolenghi et al. 2007, Benayoun et al. 2008).

The most recently discovered player in ovarian development is *R-spondin1* (*Rspo1*), part of a small family of secreted growth factors. Excitingly, it is the first identified gene that when mutated causes full female-to-male sex reversal in humans (Parma et al. 2006). It is a signaling ligand that can regulate Wnt and β-catenin signaling pathways by modulating availability of a Wnt co-receptor, LRP6 (Kim et al. 2006, Binnerts et al. 2007). Furthermore, it appears that *Rspo1*, via activation of B-catenin, and reinforced by *Wnt4* signaling, is required for mammalian ovary determination (Chassot et al. 2008, Tomizuka et al. 2008). However, *Rspo1* -/- XX mice are only partially masculinized and develop ovotestes, indicating that another upstream ovarian factor not under the control of *Rspo1* remains active in these mice (Chassot et al. 2008). The discovery of this sex-determining gene is a breakthrough in unraveling the intricacies of the

signaling and transcription network that occurs in an XX gonad. It has thus been proposed that *Rspo1* reinforces *Wnt4* in its antagonism of *Sox9/Fgf9*; in this model, a threshold amount of either pair of factors within the bipotential gonad tips the balance towards one developmental trajectory over the other, committing the bipotential organ to a sexual fate (DiNapoli & Capel 2008).

Investigation of these candidate genes in organisms exhibiting temperature-dependent sex determination

The molecular network underlying gonadogenesis in organisms with GSD began to be receive attention by researchers studying TSD in the late 1990's. Prior to the studies presented in this dissertation, *Sox9* and *Dmrt1* had been the focus of research and had been examined in four and three TSD species, respectively. The roles of *Mis, FoxL2* and *Dax1* were beginning to be explored, and *Wnt4* and *Rspo1* had never been cloned in any organism with TSD.

i. Testis pathway: Sox9, Mis, Dmrt1

Because of its critical, upstream role in mammalian testis development, *Sox9* had been investigated in four species with TSD prior to this work. However, these studies demonstrated conflicting results across taxa, and as described in Chapter Five, our work revealed that this was due to differences in the types of tissues being analyzed. Expression of *Sox9* becomes enhanced at MPT at the end of the TSP in both the leopard gecko, *Eublepharis macularius* and the Olive Ridley sea turtle, *Lepidochelys olivacea* (Moreno-Mendoza et al. 1999, Valleley et al. 2001). In contrast, expression in the American alligator does not become substantially greater at MPT as compared to FPT until during testis differentiation (Western et al. 1999a, 1999b). Furthermore, separate studies in the slider turtle gave conflicting data. *Sox9* expression appeared in one study to be enhanced at MPT late in gonadogenesis, during testis differentiation, while another study showed comparable levels of *Sox9* expression in both sexes at all stages examined (Spotila et al. 1998, Kettlewell et al. 2000). *Sox9* was the only gene whose expression had been investigated in response to sex-reversing temperature shifts, and data showed that it was indeed upregulated in response to novel MPT (Moreno-Mendoza et al. 2001)

In mammals, *Sox9* directly upregulates *Mis*, but this relationship has been altered in chicken; the interaction of these two gene products in organisms with TSD is of great interest. Prior to our work, *Mis* had been examined in two TSD organisms; however, the response of *Mis* to novel temperature changes was not explored in any study. In the American alligator, *Alligator mississippiensis,* sexually dimorphic expression of *Mis* occurs in the middle of the TSP, preceding the onset of testicular *Sox9* expression (Western et al. 1999b). In the red-eared slider turtle, *Mis* expression had also been shown to be male-specific by the middle of the TSP (Takada et al. 2004).

Dmrt1 expression had been investigated in three TSD species, and prior to the work presented here, no functional studies had been undertaken and its response to sex-reversing temperature shifts or hormone treatment had not been explored. Studies at constant incubation temperatures showed that it is likely involved in testicular development. In the Olive Ridley sea turtle, *Dmrt1* expression becomes greater in developing testes early in the TSP (Torres-Maldonaldo et al. 2002). In the American alligator, gonadal expression of *Dmrt1* before and during the TSP is also greater in males, but increases through development in both sexes, raising questions about possible function (Smith et al. 1999b). In *T. scripta*, dimorphic expression during the TSP had been reported, beginning at either stage 15 (Kettlewell et al. 2000) or stage 17 (Murdock and Wibbels 2003).

ii. Intersecting pathways: Dax1 and Wnt4

Dax1 plays a role in gonadogenesis of both the testis and the ovary in mammals, and early work in two TSD species revealed an expression pattern consistent with a similar function in TSD. *Dax1* is expressed at constant temperatures in the developing gonad of both sexes in the American alligator and the Olive Ridley sea turtle (Western et al. 2000, Torres-Maldonado et al. 2002). *Wnt4* had not been cloned in any organism with TSD prior to this research.

iii. Ovarian network: FoxL2 and Rpos1

Two genes involved in ovarian development in GSD vertebrates are *FoxL2* and the recently implicated *Rspo1*. A brief study of *FoxL2* expression in the red-eared slider turtle revealed that

transcripts are initially detected in both MPT and FPT gonads and are later restricted to the developing ovary (Loffler et al. 2003). The response to *Foxl2* to changes in temperature had not been examined. *Rspo1* was first discovered to be involved in sex determination in a ground-breaking paper published in November 2006 (Parma et al. 2006). Our studies of *Rspo1* in the slider turtle are the first, and currently remain the only, examination of this gene in an organism with TSD.

Examining the molecular network underlying gonadogenesis in an organism with temperature-dependent sex determination

For my dissertation, I address the following overall hypotheses: Firstly, components of the molecular pathway underlying gonadogenesis in organisms with temperature-dependent sex determination have been retained from genetic sex determination. Secondly, although much of this network has been conserved, new functions for some of these genes have evolved.

Specifically, I test these hypotheses in the red-eared slider turtle, *Trachemys scripta*:

I. The transcription factors *Sox9* and *Dmrt1* and the hormone *Mis* are involved in the formation of a testis and/or the repression of an ovary at a male-producing temperature.

II. The transcription factor *Dax1* and the signaling molecule *Wnt4* play roles in gonadogenesis in both sexes.

III. The transcription factor *FoxL2* and the signaling molecule *Rspo1* are involved in the formation of an ovary and/or the repression of a testis at a female-producing temperature.

IV. While *Mis* expression may be maintained by *Sox9*, the initial upregulation of *Mis* in the developing testis is modulated by some other upstream factor.

V. *Dmrt1* is an upstream factor in testicular development and may directly sense male-producing temperature, similar to its suggested master sex-determining role in other species.

VI. The development of whole gonads in an *in vitro* organ culture system mimics *in ovo* development. Furthermore, isolated gonadal tissue retains the ability to sense and respond to changes in environmental temperature, indicating an endogenous temperature-sensor.

VII. Molecular manipulation of explant gonads in culture allows previously unavailable functional experiments that are essential to elucidating the molecular network underlying TSD.

Chapter One of my dissertation has introduced temperature-dependent sex determination and the organism utilized in these studies, the red-eared slider turtle, *Trachemys scripta*. It described the key players in the molecular network underlying mammalian gonadogenesis, which these studies draw upon in a candidate gene approach. Chapter Two investigates the pathway underlying testicular development in the red-eared slider turtle. It examines the expression patterns of *Sox9*, *Dmrt1* and *Mis* in the developing turtle gonad, addressing Hypothesis I. Chapter Three investigates the pathway underlying ovarian development, examining expression of *Dax1, Wnt4*, *FoxL2* and *Rspo1*. Moreover, it extends data on these genes as well as *Sox9*, *Dmrt1* and *Mis* and examines the response of these candidate sex-determining genes to changes in temperature. This assay allows the establishment of these genes in sex-specific pathways, and addresses Hypotheses I, II and III.

Chapter Four examines the response of these seven genes to changes in temperature that last for the duration of the sex-determining period, addressing Hypotheses IV and V. It also introduces a whole organ culture system in which gonads are dissected from embryos and develop for up to several weeks *in vitro*, addressing Hypothesis VI. The utility of this assay to molecularly manipulate the gonad to investigate functional roles of sex-determining molecules is demonstrated by the misexpression of *Sox9* at female-producing temperatures, addressing Hypothesis VII. Furthermore, Chapter Four examines the strong effect of estrogen-mimicking compounds on the expression of various members of the sex-determining pathway. Chapter Five provides a summary of the work, places it in the context of other research in the field, and evaluates these seven hypotheses.

Table 1. Organisms historically used in studies examining the molecular network underlying temperature-dependent sex determination

Organism	Pattern of TSD	Temperature to produce a single -sex clutch *	Critical stages in embryonic gonadal development						Staging and gonadogenesis references	Molecular studies references
			Egg lay	Genital ridge formation	Bipotential gonad formation	TSP (in developmental stages) #	Onset of morphological differentiation	Hatch		
Red-eared slider turtle (*Trachemys scripta*)	% males / temp	MPT (26 C) FPT (31 C)	0		by 15	15 - 20 15 - 19	18/19	26	[17, 125, 126]	[41, 42, 43, 44, 54, 57, 58, 77, 51, 89, 93, 98, 99, 114, 123]
American alligator (*Alligator mississippiensis*)	% males / temp	MPT (32.5 - 33 C) FPT (30 or 35 C)	0	12 /13	by st 20	21 - 24	21/22 22/23	28 ?	[20, 127 - 130]	[47, 55, 76, 91, 92]
Olive Ridley sea turtle (*Lepidochelys olivacea*)	% males / temp	MPT (26-27.5 C) FPT (32-33 C)	0	12 - 13	21 - 23	20 - 23 24 - 27 (Days 20 - 27 for both temps)	26/27	31	[18, 131 - 133]	[85, 86, 87, 88]
Painted turtle (*Chrysemys picta*)	% males / temp	MPT (25 C) FPT (30.5 C)	0			16 - 22		26	[16, 126, 141]	[45, 56, 111]
Snapping turtle (*Chelydra serpentina*)	% males / temp	MPT (23 - 27 C, 99%) FPT (20 C, > 29.5 C)	0			14 - 19 14 -16, 14- 19		26	[126, 134 - 137]	[46]
Leopard gecko (*Eublepharis macularius*)	% males / temp	MPT (31-33 C, 90%) FPT (23-28 or 34 C)	30			32 - 37		40	[1, 138 - 140]	[90]

Notes: * *These temperatures are thought to produce 100% of the given sex under laboratory conditions, except where indicated.*
Temperature-sensitive period is defined as the period during which sex can be reversed in some individuals when a group of eggs are temperature-shifted.

Figure 1. Genetic events underlying gonad determination and differentiation in GSD mammals and TSD reptiles.
A model of the molecular network underlying mammalian genetic sex determination is given in comparison to what is known in species with TSD. It is important to note that within the model, gene names in the mammalian network represents known dimorphic function, while the reptilian network represents sex-specific gene expression. Solid lines imply direct regulatory relationships while dashed lines imply indirect or undescribed relationships. Some parts of the model have been shown conclusively, while others are supported by evidence. Developmental time proceeds from left to right. Stages of gonad development are described in the middle of the figure (B, gray box), and lines extending from this box attempt to align important gonad events across sex and sex-determining mechanism. It is also notable that other GSD species, such as chick, may have divergent timing of events and function of various factors. The mammalian GSD network was selected to provide a framework against which to compare TSD studies.

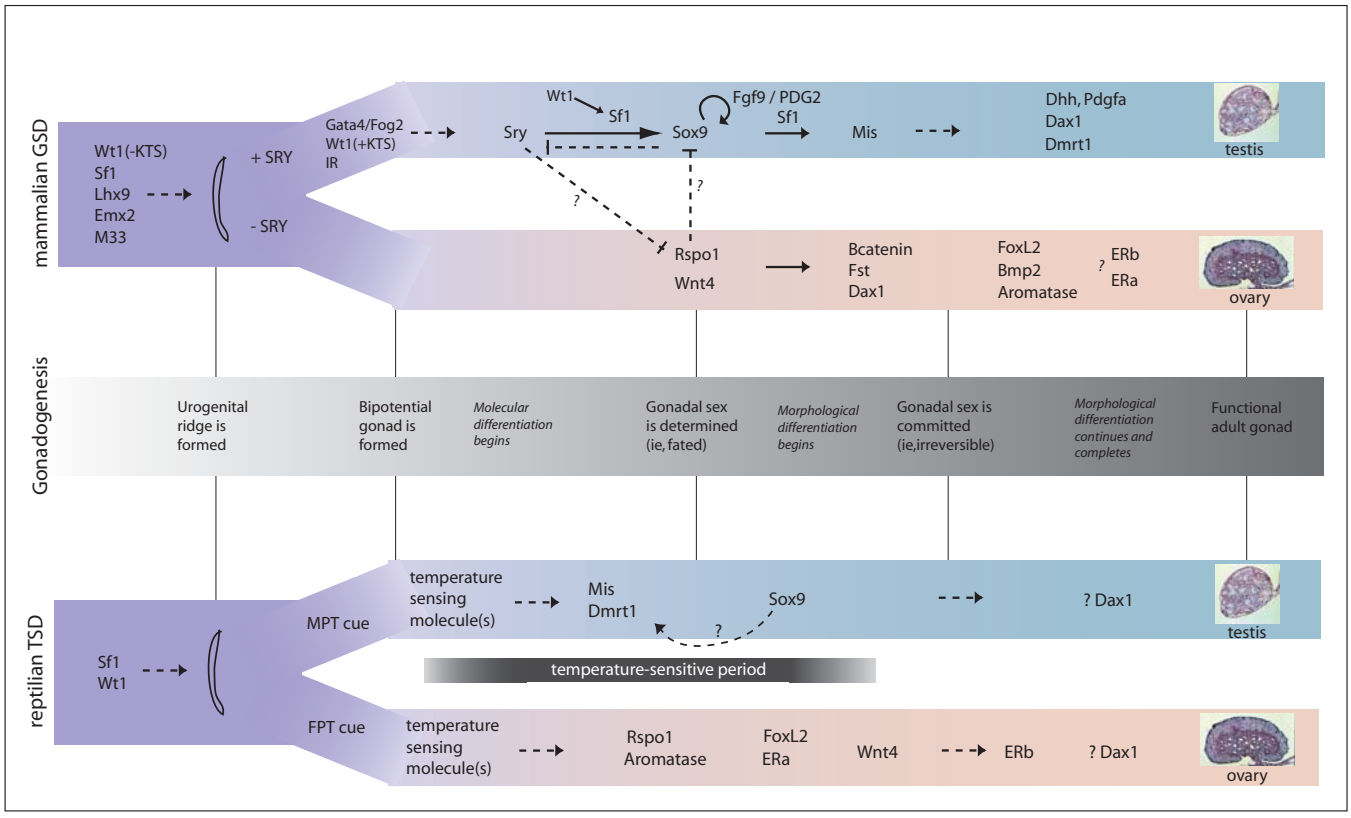

CHAPTER TWO

Expression of *Sox9*, *Mis* and *Dmrt1* in the gonad of a species with temperature-dependent sex determination*

Sex determination in vertebrates, the process of forming an ovary or testis from a bipotential gonad, can be initiated by genetic or environmental factors. Elements of the downstream molecular pathways underlying these different sex-determining mechanisms have been evolutionarily conserved. We find the first evidence that *Sox9* expression is preferentially organized in the testis early in the temperature-sensitive period in a species with temperature-dependent sex determination (*Trachemys scripta*). This pattern occurs before sexually dimorphic *Mis* expression and in a temporal hierarchy that is similar to mammals. Furthermore, we extend previous findings that *Dmrt1* expression at early stages of sex determination has a dimorphic pattern consistent with a possible upstream role in determining the fate of the bipotential gonad.

To clarify the nature of the gene regulatory network underlying testis development in organisms with TSD, we analyzed the expression patterns of *Sox9*, *Mis* and *Dmrt1* by whole mount *in situ* hybridization (ISH) and quantitative real time PCR (qPCR) during the period of sex determination and differentiation in *T. scripta*. While the expression of all three of these genes has been reported as male-specific, the localization of expression patterns and the temporal hierarchy of expression in relation to each other have not been detailed. We visualize and compare localized expression patterns of each gene at the earliest stage of bipotential gonad formation (stage 15), in the middle and at the end of the temperature-sensitive period (stages 17 and 19), as well as at two stages of gonad differentiation (stages 21 and 23). We find the first evidence in an organism with TSD that *Sox9* is expressed in a sexually dimorphic organized fashion early in the temperature-sensitive period, before the onset of testis-specific *Mis* expression. Furthermore, we support previous findings and confirm in *T. scripta* that *Dmrt1*

* Portions of this chapter appear in Shoemaker, Ramsey, Queen & Crews, 2007a.

shows sexually dimorphic expression at the beginning of the temperature-sensitive period, in a pattern that is consistent with a possible upstream role in testis determination.

METHODS

Collection and harvesting embryos

Freshly laid red-eared slider eggs purchased from Clark Turtle Farms (Hammond, LA) were maintained as previously described (Wibbels et al. 1991). Briefly, viable eggs were randomized and placed in incubators (Precision, Chicago, IL) at 26.0°C or 31.0°C. Incubator temperatures were monitored with HOBO data loggers (Onset Computer Corp., Bourne, MA) and verified with calibrated incubator thermometers. Developmental progression was monitored by assessing external characteristics in a periodic sampling of embryos.

Cloning of turtle gene homologs

Total RNA was extracted from pooled AKG tissues from a variety of sexes and stages and reverse-transcribed using oligo(dT) primers with Superscript II reverse transcriptase (Invitrogen, Carlsbad, CA). *Sox9* primers were designed to amplify a 558 bp subclone of the sequence reported by Spotila et al. (1998). Degenerate primers for *Mis* and *Dmrt1* were designed based on mouse, alligator and chicken sequences. Amplified fragments were ligated into pCR4-TOPO vector (Invitrogen, Carlsbad, CA) and sequenced using M13F and M13R primers. The sequences of the *Mis* and *Dmrt1* clones were subsequently found to correspond to base pairs 140 to 339 of *T. scripta Mis* (accession # AY235424) and base pairs 35 to 463 of *T. scripta Dmrt1* (accession # AY316537).

Whole mount in situ hybridization (ISH)

Riboprobes were reverse-transcribed in the presence of Digoxygenin-labeled UTP (Roche) using T3/T7 Megascript *in vitro* transcription kit (Ambion, Austin, TX) to produce antisense or sense DIG-labeled riboprobes. Turtle embryos were harvested from eggs at specific stages, and gonads were dissected and fixed overnight in 4% paraformaldehyde/PBS at 4°C. Following fixation, whole mount ISH was performed as described by Andrews et al. (1997) with modification.

Briefly, tissues were dehydrated in an increasing methanol/PBTX series, rehydrated and partially digested with 10ug/mL proteinase K for 15 – 45 minutes, depending on tissue stage. Following fixation in 0.2% gluteraldehyde, tissues were pre-hybridized overnight at 65°C. Hybridization of DIG-riboprobe was carried out overnight at 65°C, followed by a series of increasing stringency washes in SSC. After Anti-DIG-AP Fab fragments (Roche) were pre-blocked in turtle embyro powder, tissues were incubated in 1:2000 Ab dilution overnight at 4°C. Hybridization was visualized with BM purple (Roche) and whole tissues were photographed in 100% glycerol. AKGs were embedded in OCT medium (Fisher Scientific, Hampton, NH) and sectioned on a cryostat (2800 Reichert-Jung).

Quantitative real-time RT-PCR (qPCR)

Gonads from 20 individual turtles were pooled into one sample per stage/sex for total RNA extractions using the RNAgents Total RNA Isolation Kit (Promega, Madison, WI). Total RNA was also extracted from pooled adrenal-kidney-gonad (AKG) complexes at each stage/sex for comparison. Total RNA was treated with Turbo DNA-free DNase I (Ambion, Austin, TX) and reverse-transcribed using the SuperScript First-Strand Synthesis for RT-PCR system (Invitrogen, Carlsbad, CA) with both oligo-(dT) and random hexamers. Relative gene expression levels were quantified using SYBR Green I dye (Invitrogen, Carlsbad, CA) and an ABI PRISM 7900HT real-time PCR cycler (ABI SDS 2.2.1 software). All samples were run in triplicate, and gene-specific PCR efficiencies were calculated from gene-specific standard curves. Relative transcript abundance corrected for PCR efficiency was normalized to expression of *PP1*, a constitutively expressed transcript across both stage and sex (Muller et al. 2002, Simon 2003). Primers used to assay gene expression were designed across exon boundaries where possible using MacVector (Accelrys, San Diego, CA), and specificity was verified by agarose gel electrophoresis. Primers were as follows: ***Mis*** forward 5'-CGG CTA CTC CTC CCA CAC G-3', reverse 5'-CCT GGC TGG AGT ATT TGA CGG-3'; ***Dmrt1*** forward 5'-CAA CTA CTC CCA ATA CCA GAT GGC-3', reverse 5'-GGC TTC GCA GGC TGT TTT TC-3'; ***Sox9*** forward 5'-CCT GCC CTT CTG GTT CCG-3', reverse 5'-TCC TCG TCC CTC TCT TTC TTC AG-3'; ***PP1*** forward 5'-CAG CAG ACC CTG AGA ACT TCT TCC TGC TG-3', reverse 5-GCG CCT CTT GCA CTC ATC AT-3'.

RESULTS AND DISCUSSION

Sox9 expression is dimorphic near the beginning of the temperature-sensitive period

Previous reports have shown that levels of *Sox9* expression in *T. scripta* are similar at MPT and FPT during the temperature-sensitive period, and only become higher in the testis during differentiation (Spotila et al. 1998). While our data is consistent with this report, we also find evidence of an earlier dimorphism in the localized organization of this transcription factor. Early in the temperature-sensitive period, *Sox9* expression at MPT occurs in clusters of cells surrounding other non-expressing cells. We suggest that these clustered cells are perhaps presumptive Sertoli cells of the developing seminiferous tubules. While levels of *Sox9* expression at FPT are similar, transcript localization is diffuse and appears unorganized throughout the gonad. It is not unlikely that this differential localization corresponds to a functional dimorphism early in the sex-determining period. Thus we find the first evidence of *Sox9* expression in an organism with TSD that suggests similarity to the pattern seen in mammals. These findings are consistent with a possible upstream role for *Sox9* in TSD, although this was not investigated in the current study and warrants future attention.

At the beginning of the temperature-sensitive period (stage 15), *Sox9* is expressed at comparable levels in gonads at both male- (n=12/15; Fig. 2A) and female-producing temperatures (n=9/12; Fig. 2B). However, sections of gonads reveal that at MPT, *Sox9* transcripts are concentrated in cells surrounding non-expressing cells (Fig. 2I), while expression at FPT remains dispersed throughout the gonad (Fig. 2J). At this stage at MPT, *Sox9* is also expressed in dorsal metanephric tissue in half of the embryos examined (n=7/15; data not shown).

As the sex-determining period progresses and temperature exerts its effect (stage 17), organized *Sox9* expression persists at MPT (n=15/16; Fig. 2C, K). There is strong staining in dorsal metanephric tissue and the posterior tip of the mesonephros, although it is unclear if posterior mesonephros is actually a contributing source of gonadal cells (Fig. 2C). In addition, approximately half of MPT embryos show staining in developing Wolffian ducts (n=7/16; data not shown). Although *Sox9* expression at this stage is retained in gonads at FPT in comparable

levels to gonads at MPT (n=8/11; Fig. 2C, D), it still occurs in a diffuse pattern spread throughout the gonad (Fig. 2L). Metanephric expression is also detected in most embryos at FPT (n=7/11), but Wolffian duct expression is not. *In situ* data is confirmed by qPCR studies in which total RNA was extracted from one sample per sex/stage. Each sample was comprised of either pooled gonads or pooled AKGs dissected from at least 20 embryos. This was technically possible beginning at stage 17, and *Sox9* expression is seen at comparable levels at both MPT and FPT at this stage (Fig. 2Q).

At a stage when sexual fate is committed at a MPT but remains somewhat reversible at a FPT (stage 19), *Sox9* expression increases in virtually all gonads developing at MPT (n=7/8; Fig. 2E, Q) in a pattern that is suggestive of Sertoli cells organizing into sex cords (Fig. 2M). Expression is downregulated in all FPT gonads examined by ISH (n=0/12; Fig. 2F, N), but is still detectable by qPCR, a discrepancy we are investigating (Fig. 2Q). Expression is maintained in dorsal metanephric tissue in some embryos at both MPT (n=4/8) and FPT (n=7/12), while Wolffian duct expression disappears from males. During testis differentiation (stages 21 and 23), *Sox9* is strongly expressed in all gonads examined developing at MPT (n=13/13 and 12/12, respectively; Fig. 2G, Q). In these gonads, expression continues in an increasingly reticulated pattern, corresponding to the expansion of primitive sex cords and their subsequent transformation into seminiferous tubules (Fig. 2O). In contrast, only a few cells weakly expressing *Sox9* were observed in several differentiating ovaries at stages 21 and 23 (n=3/12 and 5/12, respectively; Fig. 2H, P, Q). In both sexes, metanephric expression remains strong in the beginning of gonad differentiation (stage 21, n=9/13 at MPT, n=11/12 at FPT; Fig. 2S) and then diminishes to a faint level (stage 23, n=9/12 at MPT, n=3/12 at FPT).

Dimorphic Mis expression occurs later in the temperature-sensitive period

It has been shown in *T. scripta* that *Mis* expression is undetectable in the bipotential gonad, is upregulated in developing testes during the temperature-sensitive period and becomes increasingly stronger as sex determination occurs and differentiation begins (Takada et al. 2004). Our data are consistent with these findings as well, and further reveal that in contrast to *Sox9*, both the level of *Mis* expression as well as its cellular organization appear similar in MPT and

FPT gonads early in development. At the start of the temperature-sensitive period, *Mis* transcripts are organized in similar clusters of cells in both sexes. It isn't until after the sex-determining period, and after *Sox9* patterns are dimorphic, that *Mis* is upregulated in males and downregulated in females. These results are consistent with a role for *Sox9* upstream of *Mis*, although a regulatory relationship between them in this species remains to be shown.

Mis expression is virtually equivalent at both male- and female-producing temperatures at the earliest stage of gonad formation (stage 15) (n=10/12 at both MPT and FPT; Fig. 3A, B, I, J). As the sex-determining period progresses (stage 17), *Mis* expression is upregulated in the gonads of embryos incubating at MPT (n=16/16; Fig. 3C, K) and persists but is downregulated at FPT (n=11/12; Fig. 3D, L). As sexual fate is committed and gonad differentiation occurs (stages 19, 21 and 23), developing testes strongly express *Mis* in a pattern similar to *Sox9*, possibly in the preSertoli cells of nascent seminiferous tubules (Fig. 3E, M, G, O, Q). Expression is also seen at MPT in dorsal metanephric tissue, as well as progressively in a cranial to caudal wave in the Müllerian ducts (Fig. 3S). In contrast, expression at FPT at stage 19 is undetectable in half of the gonads examined and faint in the rest (n=7/14; Fig. 3F, N, Q). In later stages of ovarian differentiation (stages 21 and 23), expression at FPT falls to undetectable levels (n=0/12 and 0/12, respectively; Fig. 3H, P, Q). Although qPCR levels at FPT appear close to zero in all stages examined, this is an artifact produced by the extremely high expression levels seen later at MPT (see Fig. 3Qa and Qb).

Dmrt1 expression is consistent with a possible upstream role in T. scripta

Via whole mount *in situ* hybridization, we confirm previous reports that *Dmrt1* expression is dimorphic before sex is determined. At the beginning of the temperature-sensitive period (stage 15), all embryos developing at MPT show punctate *Dmrt1* expression in the gonad (n=12/12; Fig. 4A, I), while half of FPT embryos show weaker, diffuse gonadal expression (n=6/12; Fig. 4B, J). At stage 17, expression of *Dmrt1* continues in gonads at MPT (n=14/14; Fig. 4C, K) and is detected in only a very few cells in gonads at FPT (n=2/9; Fig. 4D, L). Upregulation of expression at MPT is localized in clusters of cells surrounding non-expressing cells (Fig. 4K). qPCR confirms a difference in *Dmrt1* transcript levels at this stage, and although expression in

both sexes is low overall, relative transcript abundance is three times higher at MPT than at FPT (Fig. 4Q).

By stage 19, *Dmrt1* expression is upregulated further at MPT (n=7/7; Fig. 4E, Q). Expression at FPT declines in all ISH gonads examined (n=0/10; Fig. 4F, N), but is still detectable by the more sensitive method of qPCR (Fig. 4Q). Sectioned gonads reveal continued *Dmrt1* expression in cells organized in what are possibly developing sex cords of the testis (Fig. 4M). Finally, during differentiation (stages 21 and 23), expression at MPT continues to increase (n=12/12 and 8/8, respectively; Fig. 4G, O, Q) and is virtually undetectable in all gonads at FPT (n=0/12 and 0/12, respectively; Fig. 4H, P, Q). Throughout development, *Dmrt1* expression is not seen in other tissues of the adrenal-kidney-gonad (AKG) complex, including the mesonephros, dorsal metanephros or Müllerian and Wolffian ducts.

For a sex-determining gene to be directly downstream of temperature in an organism with TSD, its expression should be sexually dimorphic early in the temperature-sensitive period. In *T. scripta*, *Sox9* expression patterns are dimorphic early enough to be consistent with a sensitivity to temperature, and in the simplest case, *Sox9* may directly upregulate *Mis* as it does in mammals. Alternatively, an undetermined upstream factor may sense and respond to a male-producing temperature and upregulate both *Sox9* and *Mis*. Following their initial upregulation in this model, *Sox9* expression in preSertoli cells may then direct their differentiation and organize and maintain expression of *Mis*. Furthermore, our findings of the spatial and temporal patterns of *Dmrt1* expression are also consistent with the possibility that *Dmrt1* could be a target of temperature, although this was not directly tested in the current study. To gain insight into these possibilities, and shed light on the hierarchy of genes in the regulatory network underlying TSD, we are currently investigating the response of these genes to sex-reversing shifts in temperature and elimination of transcript in the gonad in an *in vitro* organ culture system.

Tissue-specific quantitative real-time PCR

Quantitative real-time PCR was performed on pooled adrenal-kidney-gonad (AKG) complexes as well as pooled gonads. Comparing relative expression levels between the two RNA sources

reveals the problems associated with retaining extraneous tissues when examining sex-determining genes by this method. *Sox9* transcript levels in the two tissues reveal wholly different relative patterns of expression. In the gonad (Fig. 2Q), *Sox9* levels are comparable at MPT and FPT during the sex-determining period (stage 17), after which expression is consistently higher at MPT. In contrast, *Sox9* expression in the AKG as a whole (Fig. 2R) causes transcript abundance at FPT to rise above MPT at stages 17 and 19. During differentiation (stages 21 and 23), levels of expression in AKGs at MPT exceed FPT, but are much less dimorphic than in the isolated gonad. In contrast, expression of both *Mis* and *Dmrt1* show a similar temporal pattern in both the gonad (Fig. 3Q, 4Q) and the AKG (Fig. 3R, 4R): values at MPT are higher than at FPT and consistently increase through development. However, transcripts are found in much greater relative abundance in the gonad as compared to mesonephric and metanephric tissues. In the future, interpretation of data produced by qPCR will be more accurate when only the tissue of developmental interest is utilized (Pieau & Dorizzi 2004, Ramsey & Crews 2007).

Exploring functional roles of genes in a non-model system

Curiously, we find *Sox9* expression at female-producing temperatures both during and after the temperature-sensitive period, and no role for *Sox9* in females has yet been described. Expression is expected early in the temperature-sensitive period, when the gonad is still bipotential and temperature has yet to be translated into a molecular signal. If *Sox9* does not play a role in ovarian development, downregulation of expression would be expected soon after. While the current study investigated only transcript abundance, examining the subcellular localization of the SOX9 protein might explain its continued gene expression. As is the case in both mouse and human, SOX9 may be localized to the nucleus of preSertoli cells in the testis, exerting transcriptional control over downstream genes, while in ovarian cells remaining cytoplasmic and thus inactive as a transcription factor (de Santa Barbara et al. 2000, Lasala et al. 2004). Future work should investigate whether a similar nuclear-cytoplasmic shuttling system is important in temperature-dependent sex determination.

Similarly, *Mis* is expressed in gonads developing at both MPT and FPT, and it is possible that *Mis* hormone receptor expression is dimorphic and controls a critical window of sensitivity to the hormone itself. *Mis* is secreted from Sertoli cells in developing mammalian testes and in an autocrine/paracrine manner binds to its highly specific receptor, *Mis-R2*, found in the membranes of both Sertoli and Leydig cells (see Josso et al. 2001). The action of MIS to induce regression of the Müllerian duct is directed by a spatial dimorphism not of the hormone itself, but of *Mis-R2*, which is expressed in a cranial to caudal wave along the duct (Allard et al. 2000). Consequently, future work includes cloning the *Mis-R2* gene homolog in *T. scripta* and examining its expression to determine if a similar mechanism could be involved. Thus, although the patterns of transcript expression of both *Sox9* and *Mis* appear more similar to mammals exhibiting genetic sex determination, the active gene products in *T. scripta* may in fact be evolutionarily conserved with other TSD species, a possibility we look forward to exploring.

Figure 2. Developmental expression of *Sox9* in embryonic gonads of the red-eared slider turtle measured by *in situ* hybridization and qPCR.
Whole mount ISH was used to examine *Sox9* expression patterns in turtle gonads dissected from embryos at indicated stages (n>8). Ventral view of representative adrenal-kidney-gonad complexes are shown (A-H, scale bar = 300um); see cartoon for morphology (T). Tissues are then sectioned to 20um thickness, producing transverse sections (I-P, scale bar = 20um). Metanephric staining at FPT is visible through the mesonephros (F), further illustrated by a dorsal view of a stage 21 AKG (S). qPCR measured as relative transcript abundance normalized to the constitutively expressed gene *PP1* shows a dramatically different pattern in the gonad (Q) versus the AKG (R), reflecting inclusion of strong metanephric expression. Dashed lines indicate external edge of gonad, g=gonad, m=mesonephros, met=metanephros, MPT=male-producing temperature, FPT=female-producing temperature, AKG=adrenal-kidney-gonad complex.

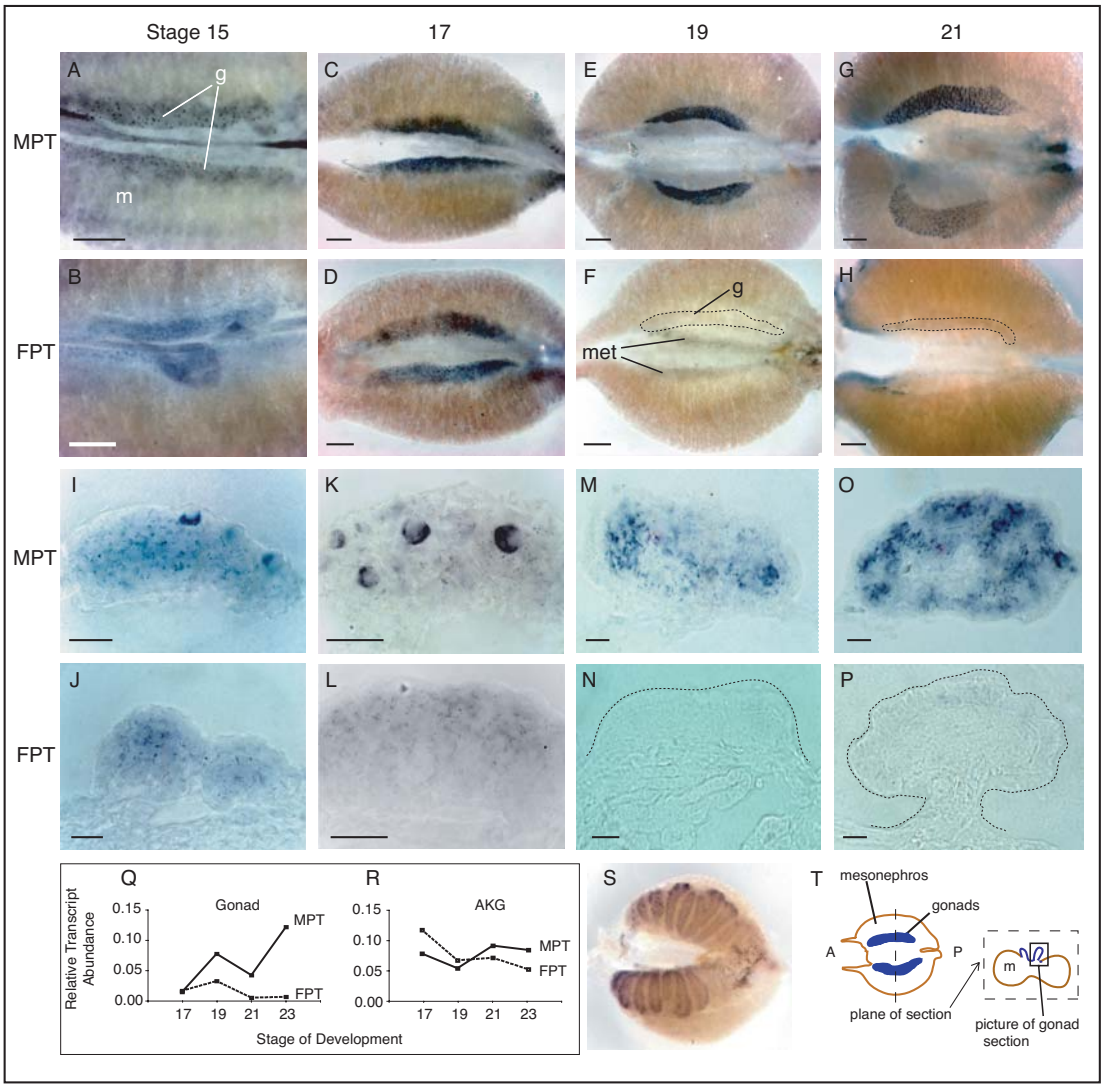

Figure 3. Developmental expression of *Mis* in embryonic gonads of the red-eared slider turtle measured by *in situ* hybridization and qPCR.
Whole mount ISH was used to examine *Mis* expression patterns in turtle gonads dissected from embryos at indicated stages (n>8). Ventral view of representative adrenal-kidney-gonad complexes are shown (A-H, scale bar = 300um). Tissues are then sectioned to 20um thickness, producing transverse sections (I-P, scale bar = 20um). A dorsal view of an MPT stage 19 AKG complex shows strong expression in metanephric tissue as well as in the anterior portion of the Müllerian ducts (S). qPCR is measured as relative transcript abundance normalized to the constitutively expressed gene *PP1*. Although metanephric expression is significant, relative levels of *Mis* expression measured from gonad tissues (Qa) are over 20-fold higher than in the AKG (R). A magnification of the scale of gonad expression reveals the decrease in FPT gonads through development (Qb). Dashed line represents external edge of gonad, g=gonad, m=mesonephros, mull=Müllerian duct, met=metanephros, MPT=male-producing temperature, FPT=female-producing temperature, AKG=adrenal-kidney-gonad complex.

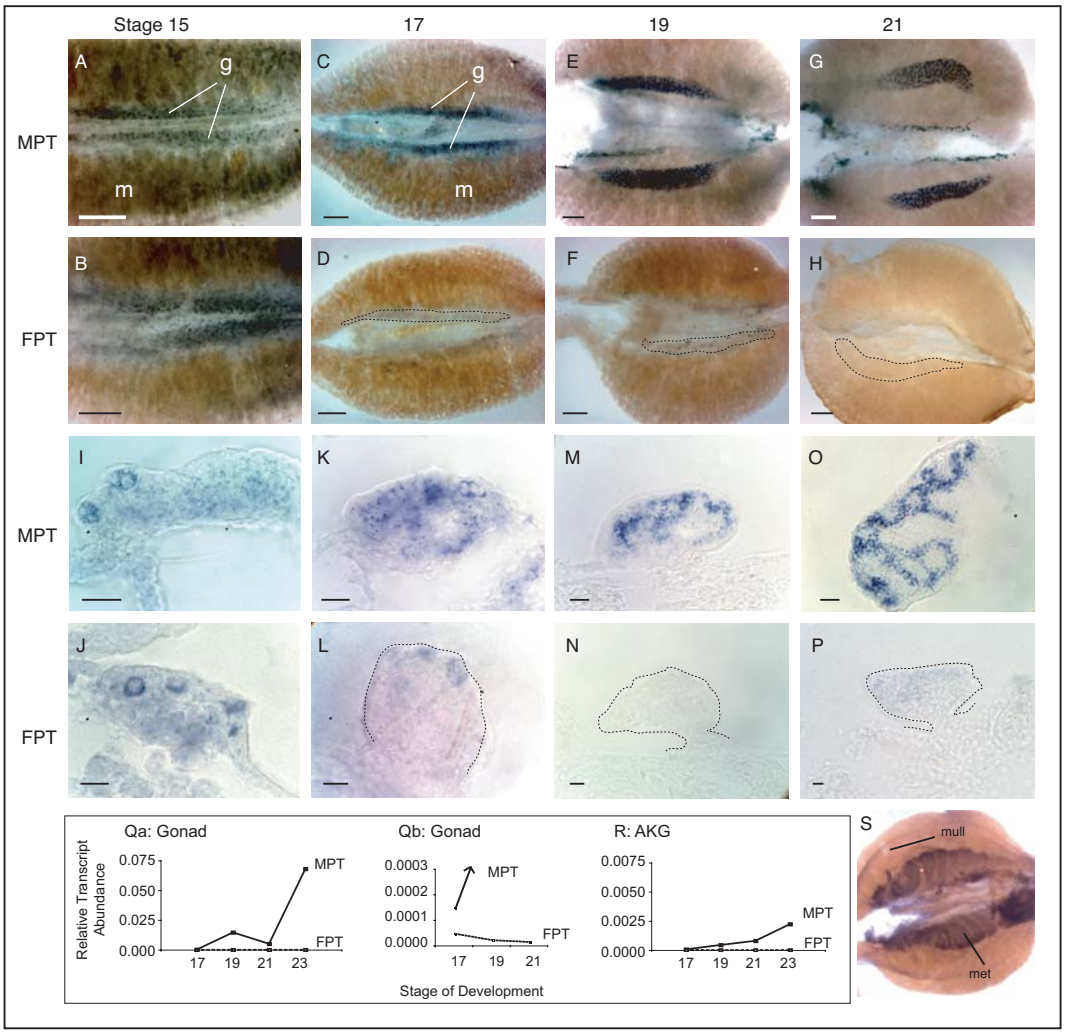

Figure 4. Developmental expression of *Dmrt1* in embryonic gonads of the red-eared slider turtle measured by *in situ* hybridization and qPCR.
Whole mount ISH was used to examine *Dmrt1* expression patterns in turtle gonads dissected from embryos at indicated stages (n>8). Ventral view of representative adrenal-kidney-gonad complexes are shown (A-H, scale bar = 300um). Tissues are then sectioned to 20um thickness, producing transverse sections (I-P, scale bar = 20um). qPCR is measured as relative transcript abundance normalized to the constitutively expressed gene *PP1* (Q, R). Dashed line represents external edge of gonad, g=gonad, m=mesonephros, MPT=male-producing temperature, FPT=female-producing temperature, AKG=adrenal-kidney-gonad complex.

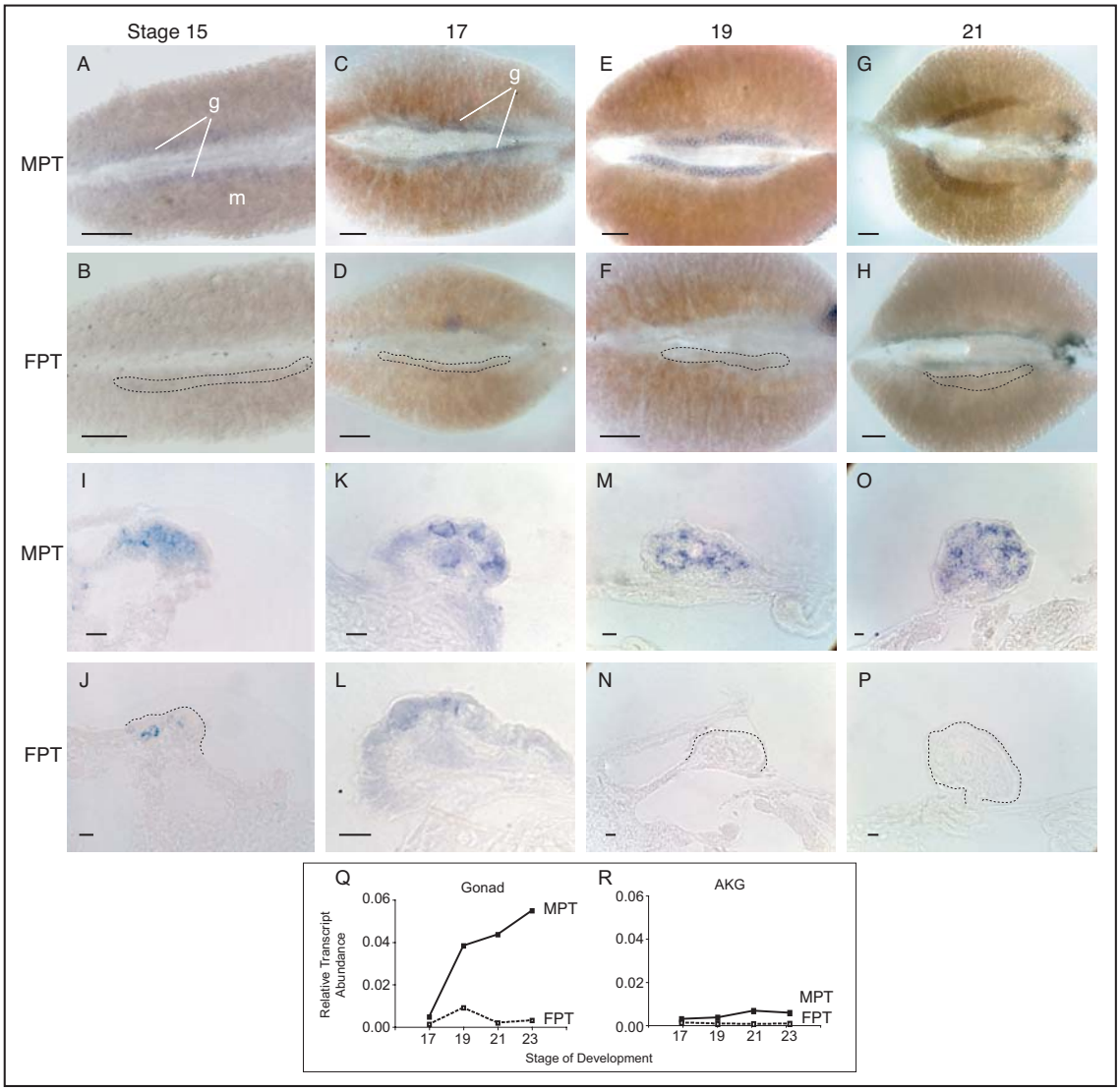

CHAPTER THREE

Response of candidate sex-determining genes to changes in temperature reveals their involvement in the molecular network underlying temperature-dependent sex determination*

Genes involved in GSD vertebrate gonadogenesis include *FoxL2, Wnt4*, *Dax1*, *Rspo1, Dmrt1* and *Mis*. While the expression of some of these factors has been examined in organisms with TSD (Spotila et al. 1998, Smith et al. 1999b, Moreno-Mendoza et al. 1999, Western et al. 1999a, 1999b, 2000, Torres-Maldonado et al. 2001, 2002, Loffler et al. 2003, Takada et al. 2004, Shoemaker et al. 2007a), their ability to respond to changes in temperature has not been investigated. Although experiments at constant incubation temperatures can correlate temporal and spatial patterns of gene expression to sexual fate, sex-reversing temperature-shift experiments represent an important functional manipulation in an organism lacking typical genetic techniques. Rapid change in gonadal expression of these genes following a temperature-shift confirms a role in the formation of the gonad, while the timing of this response provides an indication of its hierarchical placement within the molecular cascade governing organ development. In this study, we examine the ability of temperature to regulate the expression of *FoxL2*, *Wnt4*, *Dax1*, *Rspo1*, *Dmrt1*, *Mis* and *Rspo1*. The regulation of *Sox9* by temperature was demonstrated previously, and here we extend those results (Moreno-Mendoza et al. 2001).

To identify possible roles in an organism with TSD, we report cloning *Wnt4, Dax1* and *Rspo1* in the red-eared slider turtle. We analyze the expression patterns of these three genes as well as *FoxL2* throughout six stages of gonadogenesis encompassing the temperature-sensitive sex-determining period. To examine the early factors directing a bipotential gonad down an ovary or a testis developmental trajectory, we extend our previous findings on the expression patterns of three testis-specific factors, *Dmrt1*, *Mis*, and *Sox9* to earlier time points within the TSP. To investigate placement of these factors in a temporal hierarchy regulating the development of the

* Portions of this chapter appear in Shoemaker, Queen & Crews, 2007b, and in Smith, Shoemaker, Roeszler, Queen, Crews and Sinclair, 2008.

turtle gonad, we analyze their ability to rapidly respond to a shift in temperature during the sex-determining period. For the first time we report a response of *FoxL2, Wnt4, Rspo1, Dmrt1* and *Mis* to a change in temperature, confirming their role in the molecular pathway underlying temperature-dependent sex determination. As well, we provide evidence that *Dax1* is involved in gonadogenesis in both sexes, and we extend previous findings on the expression of *Sox9* in a species with TSD.

METHODS

Collection and harvesting embryos

Freshly laid red-eared slider eggs purchased from Clark Turtle Farms (Hammond, LA) were maintained as previously described (Wibbels et al. 1991), in accordance with humane animal practices under IACUC protocol #03102301. Briefly, viable eggs were randomized in trays of moistened vermiculite and placed in incubators (Precision, Chicago, IL) at 26.0°C or 31.0°C. Incubator temperatures were monitored daily with HOBO data loggers (Onset Computer Corp., Bourne, MA) and verified with calibrated thermometers. For temperature shift experiments, multiple trays of 30 eggs/tray were shifted at developmental stage 16 from incubators held at 26.0°C to 31.0°C and vice versa.

Staging

Progression of development was monitored by staging external morphological characteristics of a sampling of individuals according to Greenbaum's staging series (12). Morphological characteristics of a stage 16 slider turtle includes the initial formation of a beak, a white line that extends ventrally from the pupil of the eye, and a large digital plate with a smooth periphery with slight indications of digital ridges (Fig. 5A). By stage 17, a white caruncle, or egg tooth, has formed on the upper jaw, the white line of the eye is absent or interrupted as pigmented cells reorganize, and the periphery of the digital plate is serrated with well-developed digital ridges (Fig. 5C). We defined stage 16.5 for the purposes of this study as midway between stages 16 and 17, characterized by a caruncle that is just visible and slightly below the epidermis of the beak, a narrowing white eye line, and slight serrations around the periphery of the digital plate (Fig. 5B).

For morphological characteristics representative of other stages, see Greenbaum (Greenbaum 2002).

Cloning of turtle gene homologs

Total RNA was extracted from pooled adrenal-kidney-gonad (AKG) complexes from a variety of sexes and stages and reverse-transcribed using oligo(dT) primers with Superscript II reverse transcriptase (Invitrogen, Carlsbad, CA). Primers for *Dax1* and *FoxL2* were designed based on published mouse, human, alligator and chicken sequences where available and were: *Dax1*: 5'-AGT GCT GGA GCC TGG ACA TCG-3' and 5'-CAT CTC CAG CAG CAT GTC ATC C-3'; *FoxL2*: 5'-TCC GGC ATC TAC CAG TA-3', 5'-TTG CCG GGC TGG AAG TG-3'. *Wnt4* primers amplifying a 390 base pair fragment based on mammalian sequences were a gift from Pascal Bernard and were: 5'-GTA CCT GGC CAA GCT GTC-3' and 5'-AGC ATC CTG ACC ACT GGA AGC-3'. Amplified fragments were ligated into pCR4-TOPO vector according to manufacturer's protocol (Invitrogen, Carlsbad, CA) and sequenced using M13F and M13R primers. The sequence of the 261 base pair *FoxL2* clone was subsequently found to correspond to base pairs 73 to 330 of a previously published *T. scripta FoxL2* sequence (7, accession no. AY155535). Sequences for *Dax1* and *Wnt4* were submitted to GenBank (accession numbers EF591056 and EF591055, respectively).

In situ hybridization

Adrenal-kidney-gonad complexes were dissected from embryos, immediately frozen in OCT embedding medium and stored at -80°C. They were subsequently serially sectioned in 4 series on a 2800 Reichert-Jung cryostat at 20 microns and thaw-mounted onto SuperFrost Plus slides (Erie Sci. Co., Portsmouth, NH). Sections were fixed in cold 4% paraformaldehyde, washed in PBS and incubated in 0.25% acetic anhydride/triethanolamine. Following washes in 2X standard saline citrate (SSC), slides were dehydrated in an increasing ethanol series, air-dried, and stored at -80°C. Riboprobes were reverse-transcribed in the presence or absence of Digoxygenin-labeled UTP (Roche) using a T3/T7 Megascript *in vitro* transcription kit (Ambion, Austin, TX) to produce antisense or sense DIG-labeled or unlabeled riboprobes. Slides were warmed to room temperature, air-dried, and pre-equilibrated in hybridization buffer (50% formamide, 5X SSC,

5X Denhardt's solution, 125 ug/mL Baker's yeast tRNA, 250 ug/mL denatured herring sperm DNA) for two hours at either 50° (*Wnt4*, *FoxL2*) or 45° (*Dax1*). Sections were incubated in riboprobe overnight at the same temperatures, respectively. Experimental slides were exposed to antisense DIG-labeled probe, while control slides were incubated in either sense DIG-labeled probe or a competitive series of antisense DIG-labeled/unlabeled probes. Following RNase A treatment at 37°C, sections were washed in a decreasing series of SSC and equilibrated in 150mM NaCl/100mM Tris pH 7.5 at room temperature before incubation in 1:5000 anti-DIG-AP Fab fragments (Roche) in 0.5% Tween 20/PBS for two hours at room temperature. Sections were washed in 100mM Tris pH 7.5 and incubated in 5mM levamisole (in 100 mM Tris pH 9.5, 100 mM NaCl, 50 mM MgCl2 buffer). Chromogenic product was formed using NBT/BCIP in 100mM Tris pH 8.0 (Roche) at 30°C until desired darkness was achieved, and was terminated simultaneously for all slides within a gene. Sections were dehydrated, delipidated and coverslipped under Permount (Fisher). Sets of gonads from five embryos per sex/stage were analyzed.

Quantitative real-time PCR

Embryos were removed from the egg, staged, and sacrificed by rapid decapitation. Adrenal-kidney-gonad complexes were immediately dissected and floated in sterile PBS. Pairs of gonads were cut away from underlying mesonephric tissues using fine scissors and a dissecting microscope from 12 to 20 embryos per independent sample (n=3 at each sex/stage), pooled, immediately placed in RNA denaturing solution (Promega), vortexed to dissociate, and stored at -80°C. A maximum of five minutes elapsed from decapitation to placement in denaturing solution. Total RNA was extracted using the RNAgents Total RNA Isolation kit (Promega) and treated with DNA-Free DNase I (Ambion, Austin, TX). cDNA was reverse-transcribed using the SuperScript First-Strand Synthesis for RT-PCR system (Invitrogen, Carlsbad, CA) with both oligo-(dT) and random hexamer primers. Relative gene expression levels were quantified using SYBR Green I dye (Invitrogen, Carlsbad, CA) and an ABI PRISM 7900HT real-time PCR cycler (ABI SDS 2.2.1 software). Samples were each run in triplicate and the median value was used for analysis. PCR efficiencies were calculated from gene-specific standard curves. Relative transcript abundance was normalized to expression of *protein phosphatase 1* (*PP1*), a

constitutively expressed transcript across both stage and sex selected previously (9). A modified deltaCT method that allows for correction of differential gene PCR efficiencies was utilized, where mean normalized expression (MNE) is: MNE = mean $((E_{ref} \wedge Ct_{ref}) / (E_{target} \wedge Ct_{target}))$ where E = gene-specific PCR efficiency, Ct = cycle threshold from each independent sample, target = gene of interest, and ref = constitutively expressed reference gene (Pfaffl 2001, Muller et al. 2002, Simon 2003). To examine expression fold changes within a gene, MNE values were calibrated to the lower value at stage 23 (either MPT or FPT). Primers used to assay gene expression were designed across exon boundaries for *Wnt4* and *Dax1* using MacVector (MacVector, Inc., Cary, NC); this was not possible for *FoxL2*, which contains a single exon. Primer specificity was verified by agarose gel electrophoresis, and for *PP1*, *Dmrt1*, *Mis*, and *Sox9* were as previously described (Shoemaker et al. 2007a). qPCR primers for *FoxL2*, *Wnt4*, and *Dax1* were as follows: *FoxL2: forward* 5'-TGG CAG AAC AGC ATC CGC-3', *reverse* 5'-GGG TCC AGC GTC CAG TAG TTG-3'; *Wnt4*: *forward* 5'-CCG TAA CCG TCG CTG GAA C-3', *reverse* 5'-GGA GGA GAT GGC ATA CAC AAA AGC-3'; *Dax1: forward* 5'-GGA CTG TGC TCT TCA ACC CG-3', *reverse* 5'-GCT TGC TGT GCT TCC CTC TG-3'.

Statistical Analysis

For each gene, expression values measured by qPCR relative to the housekeeping gene (*PP1*) were plotted to test normality. *Wnt4* and *Dax1* data were found to have normal distributions, while *FoxL2*, *Dmrt1*, *Mis* and *Sox9* values were log-transformed to meet the normality assumption. A two-factor ANOVA (mixed data) on all MNE values within a gene tested for sex, stage and sex by stage interaction effects (SAS software program, SAS Institute, Inc., Cary, NC). Post-hoc pairwise comparison tests of all possible comparisons within a gene were analyzed (every combination of two MNE's), correcting for multiple tests using Tukey's HSD.

RESULTS

To investigate the role of genes possibly involved in sex determination and differentiation in an organism with TSD, we cloned *Wnt4*, *Dax1* and *Rspo1* in the red-eared slider turtle. We examine

the spatial expression patterns of *Wnt4, Dax1* and *FoxL2* at six stages of gonadogenesis by *in situ* hybridization on adjacent gonad sections from five embryos. We analyze expression levels of these three genes, as well as *Rspo1, Dmrt1, Mis* and *Sox9,* at the same six stages of development as well as in response to sex-reversing temperature shifts, by quantitative reverse-transcriptase real-time PCR (qPCR) in three independent samples. All genes were found to have highly significant temperature by stage interaction effects (two-factor ANOVA, $p<0.009$ for all genes, see Table 2). Post-hoc comparisons made between temperatures within each stage are described in this study for all genes except *Dax1,* which does not show a significant effect of temperature and is therefore examined within temperature between stages (see Tables 3 and 4).

Examining a new stage of development

The temperature-sensitive period in *T. scripta* lasts from approximately stage 14 through stage 20, and shifting embryos between constant temperatures (26°C and 31°C) during this time causes complete sex-reversal (Wibbels et al. 1991). We utilized this lability to assess the involvement of various candidate genes in TSD gonadogenesis. After development progressed along one trajectory (MPT or FPT) for several stages during the sex-determining period, eggs were shifted at stage 16 to the opposite temperature. We assessed the ability of six candidate sex-determining genes to rapidly respond to this change in temperature at two subsequent time points. Turtle embryonic development is prolonged, and the period from stage 16 to stage 17 can last up to two days at FPT (31°C) or four days at MPT (26°C). Therefore, to examine the effects of the temperature shift on a finer temporal scale, we define a stage halfway between stage 16 and stage 17, termed stage 16.5. We distinguish this stage as having morphological characteristics midway between those associated with stages 16 and 17, as described in Fig. 5.

FoxL2 expression becomes ovarian-specific at the end of the temperature-sensitive period

In situ hybridization on sectioned adrenal-kidney-gonad (AKG) complexes reveals early *FoxL2* expression throughout the bipotential gonad developing at either temperature (stage 17, Fig. 6A, B). At the end of the TSP, the spatial expression pattern of *FoxL2* in the developing ovary is localized primarily to the cortical region, although faint expression is seen in primitive sex cords that later degenerate (stage 19, Fig. 6C). Cortical expression in the ovary continues through

differentiation (stage 23, Fig. 6E). Expression is also seen faintly at MPT at the close of the TSP and through differentiation in putative testicular seminiferous tubules (stages 19, 23, Fig. 6D, F). At all stages examined, *FoxL2* expression was detected in both sexes in the dorsal metanephric tubules of the future kidney, although more strongly at FPT (Fig. 6G, H). Furthermore, expression of *FoxL2* occurs in epithelial cells lining the interior of the developing Müllerian duct of embryos at stages 19 and 23 (Fig. 6I, data not shown).

Expression levels of *FoxL2* measured by qPCR are similar between gonads developing at FPT and MPT early in the temperature-sensitive period (stages 16, 16.5, 17, Fig. 7A). However, at the end of the TSP and through ovarian differentiation, FPT expression levels rise significantly above levels at MPT (stages 19, 21, 23, $p<0.0015$, Fig. 7A). Temperature-shifting embryos at stage 16 causes gonadal expression of *FoxL2* to rise, regardless of the direction of the shift (MPT→FPT or FPT→MPT, Fig. 7A'). However, this rise was only significant in one comparison: *FoxL2* expression in stage 16.5 MPT→FPT shifted gonads is significantly higher than expression in unshifted stage 16.5 MPT gonads ($p<0.009$, Fig. 7A').

Wnt4 is widely expressed throughout the gonad, mesonephros and metanephros

A partial homolog of *Wnt4* was cloned from turtle cDNA resulting in a 390 base pair fragment. BLAST analysis indicated 85% nucleotide sequence homology to *Wnt4* in *Homo sapiens*, *Gallus gallus*, and *Mus musculus*. The putative translation deduced by MacVector software (MacVector, Inc.) is 129 amino acids long, corresponds to the coding region of exons 3, 4 and the beginning of exon 5 of the mammalian protein (see Figs. 10 and 11), and is 97% homologous to *Homo sapiens*, 97% to *Mus musculus*, and 95% to *Gallus gallus* Wnt4 amino acid sequence.

In situ hybridization detected *Wnt4* mRNA throughout the bipotential gonad during the TSP (stages 17, 19, Fig. 6K, L, M, N). This expression becomes primarily localized to the cortical region of the ovary and the seminiferous tubules of the testis during gonad differentiation, and is also retained between sex cords in the testis (stage 23, Fig. 6O, P). At all stages examined, strong *Wnt4* expression in both sexes is observed in the mesonephros and dorsal metanephric tissues destined to become the adult kidney (Fig. 6Q, R). Expression in the developing Müllerian ducts

is found at stages 19, 21 and 23 in both sexes; in FPT embryos, *Wnt4* expression increases as the duct grows, while at MPT, expression decreases with duct regression (Fig. 6S, T).

Throughout the temperature-sensitive period, *Wnt4* is expressed at comparable levels as measured by qPCR between gonads developing at FPT and MPT (stages 16 through 19, Fig. 7B). However, during ovarian differentiation, expression at FPT significantly rises above MPT by up to 4-fold (stage 21: $p=0.015$, stage 23: $p<0.0001$, Fig. 7B). In response to a FPT→MPT temperature shift, expression levels one stage later (stage 17) are increased from unshifted stage 17 FPT levels, although not significantly ($p=0.0508$, Fig. 7B'). In gonads from the converse shift (MPT→FPT), *Wnt4* expression is not significantly different from unshifted levels at either time point.

Dax1 is expressed throughout the gonad, Müllerian and Wolffian ducts

To examine its expression in the slider turtle, we cloned a 297 base pair fragment of *Dax1*. BLAST analysis identified 96% nucleotide sequence homology to *Dax1* in *Lepidochelys olivacae*, 92% to *Alligator mississippiensis*, 87% to *Gallus gallus*, and 78% homology to *Homo sapiens*. The translated 98 amino acid sequence (MacVector, Inc.) corresponds to the C-terminal ligand-binding domain of the consensus vertebrate protein (see Figs. 12 and 13) and is 95% homologous to *Lepidochelys olivacea*, 93% to *Alligator mississippiensis*, 92% to *Gallus gallus* and 76% to *Homo sapiens* Dax1.

In situ hybridization during the temperature-sensitive period reveals a diffuse pattern of *Dax1* expression in gonads developing at FPT and MPT (stage 17, Fig. 6U, V). At the end of the TSP, spatial expression patterns begin to organize (stage 19, Fig. 6W, X), and during gonad differentiation, expression is concentrated in the cortex of ovaries and in a striped pattern indicative of sex cords in testes (stage 23, Fig. 6Y, Z). At all stages examined, *Dax1* is expressed in dorsal metanephric tissue in both sexes, typified by the staining seen at stage 23 (Fig. 6AA, BB). In both developing Müllerian and underlying Wolffian ducts, *Dax1* expression occurs in the epithelial cells lining the interior of the ducts (Fig. 6CC, DD). Expression in Müllerian ducts is apparent at stages 19 (data not shown) and 23, while Wolffian duct expression is detected at

stage 23. Some sections showed punctate *Dax1* expression in a mesonephric region from which adrenal tissue is expected to develop (data not shown).

Throughout gonadogenesis, *Dax1* expression levels measured by qPCR were not significantly different between gonads developing at MPT and FPT (Fig. 7C). However, within FPT, a significant change in expression between stages is observed. In the developing ovary, *Dax1* levels are significantly greater at stages 16, 16.5 and 17 than at stages 21 and 23 ($p<0.009$ for all comparisons). In response to a shift in temperature, expression levels by stage 17 have changed in sex-typical directions, although not significantly (Fig. 7C'). Thus, following a MPT→FPT shift, *Dax1* expression levels are FPT-typical by stage 17, while after a FPT→MPT shift, are MPT-typical.

Rspo1 expression implicates its involvement in ovarian development

As examined by qPCR, *Rspo1* expression at FPT became elevated early in the TSP. In contrast, *Rspo1* levels remained low at MPT throughout gonadogenesis (Fig. 9). Expression became statistically higher in bipotential gonads developing at FPT at stage 17 ($p=0.0318$, Fig. 9A) and remained high through gonadal differentiation (stages 19, 21 and 23, $p<0.0001$, Fig. 9A). Furthermore, *Rspo1* expression levels changed in response to shifting embryos between temperatures at developmental stage 16. Following a FPT→MPT shift, expression levels were downregulated by one stage later, and were not significantly different than MPT-typical levels (stage 17, $p=0.0253$, Fig. 9B). In the converse MPT→FPT shift, *Rspo1* levels remained low and had not yet increased by one stage later (Fig. 9B).

Testis-specific genes show a rapid response to temperature shifts

Previously, we examined the spatial and temporal expression patterns of *Dmrt1*, *Mis*, and *Sox9* throughout gonadogenesis in the slider turtle (Shoemaker et al. 2007a). Here, we report an extension of those results in three independent qPCR samples, reveal dimorphic expression levels earlier in the temperature-sensitive period than we previously described, and demonstrate that *Dmrt1* and *Mis* expression is regulated by temperature.

Beginning early in the temperature-sensitive period, expression of both *Dmrt1* and *Mis* is significantly higher at MPT as compared to FPT (*Dmrt1:* stage 16.5, $p<0.027$, Fig. 8A; *Mis:* stage 16, $p<0.007$, Fig. 8B). This pattern becomes substantially more dimorphic through testicular differentiation (stages 17, 19, 21, 23, $p<0.0001$ for both genes). In response to a FPT→MPT temperature shift, *Dmrt1* expression between stages 16.5 and 17 rises significantly above unshifted gonads remaining at FPT ($p=0.0003$), and is not different from MPT expression levels (Fig. 8A'). Conversely, one stage following a MPT→FPT shift, expression levels have begun to drop but are not yet significantly lower than unshifted MPT levels. Thus, one stage after a temperature shift to MPT, *Dmrt1* expression has been significantly upregulated, but one stage after a shift to FPT, expression has not yet been significantly downregulated (Fig. 8A').

In contrast, *Mis* expression one stage after a MPT→FPT shift is significantly decreased from unshifted MPT levels ($p<0.01$), and is not significantly different from FPT levels (stage 17, Fig. 8B'). Following a FPT→MPT shift, expression has not significantly changed by stage 17 from unshifted FPT levels. Thus, expression of *Mis* has been significantly downregulated one stage after a shift to FPT, but has not yet been significantly upregulated after a shift to MPT (Fig. 8B').

While *Dmrt1* and *Mis* show significantly dimorphic expression levels early in the TSP, *Sox9* expression levels are similar between gonads at MPT and FPT (stages 16, 16.5 and 17, Fig. 8C). *Sox9* expression in the putative turtle testis becomes significantly higher than in the developing ovary at the end of the sex-determining period (stage 19, $p<0.0001$), and continues to be significantly higher through testicular differentiation (stages 21, 23, $p<0.0001$). Intriguingly, following a MPT→FPT shift, gonadal expression of *Sox9* increases significantly above unshifted MPT levels by one half stage later (stage 16.5), but are again indistinguishable from MPT by stage 17 (Fig. 8C'). Following a FPT→MPT shift, expression is not different from unshifted FPT levels at either subsequent time point.

DISCUSSION

The molecular pathway underlying the formation of a testis and an ovary from a bipotential gonad has long been studied in organisms with genotypic sex-determining mechanisms. While much of this pathway may be retained in organisms with other modes of sex determination, investigation of this has been slowed by a lack of functional manipulations in non-model organisms. Examining the response in the gonad of candidate sex-determining genes to changes in embryonic temperature allows a functional analysis of their involvement in the molecular pathway underlying gonadogenesis. Furthermore, the temporal order of expression changes triggered by sex-reversing temperature shifts may be used to infer the response to that environmental temperature regime under non-shift conditions. Thus, temperature-shift experiments provide insights into the relative hierarchical placement of gene action in this molecular cascade.

FoxL2 expression is consistent with a role in ovarian development

FoxL2 is one of the few ovarian-specific genes identified thus far, and a proposed function in mice is to repress male-specific sex-determining gene expression postnatally (Ottolenghi et al. 2005). Although its expression in mouse during embryonic gonadogenesis is solely in the developing ovary, a sex-determining role during this period has not been identified. Here we confirm and extend a previous report of its expression pattern in *T. scripta* (Loffler et al. 2003). *In situ* hybridization reveals localization of expression during differentiation in the cortex of the developing ovary, a pattern that is similar to other vertebrates. This pattern may reflect expression in the granulosa cell lineage, which is known to express *FoxL2* in mammals and localizes to the cortex, surrounding germ cells (Ottolenghi et al. 2005). Through quantitative real-time PCR, we are able to temporally define when expression at FPT significantly rises above MPT, which occurs at the close of the temperature-sensitive period. This pattern supports a role of *FoxL2* in ovarian development, and suggests it may be involved in differentiation. Because expression is similar between the sexes early in the TSP, future temperature-shift experiments should extend past this period. However, regulation of *FoxL2* by temperature is

observed, and taken together, our data provide evidence that *FoxL2* plays a role in the development of the ovary in an organism with TSD.

It should be noted that patterns of gene expression as analyzed by qPCR in this study reflect transcript abundance across the gonad as a whole, and cannot take into account cell type differences in contribution to the total transcript pool. Germ cells and the various somatic cells that make up the gonad may be, and in fact are likely to be, expressing these gene products at different levels. Thus, if a temperature-shift causes proliferation or loss of a particular cell type that is contributing to or causing an expression pattern, this subtlety may be lost in our analysis. Separating cell types of the gonad for quantitative analysis of gene expression would resolve this in future studies.

Although downstream target genes of *FoxL2* remain unknown, there is evidence for regulation of *aromatase* expression by *FoxL2* in chicken, trout, tilapia and polled goats (Baron et al. 2004, Hudson et al. 2005, Pannetier et al. 2006, Wang et al. 2007). *Aromatase* encodes the enzyme that converts androgens to estrogens. Hudson et al. showed that inhibition of aromatase in the developing chick gonad leads to reduced, but not abolished, *FoxL2* expression. This is suggested to occur by a positive feedback mechanism in which *FoxL2* upregulates *aromatase*, which then enhances *FoxL2* activation (Hudson et al. 2005). Furthermore, it was recently shown by Ramsey et al. that *T. scripta* gonadal *aromatase* expression is dimorphic between FPT and MPT embryos early in the temperature-sensitive period; expression at FPT is organized in circular clusters of expressing cells surrounding non-expressing cells, putatively pre-granulosa cells surrounding germ cells, while at MPT, expression remains unorganized (Ramsey et al. 2007). If a positive feedback loop exists between *FoxL2* and *aromatase* in an organism with TSD, exogenous aromatase inhibitor in turtle embryos should also cause decreased *FoxL2* expression.

Expression of Wnt4 is conserved across GSD and TSD vertebrates and is consistent with a role in both ovary and testis development, as well as duct and kidney formation

To our knowledge, examination of *Wnt4* in the slider turtle represents the first analysis of this signaling molecule in an organism with TSD. Here we find *Wnt4* is expressed in turtle gonads

developing at both MPT and FPT throughout the periods of sex determination and gonad differentiation, suggesting that it functions in both the developing testis and ovary. Expression at MPT begins to localize in a striped pattern indicative of developing sex cords as early as the end of the TSP, although expression in interstitial cells between cords is retained. Expression in the ovary becomes concentrated in the cortical region, and during differentiation, quantitative real-time PCR shows expression levels at FPT rise significantly above MPT. It is possible that this upregulation reflects a shift in Wnt4 function during gonad differentiation to a later female-specific role.

Mouse studies support a complex role for *Wnt4* in both male and female development, and the regulation of *Wnt4* signaling in a bipotential gonad presents an interesting problem. It was recently suggested that antagonistic action between *Wnt4* and *Fgf9* signaling pathways regulate the switch between ovarian and testicular development in the mammalian bipotential gonad (Kim & Capel 2006). However, *Wnt4* may have several sex-specific roles throughout gonadogenesis. For example, *Wnt4 -/-* XY mice retain normal *Sry* expression but have decreased levels of Sox9 and Dhh, disrupted Sertoli cell differentiation, and a substantial overpopulation of steroidogenic cells migrating into the gonad from the mesonephros (Jeays-Ward et al. 2004). Thus, an important role for Wnt4 in the developing mammalian testis includes regulating the migration of these cells, while wholly preventing this migration into developing ovaries. The expression of *Wnt4* in the turtle in the mesonephros of both sexes as well as in developing sex cords and interstitial cells of the testis may reflect a similar role. Mesonephric expression of *Wnt4* is also important in the development of other vertebrate organs, and is required for the cellular mesenchymal-to-epithelial transition that occurs during mammalian kidney tubule formation (Carroll et al. 2005). Strong turtle *Wnt4* expression in developing mesonephric and metanephric tissues destined to become the kidney is consistent with a similar function in an organism with TSD.

A testis-specific medullary coelomic blood vessel forms during mammalian gonadogenesis. It was shown that *Wnt4 -/-* XX mice ectopically develop this blood vessel, while overexpression of *Wnt4* in XY mice results in a disorganized coelomic blood vessel (Jeays-Ward et al. 2003,

Martineau et al. 1997, Brennan et al. 2002). If a similar coelomic blood vessel forms in MPT organisms with TSD, a possible role for *Wnt4* expression seen in the medullary region of the developing turtle ovary may be repressing its formation at FPT.

Finally, the role of *Wnt4* in the formation of the Müllerian ducts, anlagen which initially form in both sexes and then develop into the cervix, uterus and oviducts in females, has been examined extensively in the mouse. It is suggested that *Wnt9b* upregulates *Wnt4*, which leads to initial Müllerian duct formation in both sexes as well as inhibition of *Wnt7a* and *Pax8* (Vainio et al. 1999, Carroll et al. 2005, Parr & McMahon 1998). In males, *Mis* then causes the degradation of these ducts. Lack of either Wnt9b or Wnt4 prevents the initial formation of Müllerian ducts, while a lack of Wnt7a results in persistent ducts and prevents downstream organs from forming (Carroll et al. 2005, Parr & McMahon 1998). In the turtle, the Müllerian duct develops in both sexes in a rostral to caudal wave, and appears along the anterior/posterior axis near the gonad at the end of the TSP (stage 18/19, Wibbels et al. 1999). Mullerian duct primordia develop in both sexes for two stages and then differentiate at FPT and degrade at MPT (Wibbels et al. 1999). Our data show that before Müllerian ducts form, *Wnt4* is expressed in the mesonephric tissue from which they will derive. Furthermore, *Wnt4* expression is detected within primordial Müllerian ducts from the first stage they appear. This early expression pattern is consistent with a role for *Wnt4* signaling in the embryonic development of these ducts.

Dax1 expression is consistent with a role in gonad and adrenal development

The complexity of the role of Dax1 in vertebrate development has thus far prevented a clear understanding of its function. Expression is detected early in the development of the vertebrate gonad, and in mammals, this expression becomes female-specific through time, while in chick, expression continues in both the testis and ovary (Smith et al. 1999a, Swain et al. 1996). To examine its role in an organism with TSD, we cloned a partial *Dax1* sequence in the slider turtle and find a similar expression pattern to chick. *Dax1* is gonadally expressed throughout sex determination and differentiation at levels that are not significantly different between MPT and FPT gonads, although expression at FPT does decrease significantly through time. Furthermore, *Dax1* mRNA first appears dispersed throughout the bipotential gonad and then becomes

progressively restricted to the ovarian cortex and testicular sex cords. *Dax1* is also involved in the formation of the human adrenal cortex (Niakan & McCabe 2005, Hanley et al. 2000). Here we find *Dax1* expression in the turtle in a region of the mesonephros from which adrenal gland develops, indicating conservation of expression pattern. Interestingly, *Dax1* is the only gene examined in this study by *in situ* hybridization expressed in the developing Wolffian ducts, structures which eventually degrade in females and become functional tubules in males.

To explain its complex role in both developing mammalian testes and ovaries, a dosage-dependent mechanism has been proposed in which one copy of X-linked *Dax1* plays a role in activating male development while two copies can inhibit *Sry* action (Meeks et al. 2003a, 2003b, Bouma et al. 2005). Because organisms with TSD are thought not to have functional sex chromosomes, dosage-dependent regulation in these systems could be conserved if regulated by a different mechanism. There are presumably two *Dax1* gene copies in every diploid turtle embryo, and thus functional *Dax1* differences must be regulated at transcriptional or translational levels. Furthermore, if the role of Dax1 is dose-dependent, this regulation must at some point be correlated with incubation temperature. In this study we find that expression levels between MPT and FPT are not significantly different, and consequently, any dimorphic Dax1 function must be post-transcriptionally regulated in the turtle. During preparation of this manuscript, a model of dosage-dependent sex determination in organisms exhibiting TSD was proposed in which effects of a Z-linked male determinant depend on both temperature and copy number, and our data are not inconsistent with this mechanism (Quinn et al. 2007).

A regulatory relationship between *Wnt4* and *Dax1* has been previously postulated, in which Wnt4 signaling leads to activation of *Dax1* in a sex-specific manner (Mizusaki et al. 2003). *Wnt4-/-* XX mice show decreased *Dax1* expression at 11.5 days post-coitum (dpc), while no change in expression level is observed in 11.5 dpc *Wnt4 -/-* XY mice (Mizusaki et al. 2003). The general colocalization of expression of these factors in the developing turtle gonad is consistent with regulation of *Dax1* by *Wnt4* in an organism with TSD, and further experiments are required to explore this possibility.

Rspo1 expression is consistent with a conserved, upstream role in ovarian sex determination

We provide here the first evidence that *Rspo1* expression is sexually dimorphic during the temperature-sensitive period in an organism with TSD. Expression was significantly higher in gonads incubated at FPT than at MPT. Furthermore, sexually dimorphic expression of *Rspo1* expression occurred during the TSP, when bipotential gonads are sensitive to the action of temperature. The upstream temperature-sensing molecule in reptiles with TSD remains unknown, but genes upregulated during the critical TSP are likely to be key candidates for early mediators of gonadal development. *Rspo1* mRNA was more highly expressed in gonads incubated at FPT from stage 17 onwards, during the middle of the TSP and before the onset of gonadal sex differentiation. *Rspo1* may therefore lie upstream in the genetic cascade leading to female development in species with TSD, as inferred for birds and mammals. Furthermore, expression declined in FPT→MPT shifted embryos indicating repression of *Rspo1* by a novel male environment (Fig. 9). This is the first functional assessment of *Rspo1* in an organism with TSD, and implies that an ovarian-specific function of *Rspo1* must be repressed for male development to occur. However, *Rspo1* upregulation in MPT→FPT gonads has not yet occurred within one stage post-shift. Future studies extending analysis to later stages would clarify if temperature has the ability to upregulate *Rspo1* in response to novel female environment.

Response to temperature suggests an early role for Dmrt1, and a later role for Mis, in testicular development

As expected from our previous work (Shoemaker et al. 2007a), expression levels of *Dmrt1*, *Mis*, and *Sox9* are strongly dimorphic during gonadogenesis. By quantitative real-time PCR, both *Dmrt1* and *Mis* are expressed at significantly higher levels at MPT as compared to FPT beginning early in the temperature-sensitive period. For both genes, these levels become increasingly disparate through differentiation. In contrast, *Sox9* is expressed in both sexes during the TSP and become significantly greater at MPT at the end of the TSP and during differentiation.

For the first time we report a transcriptional response of *Dmrt1* and *Mis* to a shift in embryonic temperature. *Dmrt1* expression in the gonad shows a rapid response when embryos are shifted

from FPT to MPT: between one-half and one stage later, expression is upregulated to a level significantly greater than unshifted FPT levels, and is not different from MPT levels. The converse shift from MPT to FPT does not show a significant change one stage later, although *Dmrt1* expression has begun to drop towards FPT levels. Taken together, these data indicate that testicular development requires the rapid upregulation of *Dmrt1*, and places the action of *Dmrt1* downstream of temperature. Furthermore, it suggests an early role for *Dmrt1* function in the developing testis and an upstream position in the temporal hierarchy of genes underlying development of the gonad. Delayed response in gonads shifted towards FPT suggest that repression of this gene may be a later event in the molecular cascade governing ovarian development.

In contrast to the case with *Dmrt1*, *Mis* shows a different type of rapid response to temperature. Following a shift from FPT to MPT, gonadal *Mis* expression one stage later has begun to increase, but is not yet statistically higher than unshifted FPT levels. This suggests that the role of *Mis* is downstream of *Dmrt1* in the molecular hierarchy governing testicular development, given the assumption that *Mis* has not yet been upregulated by upstream factors. Conversely, response of *Mis* expression to a shift from MPT to FPT shows a dramatic change one stage later. Expression is significantly downregulated from unshifted MPT levels, and is not distinguishable from FPT levels. One testis-specific function of *Mis* in mammals is to induce regression of the Müllerian ducts, which otherwise differentiate into female-specific organs. The repression of this hormone is thus critical in mammalian ovaries, and our data suggest the same may be true in organisms with TSD. The extremely low levels of *Mis* observed in FPT gonads at all stages, as well as the rapid downregulation following a shift to an FPT, supports this hypothesis.

While the temporal response of gene expression to a temperature shift can be used to infer placement of gene action in the molecular hierarchy governing gonadogenesis, we cannot rule out the possibility that this response does not occur under constant conditions. Thus, it should be considered that a novel environmental temperature may not engender the same molecular response as in an embryo experiencing the same temperature in non-shift conditions.

It was previously shown in *T. scripta* that in the bipotential gonad, localization of *Sox9* expression is organized at MPT and diffuse throughout FPT gonads (Shoemaker et al. 2007a). Here we demonstrate that *Sox9* expression levels in the turtle gonad are statistically similar in both sexes early in the TSP. By qPCR, we temporally define when *Sox9* expression becomes significantly male-specific, which occurs at the end of the temperature-sensitive period. However, as is true for any monomorphic gene expression pattern, SOX9 protein may be differentially functional at an earlier time point than when dimorphic expression occurs. It was shown that in response to a MPT→FPT temperature-shift, SOX9 protein levels decreased in cultured gonad explants within the temperature-sensitive period (Moreno-Mendoza et al. 2001). Furthermore, SOX9 remains cytoplasmic in cells of the mammalian bipotential XX gonad, but is translocated to the nucleus in XY gonads where it can regulate downstream gene transcription (De Santa Barbara et al. 2000, Lasala et al. 2004). Thus, while our quantitative expression data supports a later role for *Sox9* in the development of the testis, differential *Sox9* function may occur earlier via translational regulation of SOX9 or subcellular localization of the *Sox9* mRNA or protein.

Examining the patterns of upregulation of these testicular genes may also reveal something about their role in development. *Dmrt1* and *Sox9* expression levels rise sharply early in development, showing the greatest activation in expression in the middle of the TSP, between stages 16 and 19. In contrast, *Mis* expression increases most dramatically at the end of the TSP and during differentiation, from stage 19 to stage 23, implying a later role and suggesting upregulation by earlier testis-specific genes. A candidate for activating *Mis* is *Sox9*, as it is known to directly target *Mis* in mammals (De Santa Barbara et al. 1998, Arango et al. 1999). As discussed, differential Sox9 protein translation or localization provides a mechanism by which equal levels of *Sox9* expression could differentially regulate *Mis* activation in the turtle, and while not tested in the current study, warrants future attention.

In this study, we examine the spatial and temporal response of 7 candidate sex-determining genes to a sex-reversing change in temperature. This functional manipulation in a non-model system allows an analysis of their hierarchical placement within the molecular network

governing gonadogenesis. By studying the molecular cascade regulating the development of a testis and an ovary from a bipotential gonad in an organism with temperature-dependent sex determination, we begin to identify components of the pathway that may be functionally conserved through diverse modes of sex determination.

Figure 5. Morphological development of *Trachemys scripta* during the temperature-sensitive period.
(A) Slider turtle stage 16 embryos exhibit (i) smooth tissue on the upper jaw with no indication of caruncle, (ii) a vertical line of unpigmented cells in the eye extending through the pupil (white arrow), and (iii) large paddles with a smooth periphery and indications of digital ridges (Greenbaum 2002). (B) To examine development on a finer time scale, we define stage 16.5 as having a small but visible caruncle, often still below the epidermal surface (black arrow), a diminished eyeline (white arrow), and slight indications of serrations along the paddle edge. (C) By stage 17, a distinct white caruncle is found on the ventral surface of the upper jaw (black arrow), the vertical white line in the eye is substantially interrupted or absent (white arrow), and the edges of the paddle are clearly serrated.

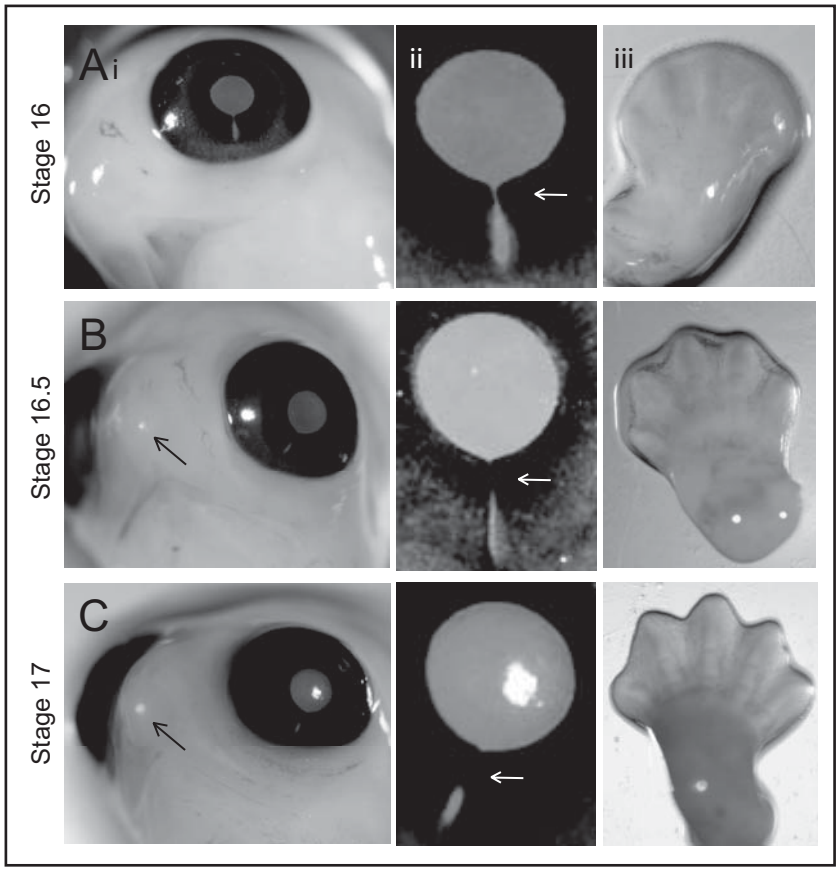

Figure 6. Expression of *FoxL2, Wnt4* and *Dax1* in the turtle adrenal-kidney-gonad (AKG) complex by *in situ* hybridization.
(A, B) *FoxL2* mRNA is found throughout bipotential gonads developing at both FPT and MPT. (C, D) During the end of the temperature-sensitive period, expression at FPT begins to be localized in the cortex, while expression in both sexes is seen in primitive sex cords. (E, F) By gonad differentiation, expression is concentrated cortically at FPT and seen faintly in putative sex cords at MPT. (G, H) View of entire AKG reveals dorsal metanephric expression of *FoxL2* at both FPT and MPT. (I) Epithelial cells lining the interior of the Müllerian ducts express *FoxL2* at FPT and MPT, typified here in a stage 23 FPT embryo. (J) View of adrenal-kidney-gonad seen in G-H, Q-R, AA-BB; dashed boxes indicate views of gonad sections seen in A-F, K-P, U-Z and of Müllerian and Wolffian duct sections seen in I, S-T and CC-DD. (K, L) *Wnt4* mRNA is found throughout bipotential gonads developing at both FPT and MPT during the temperature-sensitive period. (M, N) By the end of the TSP, expression begins to localize in the cortex at FPT and in striped medullary patterns at MPT. (O, P) Through gonadal differentiation, expression becomes further localized to the ovarian cortical region and in putative testicular sex cords. (Q, R) Dorsal metanephric tissue strongly expresses *Wnt4* at both FPT and MPT, as does the mesonephros; box indicates Müllerian duct. (S, T) Epithelial cells lining the interior of the Müllerian ducts express *Wnt4* in both sexes. (U, V, W, X) *Dax1* mRNA is found throughout gonads developing at both FPT and MPT during the temperature-sensitive period, loosely organized in the primitive sex cords that develop in both sexes. (Y, Z) During gonadal differentiation, expression is localized to the cortical region at FPT and seen faintly at MPT. (AA, BB) Dorsal metanephric tissue also expresses *Dax1* at both FPT and MPT. (CC, DD) Epithelial cells of both the Müllerian and Wolffian ducts express *Dax1*. Bar = 100 um, bar with endcaps = 200 um. g = gonad, meso = mesonephros, meta = metanephros, Md = Müllerian duct, Wd = Wolffian duct.

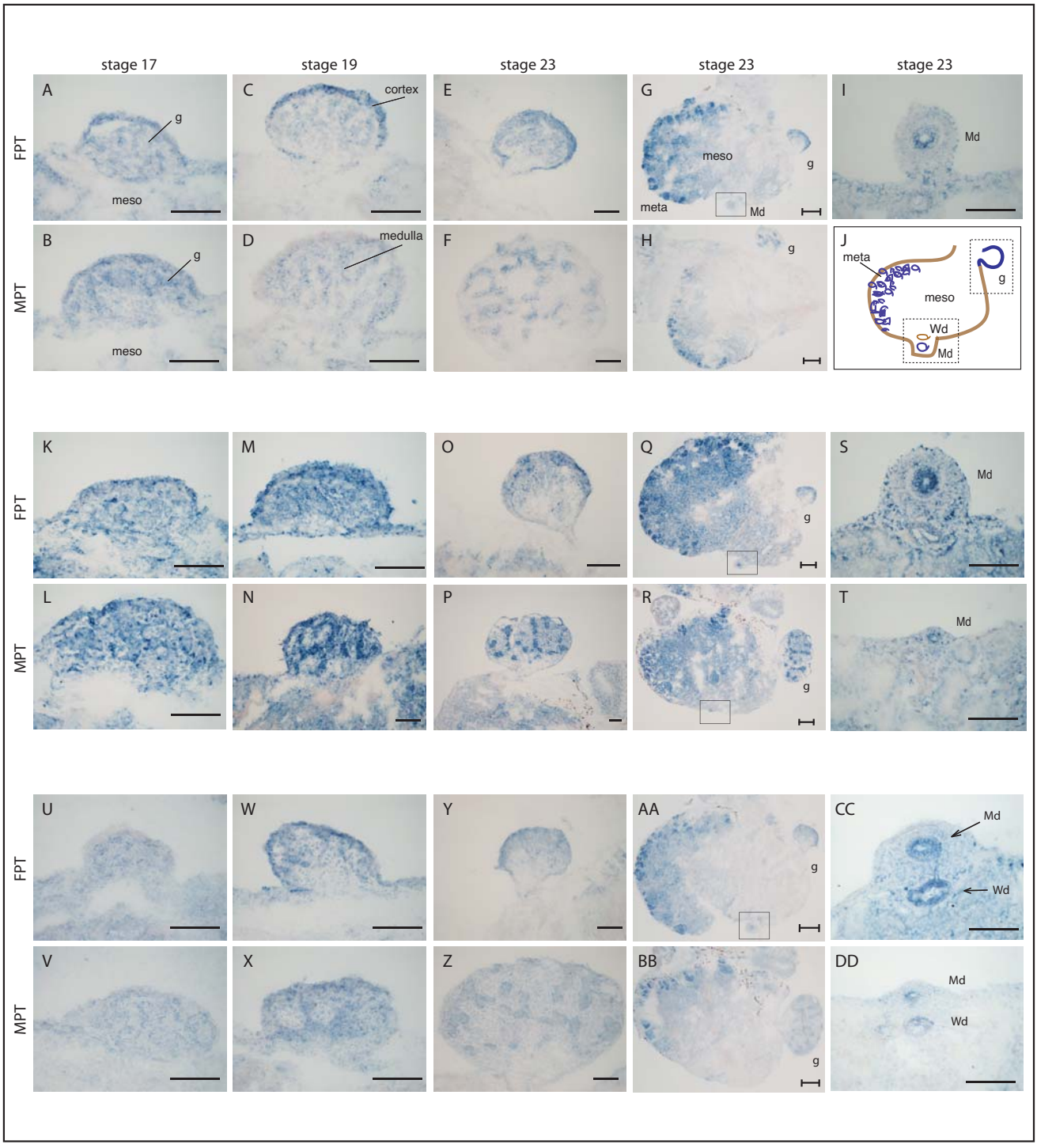
stage 17
stage 19
stage 23
stage 23
stage 23
FPT
MPT
A
B
C
D
E
F
G
H
I
J
g
meso
cortex
medulla
meta
Md
Wd
K
L
M
N
O
P
Q
R
S
T
U
V
W
X
Y
Z
AA
BB
CC
DD

Figure 7. Expression of *FoxL2, Wnt4* and *Dax1* in the turtle gonad by qPCR.
Expression levels were examined by quantitative real-time PCR in three samples per sex/stage, where each sample consisted of total RNA extracted from pooled gonads from 12-20 individuals. Average values are given with standard error bars. Left y-axis indicates expression levels normalized to the housekeeping gene *PP1*, which is constitutively expressed across development. Right y-axis indicates fold change in normalized expression calibrated to the lowest expression value at stage 23, either MPT (*FoxL2*, *Wnt4*) or FPT (*Dax1*). Asterisks indicate statistically significant difference in expression between sex within stage at the p=0.05 significance level, after correction for multiple pair-wise comparison tests by Tukey's HSD. (A, B, C) Gene expression was examined at six stages through sex determination and differentiation at both MPT and FPT. (A', B', C') Expression data at MPT and FPT at three early stages during the TSP is expanded and compared to the response of gene expression to a shift in temperature. Embryos were shifted at stage 16 from either MPT to FPT (MPT→FPT) or FPT to MPT (FPT→MPT) and gonads dissected for analysis at two subsequent time points, stage 16.5 and stage 17. (A') *FoxL2* expression in MPT→FPT stage 16.5 gonads is significantly different from MPT stage 16.5 gonads, indicated by *i*, but is not different from other values at stage 16.5. (B') *Wnt4* expression in FPT→MPT stage 17 gonads is almost significantly different from expression in unshifted FPT stage 17 gonads (p=0.0508). (C') *Dax1* expression is not significantly different in response to a temperature shift, although the direction of expression changes occurs in a sex-typical manner.

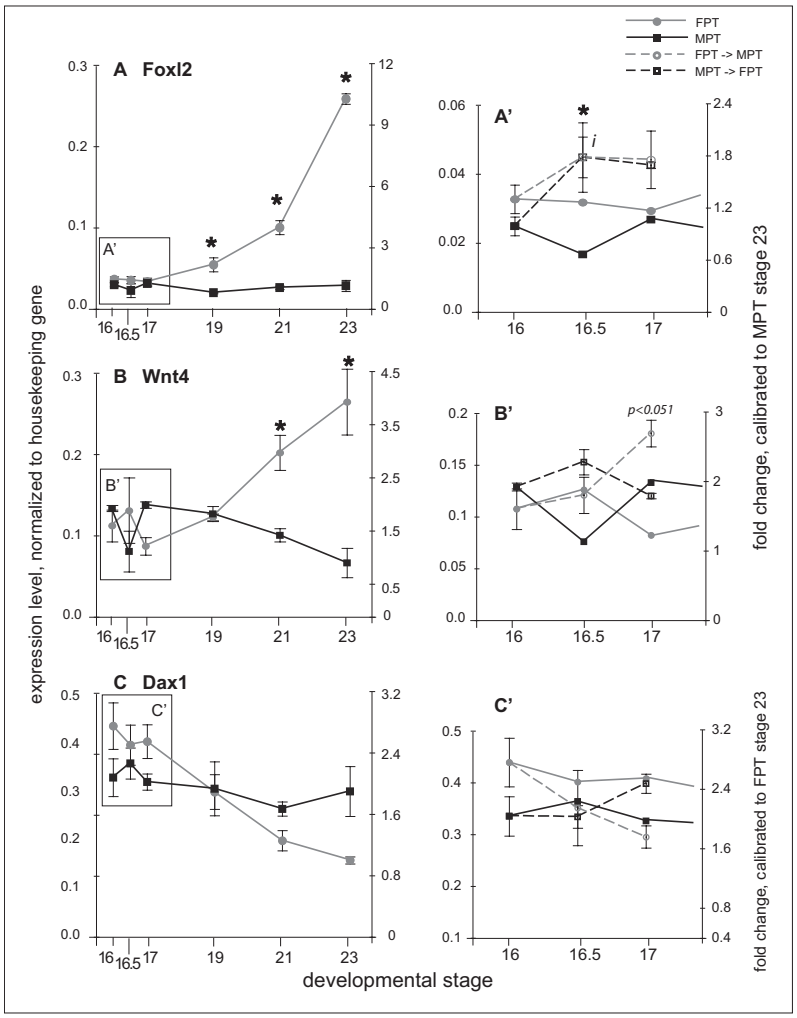

Figure 8. Expression of *Dmrt1*, *Mis* and *Sox9* in the turtle gonad by qPCR.
Expression levels were examined by quantitative real-time PCR in three samples per sex/stage, where each sample consisted of total RNA extracted from pooled gonads from 12-20 individuals. Average values are given with standard error bars. Left y-axis indicates expression levels normalized to the housekeeping gene *PP1*, which is constitutively expressed across development. Right y-axis indicates fold change in normalized expression calibrated to FPT stage 23. Asterisks indicate statistically significant difference in expression between sex within stage at the p=0.05 significance level, after correction for multiple pair-wise comparison tests by Tukey's HSD. (A, B, C) Gene expression was examined at six stages through development at both MPT and FPT. (A', B', C') Expression data at MPT and FPT at three early stages during the TSP is expanded and compared to the response of gene expression to a shift in temperature from either MPT to FPT or FPT to MPT. Embryos were shifted at stage 16 and gonads dissected for analysis at two subsequent timepoints, stage 16.5 and stage 17. (A') At stage 16.5, *Dmrt1* expression in FPT gonads is significantly lower than expression in both MPT and MPT→FPT gonads, indicated by *i*. At stage 17, expression in FPT gonads is significantly lower than all three other measurements, indicated by *ii*. (B') At stage 17, *Mis* expression in MPT gonads is significantly higher than expression at all three other measurements, indicated by *ii*. (C') At stage 16.5, *Sox9* expression in MPT→FPT gonads is significantly higher than expression in MPT gonads, indicated by *i*.

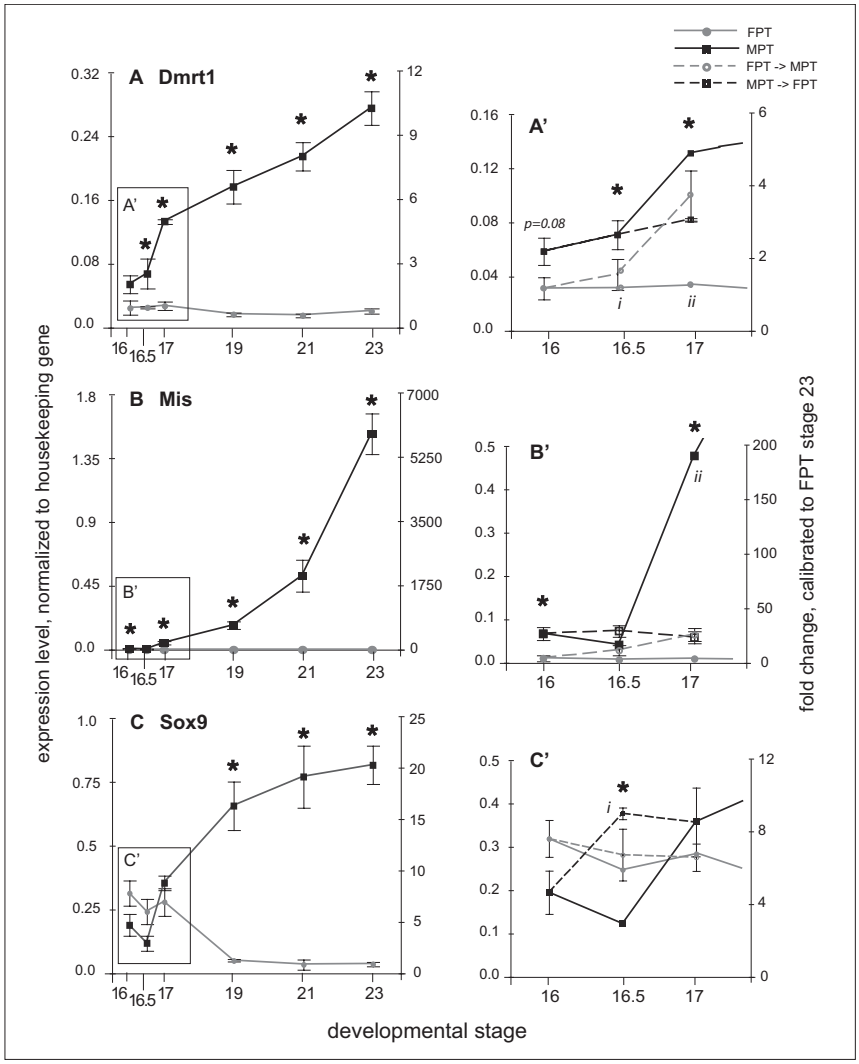

Figure 9. Expression of Rspo1 mRNA in the gonads of the slider turtle during the temperature-sensitive period by qPCR.

Expression levels were examined by quantitative real-time PCR in three samples per sex/stage. Mean +/- SEM. ● = female; ○ = male. (A) Time course of *T. scripta Rspo1* expression, showing higher expression in developing ovaries from stage 17 (p=0.0318). (B) Turtle *Rspo1* expression following temperature shifts. Expression data at MPT and FPT at three early stages during the temperature-sensitive period is expanded and compared to the response of gene expression to a shift in temperature. Embryos were shifted at stage 16 from either MPT to FPT (MPT→FPT) or FPT to MPT (FPT→MPT) and gonads dissected for analysis at two subsequent timepoints, stage 16.5 and stage 17. Following a FPT → MPT shift, expression is significantly decreased within one stage from female-typical levels (p=0.0253) and is not different from male-typical levels (p=1.0000). Following a MPT → FPT shift, expression has not yet changed from MPT-typical levels. Asterisks indicate statistically significant difference in expression between sex within stage at the p=0.05 significance level, after correction for multiple pair-wise comparison tests by Tukey's HSD.

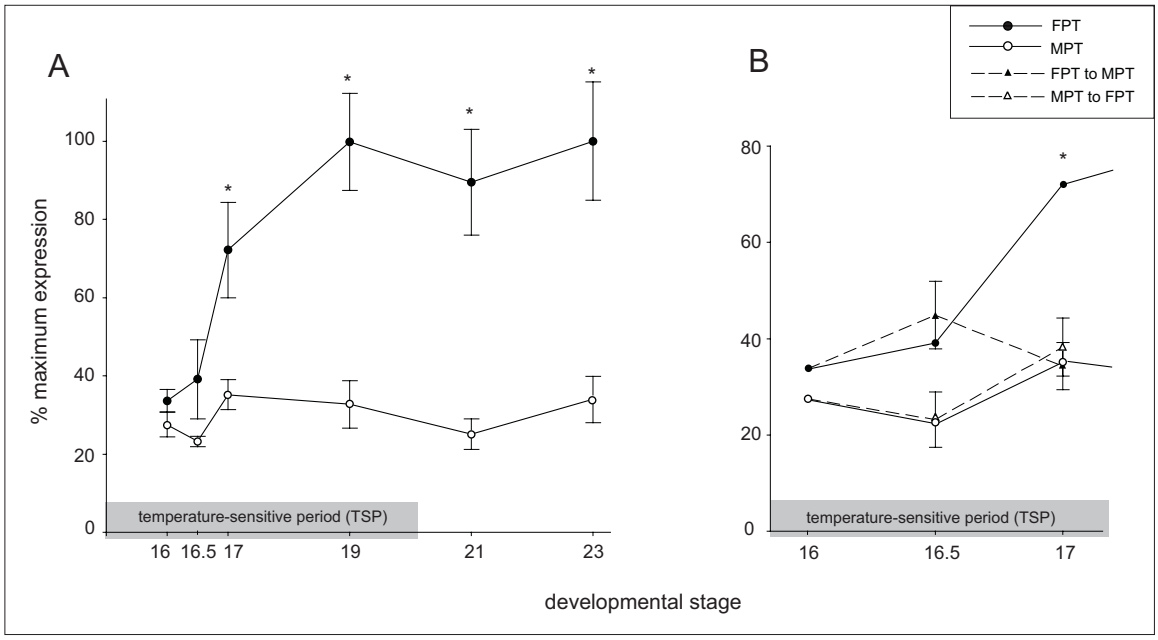

Figure 10. Nucleotide sequence and deduced translation of partial *Wnt4* in *Trachemys scripta*.

qPCR primer binding sites are indicated by bold, underlined nucleotides. Intron boundaries in human Wnt4 are denoted by asterisks above nucleotides 236/237 and 370/371; *T. scripta* sequence overlaps human exons 3, 4 and 5.

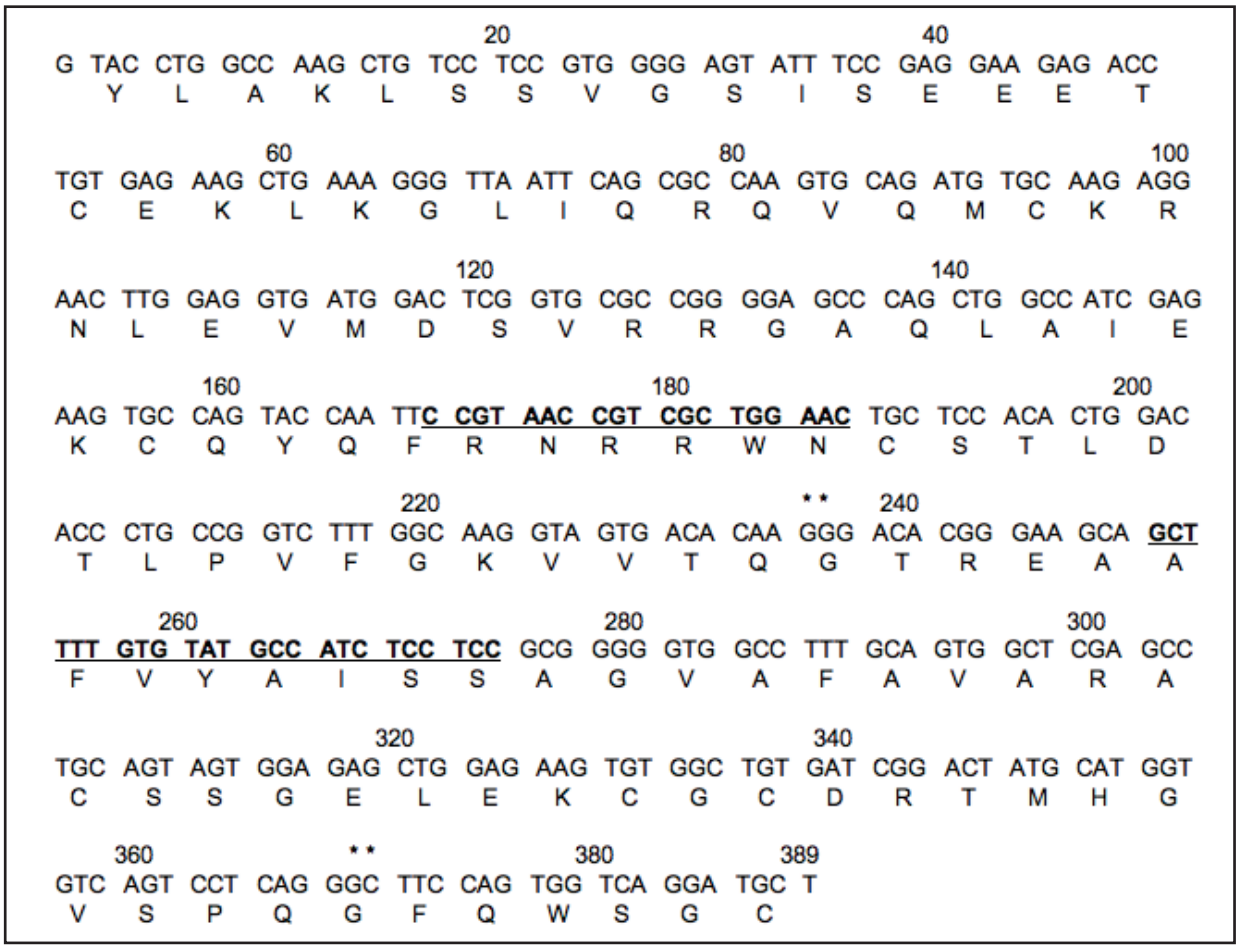

Figure 11. Alignment of vertebrate WNT4 sequences.
Deduced turtle translation is compared to chicken, mouse and human WNT4. Identical residues are shaded in dark grey, while similar residues are shaded in light grey.

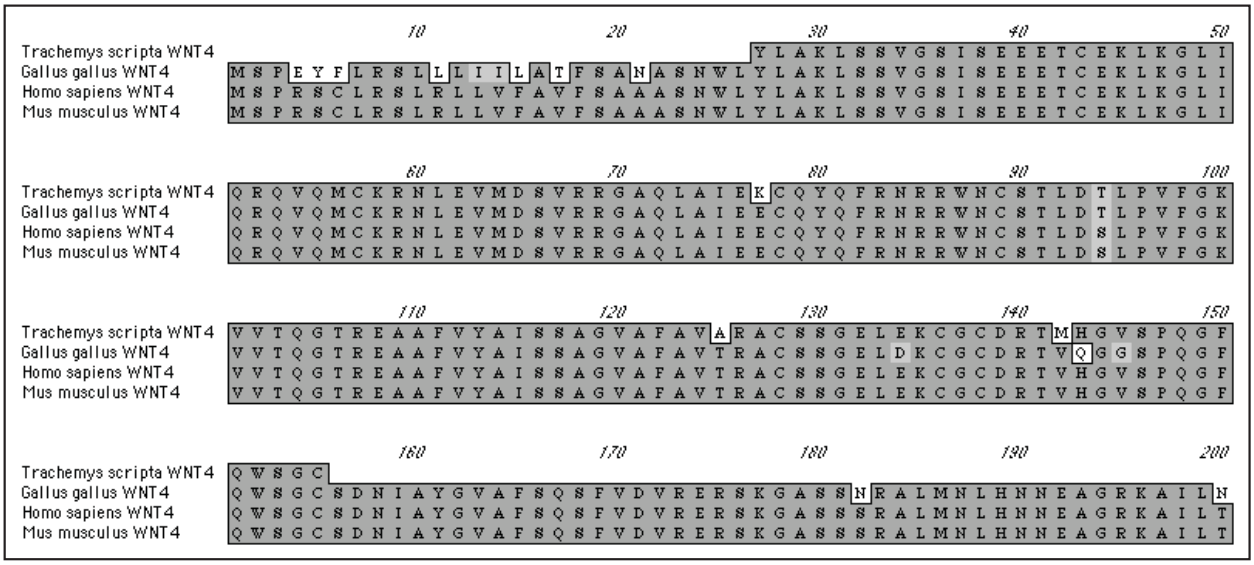

Figure 12. Nucleotide sequence and deduced translation of partial *Dax1* in *Trachemys scripta*.

qPCR primer binding sites are indicated by bold, underlined type. The intron boundary between human *Dax1* exons 1 and 2 is indicated by asterisks above nucleotides 69/70.

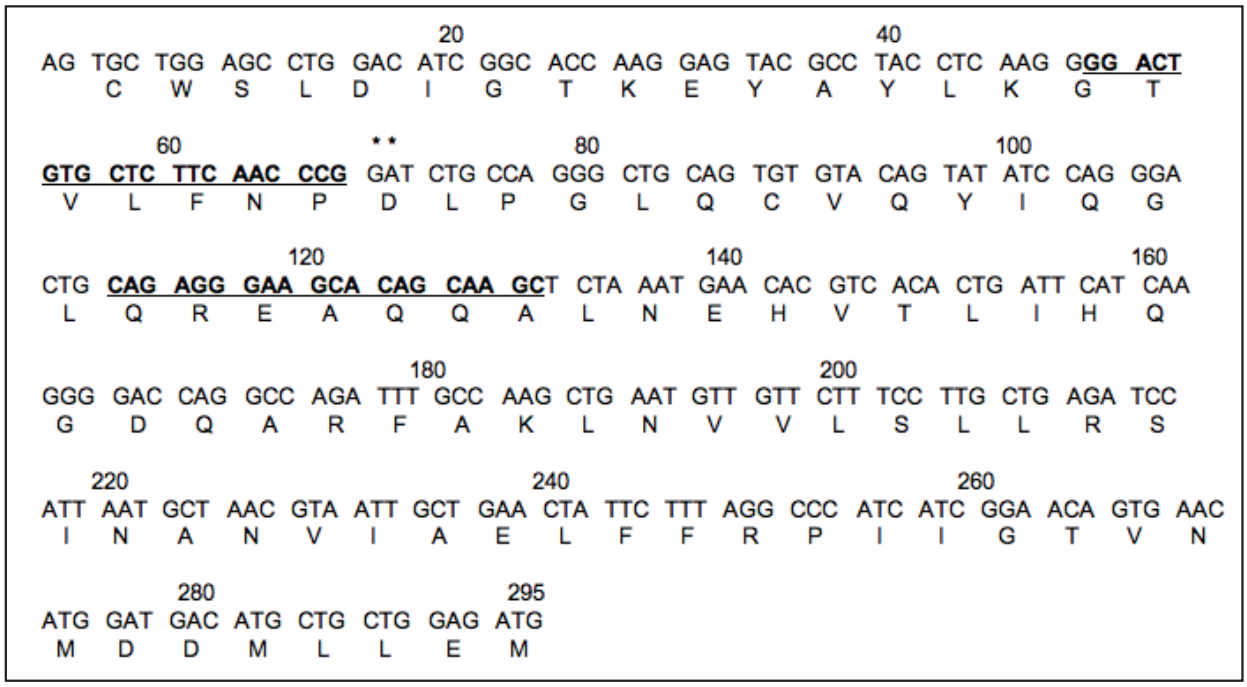

Figure 13. Alignment of vertebrate DAX1 sequences.
Deduced turtle translation is compared to C-terminal portion of Olive Ridley sea turtle, alligator, chicken, human and mouse DAX1. Identical residues are shaded in dark grey, while similar residues are shaded in light grey. Alligator, chicken and mammalian sequences show the complete C-terminus.

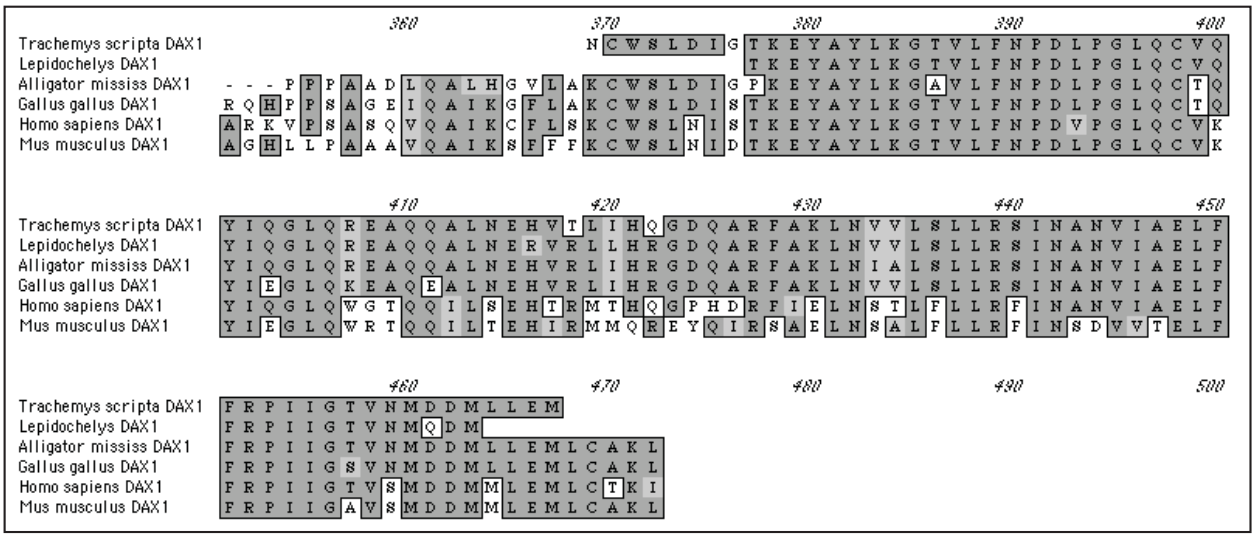

Table 2. Two-factor ANOVA tested effects of temperature, stage or temperature by stage interaction within each gene.

Gene	Effect	F Value	Pr > F
Foxl2	temperature	45.39	<.0001
	stage	15.75	<.0001
	temp * stage	10.33	<.0001
Wnt4	temperature	10.84	<.0001
	stage	3.84	0.0078
	temp * stage	10.75	<.0001
Dmrt1	temperature	132.11	<.0001
	stage	10.44	<.0001
	temp * stage	11.16	<.0001
Sox9	temperature	56.23	<.0001
	stage	3.33	0.0155
	temp * stage	38.55	<.0001
Mis	temperature	225.32	<.0001
	stage	12.25	<.0001
	temp * stage	29.94	<.0001
Dax1	temperature	1.27	0.3003
	stage	9.91	<.0001
	temp * stage	3.36	0.0085

Table 3. Significant post-hoc pair-wise comparisons within stage between temperatures after correction by Tukey's HSD.

Gene	stage	sample 1	sample 2	Estimate	t value	Adj P
Foxl2	16.5	MPT	M-F	1.5022	4.41	0.0085
	19	FPT	MPT	1.721	5.06	0.0015
	21	FPT	MPT	2.1839	6.42	<.0001
	23	FPT	MPT	3.5513	10.43	<.0001
Wnt4	17	FPT	F-M	0.0822	3.7	0.0508
	21	FPT	MPT	0.09323	4.2	0.0149
	23	FPT	MPT	0.1818	8.19	<.0001
Dmrt1	16.5	FPT	MPT	-1.1157	-3.97	0.0263
	16.5	FPT	M-F	-1.1613	-4.14	0.0174
	17	FPT	M-F	-1.3325	-4.75	0.0035
	17	FPT	F-M	1.5698	5.59	0.0003
	17	FPT	MPT	-2.0123	-7.17	<.0001
	19	FPT	MPT	-2.8979	-10.32	<.0001
	21	FPT	MPT	-3.2561	-11.6	<.0001
	23	FPT	MPT	-3.3	-11.76	<.0001
Sox9	16.5	MPT	M-F	1.6135	4.55	0.0059
	19	FPT	MPT	-3.5571	-10.03	<.0001
	21	FPT	MPT	-4.4907	-12.66	<.0001
	23	FPT	MPT	-4.34	-12.24	<.0001
Mis	16	FPT	MPT	-3.2946	-4.5	0.0067
	16.5	FPT	F-M	3.1509	4.31	0.0113
	16.5	FPT	M-F	-3.9418	-5.39	0.0006
	17	MPT	F-M	-3.7707	-5.15	0.0011

Table 4. Significant post-hoc pair-wise comparisons of *Dax1* expression within FPT between stages after correction by Tukey's HSD.

Gene	temperature	sample 1	sample 2	Estimate	t value	Adj P
Dax1	FPT	16	21	0.2404	5.26	0.0009
	FPT	16.5	21	0.2009	4.39	0.009
	FPT	17	21	0.2083	4.55	0.0059
	FPT	16	23	0.2818	6.16	<.0001
	FPT	16.5	23	0.2423	5.3	0.0008
	FPT	17	23	0.2497	5.46	0.0005

CHAPTER FOUR

Whole organ *in vitro* culture allows functional manipulation of the genetic network underlying temperature-dependent sex determination

Unraveling the molecular network that underlies TSD remains a challenge. Many genes involved in mammalian gonadogenesis have now been cloned in a variety of TSD species and their expression patterns have been examined to varying degrees (for review see Shoemaker & Crews 2009, Ramsey & Crews 2009, Moorish & Sinclair 2002, Place & Lance 2004). While descriptive studies inform our knowledge of the genes and molecules involved in TSD, progress has been hampered by technical challenges, particularly by a lack of techniques to manipulate the gonad at a molecular level. Assays such as embryonic temperature shifts and hormone treatments have been undertaken, but the data resulting from these types of experiments is limited. In this paper, we describe the application and optimization of an *in vitro* culture system, initially explored in the Olive Ridley sea turtle, *Lepidochelys olivacae* (Moreno-Mendoza et al. 2001). The gonad explant culture system facilitates manipulating the gonad at a molecular level in isolation from surrounding tissues, opening the door to functional studies classically used in traditional model organisms.

Here, we extend our previous work on four genes involved in sex determination and differentiation in the red-eared slider turtle, *Sox9*, *Dmrt1*, *Mis*, and *FoxL2* (Shoemaker et al. 2007a, 2007b). We show that the expression response to sex-reversing temperature shifts in these genes is sustained and lasts through the sex-determining period and differentiation. Because of their clear sexually dimorphic patterns of expression during gonad development, we utilize these four markers in optimizing an *in vitro* gonad explant culture system. We demonstrate that the expression patterns of these genes in gonads developing *in vitro* mimics the patterns seen *in ovo*. Furthermore, using this *in vitro* culture system, we show that expression of *Sox9*, *Mis* and *Dmrt1* is highly sensitive to estrogen-mimicking compounds. Finally, we

demonstrate that a GFP:Sox9 fusion construct electroporated into gonads *in vitro* is misexpressed in a mosaic fashion. Ectopically expressed SOX9 results in a non-significant increase in *Dmrt1* expression and no change in *Mis* or *FoxL2* expression. While this may suggest a possible functional relationship between *Sox9* and *Dmrt1*, this hypothesis requires further investigation. Taken together, these data support the use of an *in vitro* culture system to investigate *in ovo* development. This technique provides an important functional tool that can be utilized in a variety of ways to elucidate the molecular interactions occurring in the gonad during TSD.

METHODS

Embryos

Freshly laid red-eared slider eggs purchased from Clark Turtle Farms (Hammond, LA) were maintained as previously described (Wibbels et al 1991), in accordance with humane animal practices under IACUC protocol #03102301. Briefly, viable eggs were randomized in trays of moistened vermiculite and placed in incubators (Precision, Chicago, IL) at 26.0 °C or 31.0 °C. Incubator temperatures were monitored daily with HOBO data loggers (Onset Computer Corp., Bourne, MA) and verified with calibrated thermometers. For temperature shift experiments, multiple trays of 30 eggs/tray were shifted at developmental stage 16 from incubators held at 26.0 °C to 31.0 °C and vice versa. Progression of development was monitored by staging external morphological characteristics of 2-3 individuals every 3 days according to Greenbaum's staging series (Greenbaum 2002), with the addition of stage "16.5" as described previously (Shoemaker et al. 2007b). The terms "early" and "late" were utilized to describe variation observed between individual eggs laid on the same day. For example, an "early" stage 16 embryo had younger morphological characteristics than an exact stage 16, but an older phenotype than a late stage 15 embryo. Table 5 contains the individual stage data collected throughout the study and utilized for Fig. 15.

In ovo tissue collection

Eggs were incubated at 26.0 °C (MPT) or 31.0 °C (FPT) until Greenbaum's stage 16 (= Day 0), at which point some eggs were allowed to continue developing at constant temperatures. Other eggs were shifted to the opposite temperature regime (MPT→FPT or FPT→MPT). Following 1, 2, 4, 8, 12, 16, or 20 days of *in ovo* growth after Day 0, embryos were removed from the egg, staged, and sacrificed by rapid decapitation. Adrenal-kidney-gonad complexes were immediately dissected and floated in sterile PBS. Pairs of gonads were carefully separated from underlying mesonephric tissues using fine scissors and a dissecting microscope and preserved immediately for histology or gene expression analysis (Fig. 14A).

Whole gonad in vitro organ culture

Eggs were incubated at 26.0 °C (MPT) or 31.0 °C (FPT) until Greenbaum's stage 16 (= Day 0), at which point embryos were removed from the egg and sacrificed by rapid decapitation (Fig. 14B). Adrenal-kidney-gonad complexes were immediately dissected and floated in sterile PBS. Pairs of gonads were carefully separated from underlying mesonephric tissues using fine scissors and a dissecting microscope. Gonads were grown individually in culture on a sterile 0.4um Millicell membrane (Millipore) floating on 2mL culture medium. In one study (Fig. 16), culture medium contained either (A) Leibovitz's L-15 medium (+ L-Glutamine) (Gibco) supplemented with 10% charcoal-stripped fetal bovine serum (FBS) (Sigma) and 0.2% Antibiotic/Antimycotic (Gibco) or (B) L-15 medium (+ L-Glutamine, phenol red) (Gibco) supplemented with 10% unstripped FBS (Sigma) and 0.2% Antibiotic/Antimycotic (Gibco). Subsequent studies utilized culture medium A (Figs. 17-21). Gonads were cultured in sterile culture plate wells (Corning) positioned in a self-contained growth chamber unit, placed in large incubators maintained at 26.0 °C or 31.0 °C (Precision, Chicago, IL). Incubator temperatures were monitored daily with HOBO data loggers (Onset Computer Corp., Bourne, MA) and verified with calibrated thermometers. Culture medium was refreshed by replacing 1 mL every 2 days for the duration of culture. Gonads were grown at either constant temperatures (the same temperature as prior to dissection) or shifted temperatures (FPT→MPT and MPT→FPT). Following 1, 2, 4, 8, 12, 16 or 20 days of culture, gonads were preserved for histology or gene expression analysis (Fig. 14B).

Plasmid construction

An EcoRI restriction site was inserted in frame by PCR into the 5' UTR of slider turtle *Sox9* (GenBank accession #EU914820). The full length coding region (1604 base pairs) was then subcloned into pCS107:GFP:3stop containing a simian CMV IE94 promoter by restriction enzyme digest. The plasmid was a kind gift from John Wallingford, originally derived by the Harland lab (http://mcb.berkeley.edu/labs/harland/links.html) from Dave Turner's pCS2+ multipurpose expression vector (http://sitemaker.umich.edu/dlturner.vectors).

In vitro electroporation

Eggs were incubated at 26.0 °C (MPT) or 31.0 °C (FPT) until Greenbaum's stage 16 (= Day 0), at which point embryos were removed from the egg and sacrificed by rapid decapitation. Adrenal-kidney-gonad complexes were immediately dissected and floated in sterile PBS. Pairs of gonads were carefully separated from underlying mesonephric tissues using fine scissors and a dissecting microscope and placed in a sterile petri dish in 7.5 uL of 0.8 ug/uL plasmid DNA (either pCS107:GFP or pCS107:GFP:Sox9). Gonads were electroporated (2 times x 20 volts x 50 milliseconds x 3 pulses with 100 msec interval) with 0.002" bare platinum wires (A-M Systems, Inc., Carlsborg, WA) attached to a BTX Electro Square Porator ECM 830 while floating in the solution of oligonucleotides. Following electroporation, the tissue was immediately transferred to a fresh droplet of culture medium for several minutes. Gonads were then transferred to a 0.4um Millicell membrane (Millipore), cultured for 1, 2 or 3 days as above. After culture, tissues were placed in 800 uL Denaturing Solution from the RNAgents Total RNA Isolation kit (Promega) and stored at -80 °C to examine changes in gene expression (Fig. 14C). Electroporation efficiency was assessed by examining GFP fluorescence on a Olympus SZX12 microscope.

Histology

Gonads collected for histology were stored in 1mL Bouin's solution (71% picric acid, 24% formaldehyde, 5% acetic acid) and subsequently washed in 70% EtOH containing several drops of ammonium hydroxide. Gonads were dehydrated through an increasing EtOH series, cleared in xylene, and embedded in paraffin. Tissue was sectioned on an American Optical Company

microtome at 6um, stained using standard Hematoxylin and Eosin (H&E) procedures, and photographed on a Nikon microscope.

RNA extraction and cDNA synthesis

Following dissection from the egg or *in vitro* culture, individual gonads were placed immediately in 800 uL of RNA Denaturing Solution (Promega), vortexed for 1 minute to dissociate, and stored at -80 °C. Total RNA was extracted using the RNAgents Total RNA Isolation kit (Promega) and treated with DNA-Free Turbo DNase I (Ambion, Austin, TX). All RNA extracted from each individual gonad was reverse-transcribed into cDNA using the SuperScript First-Strand Synthesis for RT-PCR system (Invitrogen, Carlsbad, CA) with both oligo-(dT) and random hexamer primers and stored at -20 °C for gene expression analysis by quantitative real-time PCR (qPCR).

Quantitative real-time PCR

Relative gene expression levels were quantified using SYBR Green I dye technology (Invitrogen, Carlsbad, CA) and an ABI PRISM 7900HT real-time PCR cycler (ABI SDS 2.2.1 software). Samples were each run in triplicate and the median value was used for analysis. Gene-specific PCR efficiencies were calculated from standard curves. To compensate for variation in RNA extraction between individual gonads, relative transcript abundance was normalized to expression of *protein phosphatase 1* (*PP1*), a constitutively expressed transcript selected previously (Shoemaker et al. 2007a). A modified deltaCT method that allows for correction of differential gene PCR efficiencies was utilized, where normalized expression (NE) for each sample was:

$$NE = ((E_{ref} \wedge \text{median } Ct_{ref}) / (E_{target} \wedge \text{median } Ct_{target}))$$

where E = gene-specific PCR efficiency, Ct = cycle threshold, target = gene of interest, and ref = reference gene (Pfaffl 2001, Muller et al. 2002, Simon 2003). To examine gene expression fold changes both *in ovo* and *in vitro*, NE values were calibrated to the lowest *in ovo* expression value. These time points were: for *FoxL2*, *in ovo* Day 20 MPT; for *Sox9* and *Dmrt1*, *in ovo* Day 20 FPT; for *Mis*, the value of 0.00001. *Mis* expression at Day 20 FPT was below the level of detectability; 0.00001 is the threshold of detection for *Mis* expression as determined by the ABI

7900, and therefore is used to approximate the lowest point of detectable expression. qPCR primers were the same as used previously (Shoemaker et al. 2007a, 2007b).

Whole mount in situ hybridization

Sox9 riboprobes were reverse-transcribed in the presence of Digoxygenin-labeled UTP (Roche) using T3/T7 Megascript *in vitro* transcription kit (Ambion, Austin, TX) to produce antisense or sense DIG-labeled riboprobes. Turtle embryos were harvested from eggs at Greenbaum's stage 15 and adrenal-kidney-gonad complexes (AKGs) were dissected and fixed overnight in 4% paraformaldehyde/PBS at 4°C (n=10 at FPT and n=5 at MPT). Following fixation, whole mount ISH was performed as described by Andrews et al. (1997) with modification. Briefly, tissues were dehydrated in an increasing methanol/PBTX series, rehydrated and partially digested with 10ug/mL proteinase K for 20 minutes. Following fixation in 0.2% gluteraldehyde, tissues were pre-hybridized overnight at 65°C. Hybridization of DIG-riboprobe was carried out overnight at 65°C, followed by a series of increasing stringency washes in SSC. After Anti-DIG-AP Fab fragments (Roche) were pre-blocked in turtle embyro powder, tissues were incubated in 1:500 Ab dilution overnight at 4°C. Hybridization was visualized with BM purple (Roche) and whole tissues were photographed in 100% glycerol. AKGs were embedded in OCT freezing medium (Fisher Scientific, Hampton, NH), sectioned on a 2800 Reichert-Jung cryostat and photographed on a Nikon microscope.

Statistical analysis

For each gene, expression values measured by qPCR relative to the housekeeping gene (*PP1*) were tested for normality and variance assumptions. For *Mis*, values below the level of qPCR detectability (=0.0) were replaced with threshold value 0.00001 (see above) and all values were log-transformed to meet the normality assumption. A model was selected to account for heterogeneity of variance among groups. A two-factor ANOVA (mixed data, factors sex and group, with day as a continuous variable) on all NE values within a gene tested for sex or day main effects and a sex by day interaction (SAS software program, SAS Institute, Inc., Cary, NC). Sex by day interactions for all genes were found to be highly statistically significant (Table 6).

Post-hoc pairwise comparison tests examined differences within gene between sex within each day, correcting for multiple tests using Tukey-Kramer adjustment (Table 7).

RESULTS

Rate of development changes throughout embryonic incubation

Embryos incubating *in ovo* were dissected between 1 and 20 days post-embryonic stage 16 (= Day 0) for analysis, allowing a comparison of developmental rate at the two incubation temperatures. Embryos incubating at FPT develop faster than those developing at MPT, such that after 20 days of development in the egg post-Day 0, an FPT embryo has reached stage 23, while an MPT embryo has reached early stage 21 (Fig. 15A, B). Embryos that are shifted at Day 0 from one temperature to the other sense the new environment and morphological rates of development are altered. Thus, the developmental rate of embryos at FPT shifted to MPT (FPT→MPT) decreases, while rate of embryos at MPT shifted to FPT (MPT→FPT) accelerates. It takes approximately 12 days for this adjustment period to occur, regardless of the direction of shift (Fig. 15A). By Day 12, MPT→FPT shifted embryos reach the same overall morphological phenotype as their FPT counterparts, indicating an acceleration of development. Similarly, FPT→MPT shifted embryos reach the same morphological phenotype as MPT embryos by Day 12, indicating a deceleration in the original FPT rate of development. From Day 12 to Day 20, shifted embryos develop at temperature-typical rates. The data graphed in Fig. 15A is given in tabular form for reference (Fig. 15B). It should be noted that this correlation between days of development and developmental stage only applies to embryos and gonads *in ovo*, and is not applicable to *in vitro* samples.

Developmental rate within each temperature regime does not stay constant. The slope of a line through data points in these graphs is a measure of change in stage per day. From Day 0 to Day 8 at MPT embryos develop at a relatively constant rate, or roughly 1.5 stages in eight days ($m = 0.18$, Fig. 15C). From Day 8 to Day 12, development speeds considerably ($m = 0.47$) and within these four days the embryo develops almost 2 full stages. Subsequently, development slows to

the previous rate, and the embryo again progresses 1.5 stages in eight days (Day 12 to Day 20, m = 0.21). At FPT, a similar phenomenon is observed. From Day 0 to Day 4, development occurs at a relatively constant rate and the embryo progresses 1.5 stages in four days (m = 0.35, Fig. 15D). Growth rate accelerates from Day 4 to Day 8, during which the embryo develops 2.5 stages in four days (m = 0.55). Finally, development slows again, progressing 3.5 stages in the subsequent twelve days (m = 0.28).

Estrogenic phenol red strongly regulates gene expression patterns in the gonad

The effect of an estrogen-mimicking compound on gonad explants cultured *in vitro* was studied. Gonads were cultured in either Leibovitz's L15 medium supplemented with 10% charcoal-stripped FBS (Fig. 16A) or Leibovitz's L15 medium containing estrogenic phenol red supplemented with 10% unstripped fetal bovine serum (FBS) containing trace levels of steroid bovine hormones (Fig. 16B).

Gonads cultured at MPT in phenol red-free L15 medium and charcoal-stripped FBS showed an increase in *Sox9*, *Dmrt1*, and *Mis* expression, and *FoxL2* expression at MPT was not induced (Fig. 16B). These results are consistent with previous observations *in ovo* (Shoemaker et al. 2007b), suggesting phenol-red free *in vitro* culture method was more comparable to physiological development. In contrast, gonads cultured at MPT in the presence of phenol red and serum hormones exhibit dramatic repression of *Sox9*, *Dmrt1* and *Mis* mRNA expression (Fig. 16A). *Sox9* expression never raised substantially above FPT levels, *Dmrt1* followed a slow pattern of repression, and *Mis* was rapidly repressed to undetectable levels by the first time point examined. Furthermore, expression of *FoxL2* at MPT was slightly upregulated after 16 days of culture. Thus, estrogen mimicking compounds in the culture medium repress MPT-typical patterns of expression and induce FPT-typical patterns for 3 of the 4 genes. All subsequent *in vitro* experiments were conducted using phenol red-free medium supplemented with charcoal-stripped FBS.

Morphological development of gonads in ovo and in vitro

The histology of gonads developing within the embryo under both constant and shifted temperature conditions is presented in Fig. 17A. In developing ovaries, somatic cells reorganize into two regions, the cortex and the medulla, separated by the basal lamina. While the medullary region lacks obvious structure, primordial germ cells and granulosa cells migrate into the cortex where they later will develop into follicles in the adult. This occurs in gonads developing under either constant FPT or MPT→FPT conditions (Fig 17A, i and iv), revealing the ability of an embryo to sense and respond to its temperature environment at the level of gonadal morphological structure. In gonads shifted MPT→FPT, cells begin to reorganize and move away from male-typical morphology by 12 days post-shift (Fig. 17A, iv). Remnants of sex cords are observable at Day 16, as well as the initial formation of a thickening cortex. By Day 20 post-shift, sex cords are no longer visible and the basal lamina boundary between cortex and medulla is distinct.

In developing testes, somatic preSertoli cells organize into medullary sex cords surrounded by interstitial tissue composed of Leydig cells and peritubular myoid cells, and eventually lack any substantial cortical region. This occurs in embryonic gonads developing at either constant MPT or shifted FPT→MPT (Fig. 17A, iii and ii). In response to a FPT→MPT shift, male-typical sex cords can be seen forming as early as 12 days post-shift (Fig. 17A, ii). The sex cords continue to condense through development, and by 20 days post-shift, the cortex has fully dissolved and sex cords are distinct.

The morphological development of gonads removed from embryos at developmental stage 16 (=Day 0) and cultured *in vitro* for up to 20 days was examined (Fig. 17B). Transverse sections of *in ovo* gonads are characteristically round (Fig. 17A), and this morphology changes during *in vitro* culture. As the gonad becomes flattened from resting on the culture membrane, transverse sections taken along the same axis appear more oval-shaped (Fig. 17B). Following culture at FPT, a cortical region begins to emerge and the medullary region shows signs of reorganization by Day 12 (Fig. 17B, v). Primordial germ cells continue to migrate to the cortex, visible at Day 16, and by 20 days of culture, a more distinct boundary between cortex and medulla is apparent.

These female-typical changes are observable but less apparent in gonads shifted from MPT→FPT for the culture period; a thickened outer cortex begins to form next to a disorganized medulla by Day 20 (Fig. 17B, viii). During gonad culture at MPT, male-typical sex cords begin to form after 20 days of incubation (Fig. 17B, vii). At this point, sex cord morphology shows the expected migration of somatic cell nuclei towards the outside of the cord, leaving the cytosol of each somatic cell towards the center. These male-typical changes are not apparent in cultured gonads shifted from FPT→MPT (Fig. 17B, vi). Thus, in general, removing the gonad from its embryonic environment slows morphological development and hinders sex cord formation, especially in gonads shifted FPT→MPT.

Temperature regulates the molecular network underlying gonadogenesis in ovo and in vitro

Gene expression patterns in gonads developing *in ovo* or *in vitro* for up to 20 days post-Greenbaum's stage 16 at either constant or shifted incubation temperatures were analyzed by qPCR. The patterns observed in individual *in ovo* gonads supports previous pooled data and reveals the ability of the embryo to sense and respond to change in environmental temperature by regulating expression of the sex-determining molecular network (Shoemaker et al. 2007b). Previous data demonstrated the response of these genes at two early time points following a temperature shift (Shoemaker et al. 2007b). Here, we clarify and extend those responses by investigating time points throughout the entire sex-determining period. We observe sustained expression changes in *Sox9*, *Mis*, *Dmrt1* and *FoxL2* in response to temperature shifts that are maintained into differentiation. Explant gonads developing *in vitro* were also examined at the molecular level, and similar strong, sustained responses to changes in temperature were observed for all four markers. This demonstrates the endogenous ability of an isolated slider turtle gonad to sense and respond to changes in temperature by regulation of transcription, independent of the rest of the embryo (Moreno-Mendoza et al. 2001). Statistical estimates showing main effects of sex and day as well as sex by day interaction effects are given in Table 6. All genes were shown to have highly significant sex by day interaction, and therefore pairwise posthoc comparisons within gene within day between sex were conducted; p-values for all comparisons are given in Table 7.

Sox9 expression* in ovo *shows a strong, sustained temperature-sensitive response

In ovo patterns of *Sox9* expression at constant temperatures (MPT and FPT) in individual gonads was similar to that previously reported for pooled samples (Fig. 18A, Shoemaker et al. 2007b). From embryonic stage 16, *Sox9* expression levels at MPT more than doubled through stage 17, and were then maintained through stage 21 (Fig. 18A). Initially, *Sox9* expression was higher in FPT gonads than in MPT gonads, and subsequently decreased to negligible levels by stage 20 (Fig. 18A). This decrease at FPT is known to occur even earlier at a time point not examined here, by stage 19 (Shoemaker et al. 2007b).

We extend previous findings by examining *Sox9* expression in response to temperature shifts lasting throughout gonadogenesis, and reveal significant changes in *Sox9* levels. In gonads developing at MPT and shifted to FPT at stage 16 (MPT→FPT), *Sox9* expression initially decreased slightly, and then more dramatically by late stage 19. From this point forward, *Sox9* expression in these gonads was maintained at baseline levels (Fig. 18A). In gonads shifted in the opposite direction (FPT→MPT), *Sox9* expression also responded significantly to the new temperature. Through late stage 17, expression was indistinguishable from FPT-typical levels, but by late stage 18, the gonad began to follow a new trajectory in response to the MPT environment. While *Sox9* expression in FPT counterparts at this stage declined, expression in FPT→MPT gonads was maintained at MPT-typical levels from late stage 18 onwards (Fig. 18A).

The gene expression data described above are presented in Fig. 18 plotted against two measures of time: developmental stage (Fig. 18A) and days of *in ovo* development (Fig. 18B). The conventional use of embryonic stage when examining *in ovo* gene expression patterns becomes nonsensical in the *in vitro* culture system, as the morphological characteristics of the embryo used to assess stage no longer exist. Thus, because *in vitro* gonad development must be tracked by day, *in ovo* comparison experiments are described by day as well. To illustrate this phenomenon, a comparison between stage and day is described for *Sox9* expression, and is not repeated in further gene expression analyses. Moreover, development at warmer FPT occurs at a faster rate than at cooler MPT, due to metabolic reasons (McCue 2004). Therefore, after 20 days

of *in ovo* development post-stage 16, embryos developing at MPT reach early stage 21, while those at FPT reach stage 23. The discrepancy within Fig. 18A is not due to missing MPT data, but due to a compression of data points collected at Days 1 - 20 into earlier stages as compared to FPT counterpart data.

Thus, in terms of days of development, expression at MPT became significantly higher than FPT at Day 8 (Fig. 18B). In MPT→FPT gonads, *Sox9* expression dropped quickly in response to the novel female environment and became significantly lower than MPT levels at Day 2. In FPT→MPT gonads, expression also responded quickly; *Sox9* expression was indistinguishable from MPT levels from Day 2 onwards, and significantly higher than FPT levels from Day 8 forward.

Here, we also extend previous results examining the localization of *Sox9* transcripts in the developing gonad early in the TSP using *in situ* hybridization (ISH, Shoemaker et al. 2007a). Whole mount ISH was conducted on adrenal-kidney-gonad complexes (AKGs) dissected from Greenbaum's stage 15 embryos incubating at FPT (n=10) and at MPT (n=5). Clusters of cells expressing *Sox9* grouped around non-expressing cells were seen in gonads developing at both temperatures (Fig. 18D, E). The number of *Sox9*-expressing cell clusters were counted in all sections per AKG in a blind experimental design and averaged. The total number of clusters observed per AKG section was the same for FPT and MPT, ranging from 0 to 7 clusters/section. Furthermore, the average number of clusters per section was not different between temperatures (FPT mean = 3.7, MPT mean = 3.8).

***Gonadal Sox9 expression* in vitro *mimics patterns observed* in ovo**

Expression of *Sox9* in gonads developing in culture was nearly identical to patterns observed *in ovo*. At MPT, expression increased from Day 0 through Day 12, reaching a peak expression slightly higher than that seen in *in ovo* gonads (Fig. 18C). Within this increase, expression at MPT became significantly higher than FPT at Day 4. Expression from Day 12 declined, returning to levels similar to MPT *in ovo* gonads. At FPT, *Sox9* expression decreased

substantially by Day 1 of *in vitro* culture. Expression continued to decrease in these gonads through Day 4 and remained at baseline for the duration of the culture period (Fig. 18C).

Gonads that were grown *in ovo* at MPT through stage 16 (= Day 0) and then shifted to FPT for the culture period (MPT→FPT) responded immediately to the new temperature environment (Fig. 18C). After one day of *in vitro* culture, *Sox9* expression increased to Day 0 FPT-typical levels. Expression remained there for one day (Day 1 to Day 2) and then decreased, reaching basal levels not significantly different from FPT expression, and significantly lower than MPT levels, by Day 8. In the opposite shift, gonads grown *in ovo* at FPT through Day 0 and then shifted to MPT for the culture period (FPT→MPT) exhibited a delayed response to the novel MPT environment (Fig. 18C). Through Day 4, *Sox9* expression in FPT→MPT gonads followed an FPT-typical pattern of decline. From Days 8-12, gonads responded to the MPT environment with increased *Sox9* expression, and became significantly greater than FPT levels at Day 16. This expression was maintained for the duration of culture at levels indistinguishable from MPT gonads.

Gonadal Dmrt1 expression* in ovo *reveals an immediate, sustained response to temperature

Similar to *Sox9*, expression of *Dmrt1* in individual gonads developing at constant temperatures *in ovo* mimicked expression in pooled samples reported previously (Shoemaker et al. 2007b). *Dmrt1* expression at MPT was significantly greater than FPT at Day 0; expression increased throughout gonadogenesis and remained higher than FPT for the entire period (Fig. 19A). At FPT, gonads exhibited baseline *Dmrt1* expression for the duration of development post-stage 16 (Fig. 19A).

We demonstrated previously that Dmrt1 rapidly increases in response to a FPT→MPT shift at two early time points during the TSP (Shoemaker et al. 2007b). Here we validate and extend this response through gonad differentiation. Gonads shifted FPT→MPT at Day 0 responded rapidly to the MPT new temperature environment with an increase in expression that was apparent by Day 1 and significantly greater than FPT expression by Day 2 (Fig. 19A). This expression continued to increase through Day 8, after which levels were maintained through Day 20.

However, while expression in FPT→MPT gonads was higher than at FPT, it never reached MPT-typical levels (Fig. 19A). In the opposite shift, MPT→FPT gonads also responded quickly; expression was repressed significantly lower than MPT-typical levels by Day 2 and remained at baseline levels (Fig. 19A).

Dmrt1 expression in gonads* in vitro *mimics* in ovo *patterns

In cultured gonads, expression of *Dmrt1* showed a strongly sexually dimorphic pattern that closely mimicked what was observed *in ovo* (Fig. 19B). Expression was significantly greater at MPT than FPT for all time points examined. *Dmrt1* levels at MPT increased quickly from Day 0 to 4 and were maintained through Day 12; expression then decreased slightly through the end of the culture period (Fig. 19B). Peak MPT expression *in vitro* was roughly 2 times lower than peak levels observed *in ovo* (Fig. 19A, B). Expression at FPT remained low for the duration of the culture period.

In cultured gonads, the response of *Dmrt1* expression to temperature shifts mimicked that seen *in ovo* in both directions (Fig. 19B). In MPT→FPT gonads, *Dmrt1* expression was significantly rapidly repressed compared to MPT levels and not significantly different from FPT levels by Day 2. This response occurred at the same time as the respective *in ovo* response. From Day 2, expression continued to decrease through culture. In FPT→MPT gonads, *Dmrt1* expression through Day 4 was maintained at FPT-typical levels and increased significantly above FPT levels by Day 8. This increase was delayed compared to the respective increase observed *in ovo* (by Day 2). Expression continued to increase through Day 12, and was then maintained at MPT-typical levels. FPT→MPT shifted gonads exhibited roughly the same peak level of *Dmrt1* expression in both *in ovo* and *in vitro* experiments (Fig. 19A, B).

Gonadal Mis expression in ovo reveals a strong, immediate temperature-response

Mis expression in individual gonads grown at constant temperatures *in ovo* was strongly sexually dimorphic, a finding consistent with results from pooled gonads (Shoemaker et al. 2007b). MPT levels were greater than FPT levels beginning at Day 0 and continued for all time points examined. A second dramatic increase in *Mis* expression at MPT occurred later in the sex-

determining period from Day 12 to Day 20. FPT expression hovered at a minimal baseline level early in the TSP, and dropped below qPCR detectability from Day 4 onwards (Fig. 19C).

We validate and extend previous *in ovo Mis* expression data that demonstrated an early repression of *Mis* in response to MPT→FPT shift (Shoemaker et al. 2007b). The present study revealed that this repression occurred rapidly by Day 1 post-shift, and was maintained through a 20 day *in ovo* incubation period, despite a slight increase at Day 4 (Fig. 19C). Prior to this study, there was no evidence to support the prediction that *Mis* expression would increase in response to a FPT→MPT shift in any organism with TSD. Here we show for the first time that *Mis* expression in FPT→MPT gonads rose significantly above FPT-typical expression by Day 2. This increase in expression in response to novel MPT continued for the duration of gonadogenesis.

Expression of Mis* in vitro *is strongly sexually dimorphic and responsive to temperature

In cultured gonads, expression of *Mis* generally mimicked patterns observed *in ovo*. At MPT, *in vitro* gonads expressed *Mis* at significantly greater levels than at FPT for all time points examined. MPT gonads showed an initial increase in *Mis* expression from Day 2 through Day 8 (Fig. 19D). Expression then decreased slowly for the duration of the culture period, diverging from the *in ovo* pattern of continued increase. Furthermore, while *in vitro Mis* expression at MPT was consistently greater than at FPT, peak expression was 10 times lower than that observed *in ovo*. Expression at FPT *in vitro* was below the level of qPCR detectability at all time points examined.

In response to temperature shifts, *in vitro* gonads exhibited a strong endogenous ability to regulate *Mis* expression that mimicked regulation *in ovo* (Fig. 19D). Gonads shifted MPT→FPT revealed an immediate downregulation of expression by Day 1 that reached baseline levels by Day 2, and became undetectable by Day 8. Gonads shifted FPT→MPT showed a strong increase in response to a new MPT environment that was significantly greater than FPT expression by Day 4, slightly delayed from this increase *in ovo*. Expression then increased more substantially through Day 12, and was maintained for the duration of culture.

In ovo *FoxL2 expression reveals a response to changes in temperature*

At constant temperatures, *FoxL2* expression in individual gonads mimicked patterns detected in pooled samples described previously (Shoemaker et al. 2007b). Expression was indistinguishable between MPT and FPT early in the TSP, from Day 0 through Day 4. At MPT, *FoxL2* expression remained low throughout gonadogenesis (Fig. 19E). At FPT, *FoxL2* increased significantly above MPT by Day 8, and continued to increase during the end of the TSP and ovarian differentiation.

Previous data in the snapping turtle demonstrated an increase in expression in response to MPT→FPT shifts (Rhen et al. 2007). We find a similar response in the slider turtle and extend these observations to include shifts in both directions through the entire sex-determining period (Fig. 19E). In gonads shifted from MPT→FPT, *FoxL2* expression significantly increased above MPT levels by Day 12, and continued to increase through Day 20. In gonads shifted from FPT→MPT, *FoxL2* expression was maintained at low levels similar to FPT for the duration of gonadogenesis.

FoxL2* in vitro *expression is strongly temperature-sensitive, and similar to* in ovo *patterns

FoxL2 expression in gonads developing *in vitro* mimicked *in ovo* patterns. At MPT, expression *in vitro* remained at baseline levels throughout the culture period. At FPT, cultured gonads showed a significant increase in expression at the same time as *in ovo* gonads, from Day 8 onwards (Fig. 19F). Differing from *in ovo*, a dip in expression at FPT occurred at Day 20. Peak *FoxL2* expression at FPT was roughly 1.5 times greater *in vitro* than that observed *in ovo*.

FoxL2 expression was also strongly regulated by temperature shifts *in vitro*. Following an MPT→FPT shift, *FoxL2* expression remained at typical levels through Day 8, and then increased significantly above MPT by Day 12, at the same time this increase was observed in respective *in ovo* gonads. Expression then plateaued and was maintained for the duration of the culture period, rather than continuing to increase as occurred *in ovo.* In gonads shifted from FPT→MPT, expression remained at baseline levels throughout the culture period, with a slight non-significant increase observed at Day 20.

Individual variation within shifted gonads

When embryos developing *in ovo* are shifted between temperatures at embryonic stage 16, there is little individual variation observed within the average responses previously described (Figs. 18B, 19A, 19C, 19E). Thus, individual *in ovo* gonads shifted MPT→FPT all show similar levels of increased *FoxL2* and decreased *Sox9*, *Mis* and *Dmrt1*. Similarly, gonads shifted FPT→MPT reveal little variation in levels of increased *Sox9*, *Mis* and *Dmrt1*, and decreased *FoxL2* (data not shown).

However, *in vitro* cultured gonads exhibit individual variation in response to shifts. When gonads are shifted from FPT→MPT and grown in an *in vitro* culture system, expression of *Sox9*, *Mis* and *Dmrt1* rise in response, and *FoxL2* is repressed, as previously described (Figs. 18C and 19B, 19D, 19F). Although these average differences are often statistically significant, there is some individual variation within this shift that is masked by the average response. Therefore, we find it useful to plot expression in individual FPT→MPT cultured gonads in comparison to average FPT expression (Fig. 20A). Most gonads respond to the novel MPT environment with increased *Sox9*, *Mis* and *Dmrt1* expression and repressed *FoxL2* expression; we term these gonads "responsive". Alternatively, some gonads exhibit low expression of all four genes, and are termed "repressed". Finally, one gonad did not sense the new MPT environment and maintained female-typical levels of expression of all four genes; it is termed "non-responsive".

Gonads shifted MPT→FPT and grown in culture exhibit decreased expression of *Sox9*, *Mis* and *Dmrt1* and increased expression of *FoxL2*, as described (Figs. 18C and 19B, 19D, 19F). This pattern shows little variation among individual gonads. All gonads were "responsive" to the novel temperature environment (Fig. 20B). Similar to *in ovo* gonads, none of these individual gonads exhibit pervasive repression of gene expression or a nonresponsive effect.

Misexpression studies

Gonads were dissected from stage 16 embryos incubating at FPT and a fusion construct (pCS107:GFP or pCS107:GFP:Sox9) was introduced by electroporation. The gonads were cultured *in vitro* for up to 3 days and preserved for gene expression analysis by qPCR. The

efficiency of electroporation was examined by fluorescence microscopy, revealing a mosaic GFP expression pattern throughout the gonad (Fig. 21A, B). Higher levels of GFP fluorescence were observed in gonads electroporated with control GFP plasmid as compared to fusion GFP:Sox9.

At Day 1 post-electroporation, *Sox9* levels are substantially greater in pCS107:GFP:Sox9 gonads as compared to pCS107:GFP gonads (Fig. 21C). This increase drops by Day 2 and is gone by Day 3. At both Days 1 and 2, *Dmrt1* expression in gonads electroporated with pCS107:GFP:Sox9 is increased above control levels. However, variation within these groups is substantial and this increase is not statistically significant. By Day 3, this effect is gone. Expression of *FoxL2* is not different between gonads electroporated with each plasmid. Expression of *Mis* was below the level of qPCR detectability for all gonads electroporated with either GFP or GFP:Sox9, indicating that neither plasmid had an effect on *Mis* expression on gonads incubating at FPT (data not shown).

DISCUSSION

Temperature-sensitive period is a time of rapid overall development

In general, body temperature in most organisms is correlated to rates of metabolism and development, among other traits (McCue 2004). In the slider turtle, this results in growth being faster at the warmer FPT and slower at the cooler MPT. However, here we also show that the developmental rate of embryos does not remain constant within each incubation temperature throughout the time points examined (Fig. 15). A period of accelerated growth occurs in the middle of gonadogenesis in both putative males and females. This period spans different days of development at each temperature, lasting from Day 8 - 12 at MPT and from Day 4 - 8 at FPT. Interestingly, the timeframe of these growth spurts overlap similar developmental stages, from late stage 17 to late stage 19 at MPT, and from stage 17.5 to early stage 20 at FPT. Furthermore, this period occurs during the TSP in this species. While it seems obvious that the sex-determining period is a time of massive reorganization and change within the gonad, we find that it is also a period of increased rate of change in the embryo as a whole.

Expression of the molecular network underlying gonadogenesis is altered by estrogen-mimicking compounds

We compared the effect of two culture media preparations on gonads developing *in vitro*; one lacked phenol red and utilized stripped FBS, while the other contained estrogen-mimicking phenol red and unstripped FBS. The estrogenic properties of phenol red have been well-documented (Welshons et al. 1988, Berthois et al. 1986). Furthermore, nonstripped FBS most likely contains trace amounts of circulating hormones remaining in the serum, and stripping serum with charcoal removes hydrophobic, low molecular weight molecules, including steroid hormones (e.g., Chen et al. 2004).

In vitro culture in medium lacking phenol red and using stripped FBS results in expression patterns of *Sox9, Dmrt1, Mis* and *FoxL2* similar to those observed previously in gonads developing in the embryo (Fig. 16A, Shoemaker et al. 2007b). *Sox9*, *Dmrt1* and *Mis* expression is greater at MPT, while *Foxl2* expression is high at FPT. In comparison, either phenol red or traces of hormones in unstripped FBS strongly repress the expression of *Sox9, Dmrt1,* and *Mis* in gonads culturing at MPT (Fig. 16B). The repression of these three factors occurs at different rates. *Mis* expression is rapidly downregulated by the first time point sampled, indicating a high sensitivity to estrogen-mimicking compounds. In contrast, *Dmrt1* is more slowly downregulated, and *Sox9* expression remains constant at basal levels. At both MPT and FPT, phenol red caused *FoxL2* gene expression to rise slightly at the end of the culture period.

These data indicate that the expression of these genes is sensitive to regulation by estrogen-mimicking compounds. It is quite probable that estradiol itself would have a similar effect, and exploring this would be a fruitful avenue of future research. It is now known that, in contrast to the case in mammals, estradiol is critical to early patterning of the ovary in the red-eared slider turtle (Pieau & Dorizzi 2004, Ramsey & Crews 2009). Furthermore, estradiol treatment to the eggshell of developing embryos overrides the effect of MPT *in ovo*, feminizing the resulting gonad (Crews et al. 1991). The interactions between estradiol and the molecular network underlying gonadogenesis has begun to be explored in studies examining *ERα*, *ERβ*, *aromatase*, *AR* and *Sf1* (Fleming & Crews 2001, Ramsey et al. 2007, Ramsey & Crews 2007b). It is also

probable that estradiol-induced sex-reversal is modulated in part by the repression of gene products required for testis development, and our data suggest these repressed factors may include *Sox9*, *Mis* and *Dmrt1*.

These results are supported by findings in organisms with GSD. In mouse, the expression of both *Sox9* and *Mis* are strongly responsive to estrogen. *Aromatase* -/- mice are estrogen-deficient and produce testicular Sertoli and Leydig cells during puberty; however, when embryos are treated with estradiol, significant downregulation of both *Sox9* and *Mis* occurs, leading to somatic cell transdifferentiation towards an ovarian phenotype (Britt et al. 2004). *ERα* and *ERβ* double knockout mice show upregulation of both *Sox9* and *Mis* (Couse et al. 1999). Furthermore, these mice develop Sertoli-like cells that express *Sox9* from granulosa precursor cells; in the absence of estrogen, *Sox9* expression is thought to cause the transdifferentiation of these somatic cells from an ovarian phenotype to a testicular phenotype, implying that a normal role of estrogen is to directly or indirectly repress *Sox9* (Dupont et al. 2003). In the Nile tilapia (*Oreochromis niloticus*), adults can be sex-reversed by the application of exogenous steroid hormones; estrogen treatment of males results in the downregulation of *Dmrt1*, while exogenous androgen to females causes upregulation of *Dmrt1* expression in both Sertoli and epithelial testis cells (Kobayashi et al. 2008). In mammals, *FoxL2* upregulates *aromatase* expression, which is required for estrogen production (Pannetier et al. 2006, Wang et al. 2007). Inhibiting *aromatase* results in decreased *FoxL2* expression in chicken (Hudson et al. 2005). Taken together, these results indicate that a positive feedback loop may exist between *FoxL2* and *aromatase*, and it is not unlikely that estradiol plays a role in modulating this interaction (Smith et al. 2008).

The ability of estradiol to moderate expression of these four genes in an organism with TSD has been explored in only one other case. When estrogen is applied to slider turtle eggshells incubating at MPT before the TSP, expression of *Dmrt1* is downregulated to FPT-typical levels; effects on other genes were not examined (Murdock & Wibbels et al. 2006). The modulation of this interaction remains to be elucidated, but as indicated by our data, it would be revealing to expand hormone treatment studies to these components of the sex-determining pathway. It will be of critical importance in the upcoming decades for research on the TSD molecular network to

examine interactions downstream of temperature between endogenous steroid hormones and gene products. Understanding the complex interactions of these two systems, hormonal and genetic, is necessary in order to fully understand how a gonad is formed in organisms with TSD.

Mis, Dmrt1 and FoxL2 exhibit previously undetected sustained responses to changes in temperature during in ovo development

We previously investigated the ability of sex-determining genes to respond rapidly to changes in incubation temperature at two early time points of the TSP (Shoemaker et al. 2007b). *Dmrt1* and *Mis* showed a temperature response in one shift direction but not the other, and *FoxL2* did not exhibit the expected response; while we were interested in the ability of these genes to change rapidly in response, the timeframe examined did not last long enough to elucidate downstream responses. Here we extend those results to examine changes throughout the entire sex-determining period and reveal previously undetected sensitivity to changes in temperature in both shift directions in *Dmrt1*, *Mis* and *FoxL2*. Furthermore, we confirm previous findings in other species that *Sox9* expression is regulated by temperature shifts in both directions as well (Moreno-Mendoza et al. 2001).

We previously reported *Dmrt1* expression in gonads shifted FPT→MPT increases by one stage post-shift (Shoemaker et al. 2007b). Here we extend these results and demonstrate that expression is significantly upregulated by 2 days post-shift, at stage 16.5, and continues to increase for the duration of gonadogenesis (Fig. 19A). Moreover, in gonads shifted MPT→FPT, we reveal for the first time a significant, rapid decrease in expression below MPT-typical levels by 2 days post-shift, at stage 16.5. These results confirm the temperature-sensitivity of *Dmrt1* and validate a critical function in the developing testis of the slider turtle. Furthermore, the data indicate that it is important to repress this function in gonads at FPT destined to form ovaries. The sexually dimorphic pattern of *Dmrt1* expression from very early in the TSP suggests that it may play a more upstream role in the developing testis of the slider turtle, as opposed to its downstream role in mammalian testis differentiation.

A significant increase in *Mis* expression in FPT→MPT shifted gonads was not detected when two early time points were examined (Shoemaker et al. 2007b). However, here we clarify this response to show that expression is significantly upregulated by 2 days post-shift, equivalent to a stage 16.5 embryo (Fig. 19C). This increase continues through the sex determining-period and into differentiation. In embryos shifted in the opposite direction, from MPT→FPT, we confirm previous findings of a rapid repression of *Mis* expression. Expression is significantly downregulated below MPT levels by 1 day post-shift, in a late stage 16 embryo, and repression is sustained throughout gonadogenesis. Taken together, these data indicate that *Mis* plays a critical role in the development the testis, and this function must be repressed in developing ovaries. Whether *Mis* is responsible for the inhibition of Mullerian duct differentiation into female-specific ducts in developing male slider turtles, as it does in mammals, would be productive to investigate.

Because expression of *FoxL2* is indistinguishable early in the TSP between MPT and FPT gonads, previous investigations of a rapid response to temperature shifts were not revealing (Shoemaker et al. 2007a). However, here we extend examination later in the TSP and show for the first time that *FoxL2* significantly increases in gonads shifted MPT→FPT by 12 days post-shift, at stage 21 (Fig. 19E). This upregulation occurs at a similar time as the increase in expression observed in FPT gonads (Day 8, stage 19), indicating that the gonad maintains a developmental clock even when shifted between temperatures. Furthermore, *FoxL2* expression in gonads shifted FPT→MPT remains low at MPT-typical levels for the duration of gonadogenesis. These data suggest a role for *Foxl2* in the developing ovary of slider turtles. Because *FoxL2* expression increases near the end of the female TSP, it is unclear whether it plays a role in the repression of male-typical gene expression as in GSD organisms; this would be worthwhile to examine in future studies.

***Sox9* localization early in the temperature-sensitive period is not sexually dimorphic**

We previously demonstrated a sexually dimorphic localization of *Sox9* early in the TSP (Shoemaker et al. 2007a). At stage 15, *Sox9* transcripts were found to be preferentially organized in gonads developing at MPT in clusters of cells surrounding non-expressing cells, while

expression remained diffuse at FPT. Here we clarify those results and find that while in some gonads at FPT, *Sox9* expression does remain diffuse (data not shown), FPT gonads also exhibit clusters of *Sox9*-expressing cells surrounding non-expressing cells (Fig. 18D). Overall, there were no differences in the range or average number of clusters found at MPT versus FPT. In light of this new evidence, it is concluded that *Sox9* becomes sexually dimorphic in the gonads of the red-eared slider turtle after *Mis* expression is enhanced at MPT. This is similar to the case in both the American alligator and chicken (Oreal et al. 1998, Smith et al. 1999a, Western et al. 1999b). While *Sox9* may still be found to play a role in the commitment of the developing gonad in organisms with TSD as was previously proposed, it appears not to be involved early in the opening of the temperature-sensitive window in the slider turtle.

Gonads cultured in vitro exhibit gene expression patterns strongly similar to in ovo development

Taken together, the data presented here indicate that gonad explants developing in a whole organ *in vitro* culture system are a useful tool to investigate *in ovo* development in organisms with TSD. According to morphological characteristics, gonad development slows upon isolation from the embryo (Fig. 17). At FPT, it takes longer for ovarian-specific structures to form *in vitro*, and by Day 20, a thickened cortex separated from the degrading medullary region by a basal lamina is distinct. In MPT→FPT shifted gonads, ovarian morphology is less apparent, although a cortical/medullary distinction begins to form by Day 20. At MPT, sex cord formation is hindered by a lack of supporting tissues; by Day 20 sex cord-like structures begin to appear. In FPT→MPT gonads, sex cords are nonexistent. These results are not unexpected and may be due to the lack of the underlying mesonephric tissue which the gonad requires for full differentiation. In the slider turtle, the mesonephric coelomic epithelium invaginates into the gonad and is required for fully formed sex cords in the developing testis (Yao et al. 2004b). Thus, when this coelomic epithelium is removed, the formation of sex cords is predicted to be inhibited. Unfortunately, whole adrenal-kidney-gonad complexes cultured with the underlying mesonephric tissue intact undergo rapid degradation and cell death, and development does not proceed (N. Moreno-Mendoza, pers. comm.).

While the morphology of gonads developing *in vitro* is hindered by isolation, gene expression of components of the sex-determining pathway tell a different story. As described, gene expression *in vitro* closely mimics *in ovo* patterns (Figs. 18, 19). *Sox9*, *Dmrt1* and *Mis* were all strongly upregulated in MPT and FPT→MPT gonads, and expression was strongly repressed in FPT and MPT→FPT gonads. Conversely, *FoxL2* was upregulated at both FPT and MPT→FPT, and was downregulated at MPT and FPT→MPT. The timing of these gene expression changes was also generally similar between *in ovo* and *in vitro* samples, although the differences are illuminating. Differences include a delay in the upregulation of *Sox9*, *Dmrt1* and *Mis* in FPT→MPT shifted gonads *in vitro* as compared to *in ovo*. Thus, gonads encountering a new male-producing environment took longer to induce a male-typical gene cascade in isolated gonad tissue than when the gonad was incubating within the embryo. However, the repression of *Dmrt1* and *Mis* in MPT→FPT gonads occurred at the same time *in vitro* as *in ovo*, indicating that FPT repressed the male pathway without delay in isolated tissue. The exception to this was *Sox9*, whose decreased expression was delayed in MPT→FPT tissues. The timing of *FoxL2* expression changes in both FPT→MPT and MPT→FPT was exactly the same *in vitro* and *in ovo*, indicating that the expression of this gene is highly correlated to an internal "developmental clock". It is dangerous to make generalizations based on one marker, but according to our findings of *FoxL2* expression patterns, gonads encountering a new female-producing environment upregulate the female cascade at the appropriate time.

The duration of the culture period in this study was 20 days, and during this time, each marker showed different levels of similarity to *in ovo* expression. At constant temperatures, *Sox9* expression *in vitro* was similar to *in ovo* patterns for the duration of culture, except for a brief spike in expression at MPT above what was observed *in ovo* (Fig. 18). In contrast, *Dmrt1* showed slightly different gene expression patterns from *in ovo* beginning at Day 12, and *Mis* differed from Day 8 onwards (Fig. 19). In these two genes, expression at MPT began to decrease instead of continuing to increase as occurred *in ovo*. Finally, *FoxL2* expression appeared to be maintained through Day 16, at which point expression at FPT began to decline (Fig. 19). Thus, the optimal length of culture will vary depending on which marker is used for justification, but *in vitro* development mimicked *in ovo* patterns at least through Day 8 for all genes examined here.

We confirm here that in the red-eared slider turtle, an isolated gonad endogenously retains the ability to sense changes in environmental temperature, a finding similar to that of Moreno-Mendoza et al. (2001) in the Olive Ridley sea turtle. Importantly, individual cultured gonads respond to temperature with gene transcription changes of multiple components of the molecular network underlying sex determination and differentiation in the absence of other possible temperature-sensing systems (e.g., the brain, Merchant-Larios et al. 1989, Gutierrez et al. 1999). The data presented here indicate that the gene expression pathways initiated by temperature progress normally for some time despite limits placed on gonad development by altered cellular behavior. *In vitro* molecular interactions proceed normally for at least 8 and up to 20 days, while cellular interactions are more strongly hindered by the gonad's isolation from neighboring tissues. Thus, the utility of this culture system may be limited to molecular studies observable in a one-to-three week time period.

In vitro gonads allow functional manipulation of the sex-determining molecular network

Gonads electroporated with either control GFP or a GFP:Sox9 fusion construct exhibit mosaic GFP fluorescence throughout the tissue (Fig. 21). GFP fluorescence was brighter in gonads electroporated with control plasmid than in samples electroporated with GFP:Sox9 (Fig. 21A, B). This could be due to several reasons: electroporation efficiency may differ between the two plasmids, expression of the two plasmids may differ within gonadal cells, or fusing Sox9 to GFP may inhibit correct folding and thereby decrease fluorescence. We were not able to distinguish between these possibilities in this study, but future examination of protein levels by Western blot or immunocytochemistry may elucidate this discrepancy. In any event, it is clear that both constructs entered gonadal cells and were misexpressed, as evidenced by GFP fluorescence.

Gonads were analyzed by qPCR to determine the effect of electroporation on gene expression. *Sox9* expression was significantly increased in gonads electroporated with GFP:Sox9 over control gonads (Fig. 21C). Because all gonads were incubated at FPT, this increase can be attributed to the plasmid treatment. The effect of increased Sox9 on endogenous *Dmrt1* expression is unclear. There appears to be an increase in expression at 1 and 2 days post-electroporation, but due to large variation between individuals, this difference is not statistically

significant. It is possible that further optimization of the culture technique will clarify this response. There was no difference in *FoxL2* or *Mis* expression between the two plasmids.

Evidence Sox9 may not regulate Mis in the slider turtle gonad

Sox9 directly upregulates the expression of *Mis* in the developing mammalian testis, and this relationship is not conserved through taxa. In chicken, alligator and slider turtle, sexually dimorphic expression of *Mis* in developing gonads precedes dimorphic *Sox9*, indicating that the initial upregulation of *Mis* has been coopted by other molecule(s) (Shoemaker et al. 2007b, Takada et al. 2004, Western et al. 1999b, Oreal et al. 1998, Smith et al. 1999a). While any possible functional relationship between these two molecules in organisms with TSD is as yet undescribed, the data here continue to support the hypothesis that *Mis* is regulated by something other than *Sox9* in the red-eared slider turtle.

Firstly, in gonads shifted FPT→MPT, upregulation of *Mis* occurred more rapidly than upregulation of *Sox9*. *In ovo* and *in vitro*, *Mis* expression in FPT→MPT gonads is statistically significantly greater than MPT expression by Day 2 and Day 4, respectively. In contrast, *Sox9* expression in FPT→MPT gonads became statistically greater than MPT expression *in ovo* and *in vitro* by Day 8 and Day 16, respectively. This indicates that initial upregulation of *Mis* in this species has been coopted from *Sox9* by some other molecule.

Secondly, MPT→FPT shifted gonads reveal that *Mis* expression responds more rapidly to the new FPT environment than *Sox9* expression, in both *ovo* and *vitro* samples. *Mis* is immediately downregulated by novel FPT temperature, exhibiting statistically lower expression by Day 1 *in ovo* and *in vitro* (Fig. 19C, D). The transient increase in *Mis* expression in MPT→FPT gonads at Day 4 *in ovo* and *in vitro* is driven by only one individual gonad in each case (data not shown). In contrast, *Sox9* downregulation in MPT→FPT gonads occurs later than *Mis* repression (Fig. 18B, C). *In ovo*, *Sox9* is significantly lower than MPT by Day 2, while *in vitro* MPT→FPT gonads show an initial rise in *Sox9* expression at Days 1 and 2 followed by a similar slow descent to baseline levels by Day 8 (Fig. 18). This data indicates that *Mis* has a strong temperature sensitivity, and that *Mis* repression in MPT→FPT gonads is not due to a simple lack

of upregulation by *Sox9*. In fact, this initial upregulation *in vitro* of *Sox9* in MPT→FPT gonads would be predicted to cause a corresponding increase in *Mis* if this was its normal function. It is possible that *Mis* is directly sensing temperature, or is being regulated via a separate temperature-sensing molecule, hypotheses that would be fruitful to examine.

Thirdly, when exogenous *Sox9* is misexpressed in gonads developing at FPT *in vitro*, *Mis* expression remains undetectable in all cases (data not shown). Since *Sox9* upregulation is transient and only lasts for one day (Fig. 21), it is possible that an effect on *Mis* is not observed due to timing of the experiment, and given stable expression of *Sox9* at FPT for a longer period, *Mis* would be upregulated. In this initial study, however, the repression of *Mis* by FPT was not altered by a significant increase in Sox9 levels. Therefore, while our data do not rule out the possibility that *Sox9* upregulates *Mis*, they do support the hypothesis that some other factor upstream of *Mis* controls its initial expression. The ability to have sustained misexpression *in vitro* would clarify between these two possibilities and is a goal of future experiments.

In all likelihood, there are multiple mechanisms regulating the expression of *Mis*. For example, *Mis* expression may be initially upregulated by an unknown male-typical factor, maintained by *Sox9*, repressed by estrogen, and repressed directly by female-producing temperatures or indirectly via a female-typical factor. These possibilities could be explored further beginning with a functional analysis of the *Mis* promoter, as well as future experiments manipulating the gonad at the molecular level *in vitro*.

Evidence that Dmrt1 does not directly sense temperature in the slider turtle

Expression of *Dmrt1* in slider turtle gonads is sexually dimorphic at the earliest stages examined both *in ovo* and *in vitro*, beginning at stage 16 (Day 0) and continuing through gonadogenesis (Fig. 19A, B, Shoemaker et al. 2007b). This data might lead to the hypothesis that *Dmrt1* may be a temperature-sensing molecule, similar to the master sex-determining role proposed in chicken and medaka studies. We present two lines of evidence suggesting that this is not true in the red-eared slider turtle. First, in response to a FPT→MPT shift, expression in both embryonic and cultured gonads becomes significantly greater than basal FPT expression levels at Day 2 post-

shift *in ovo* and Day 8 *in vitro*. Furthermore, *in ovo* FPT→MPT gonad expression never reaches *in ovo* levels. It is likely that if *Dmrt1* was the primary factor determining sex downstream of temperature, its expression would rise more dramatically and swiftly in response to a novel MPT. Second, when *Sox9* is misexpressed at FPT in culture, *Dmrt1* expression in response is higher than in control gonads, albeit non-significantly (Fig. 21C). If *Dmrt1* was upstream of *Sox9* and sensed temperature directly, one might expect FPT repression of *Dmrt1* to override downstream exogenous *Sox9*. This would result in *Dmrt1* expression equal to control levels, rather than an upregulation of expression. However, because the observed *Dmrt1* increase is not significant, further studies are needed before any conclusions can be made concerning the relationship between *Sox9* and the regulation of *Dmrt1* expression.

Here we demonstrate that expression of *Sox9, Dmrt1, Mis* and *FoxL2* all exhibit sustained changes in expression in response to sex-reversing temperature shifts that last through embryonic gonadogenesis. We present optimization of a whole organ *in vitro* culture system in the red-eared slider turtle and show that in culture, expression patterns of these four genes mimic *in ovo* patterns at both constant and shifted temperature regimens. We demonstrate the ability to introduce fusion plasmid constructs by electroporation into gonadal cells, which are then misexpressed. Importantly, this opens the door to functional manipulation of the gonad by misexpression of gene products. Taken together, these data lend support to using an *in vitro* culture system in future experiments examining the molecular network underlying gonad development.

Figure 14. Experimental design.
(A) Developmental progression of red-eared slider turtle (*Trachemys scripta*) embryos incubating *in ovo* at male-producing temperature (MPT) or female-producing temperature (FPT) was monitored. At Greenbaum's embryonic stage 16 (= Day 0), some eggs were shifted to the opposite temperature while others remained at constant temperatures. Following up to 20 days further *in ovo* incubation, embryos were sacrificed and gonads dissected for individual quantitative real-time PCR (qPCR) and histological analysis. (B) Developmental progression of embryos incubating *in ovo* at MPT or FPT was monitored and at Greenbaum's embryonic stage 16 (= Day 0), embyros were sacrificed, adrenal-kidney-gonads were dissected, and gonads were separated. Gonads from each original incubation temperature were cultured *in vitro* at either constant and shifted temperatures for up to 20 days and preserved for individual qPCR and histological analysis. (C) Developmental progression of embryos incubating *in ovo* at MPT or FPT was monitored and at Greenbaum's embryonic stage 16 (= Day 0), embyros were sacrificed and gonads dissected. Gonads were electroporated with pCS107:GFP:Sox9 or pCS107:GFP, cultured *in vitro* for up to 3 days, and preserved for individual qPCR analysis.

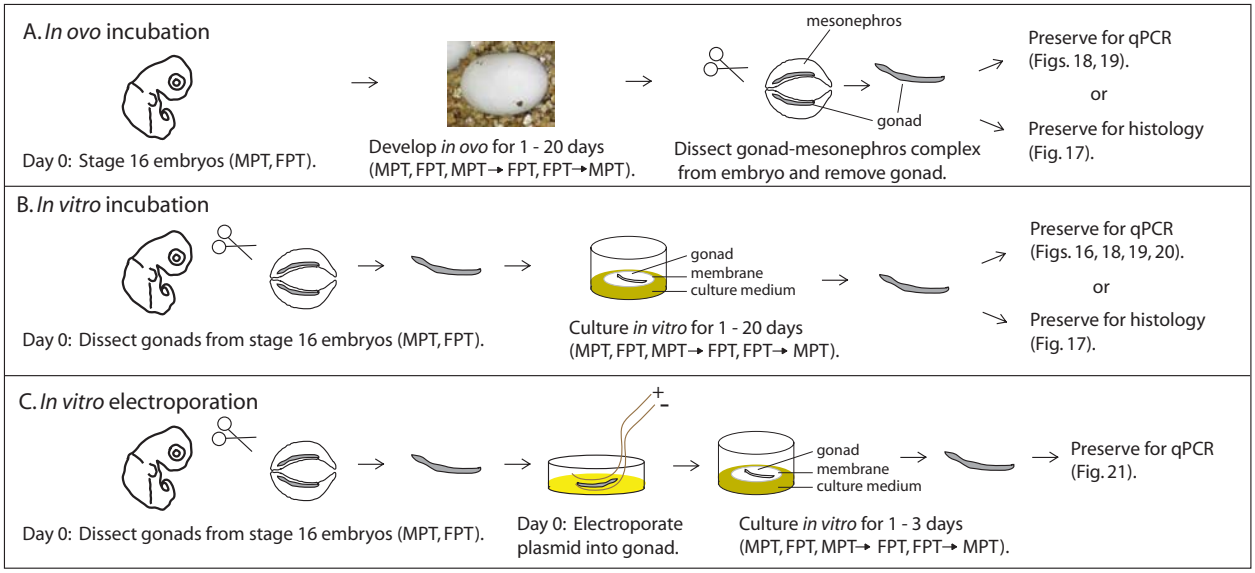

Figure 15. Developmental rate variation at different incubation temperatures.
Red-eared slider turtle embryos developing *in ovo* were dissected and staged by a variety of morphological characteristics, including digit, limb, eye, head, caruncle, carapace, plastron, and body size phenotype (Greenbaum 2002). The number of days development post-stage 16 (= Day 0) is plotted against corresponding developmental stage to show overall rate of embryonic morphological development (n = 7-10 embyros per data point). (A) Comparison of variation in rates of development between MPT, FPT, MPT→FPT and FPT→MPT. (B) Data graphed in (A) is given for reference. (C, D) Rates of development within a constant temperature varies through time, shown at MPT and FPT, respectively. Equations of lines through various subsets of data points are given; particular data points included are indicated by brackets. The slope of the line is a measure of the amount of morphological change occuring in stages per day. Data from individuals is presented in Supplementary Data Table 1.

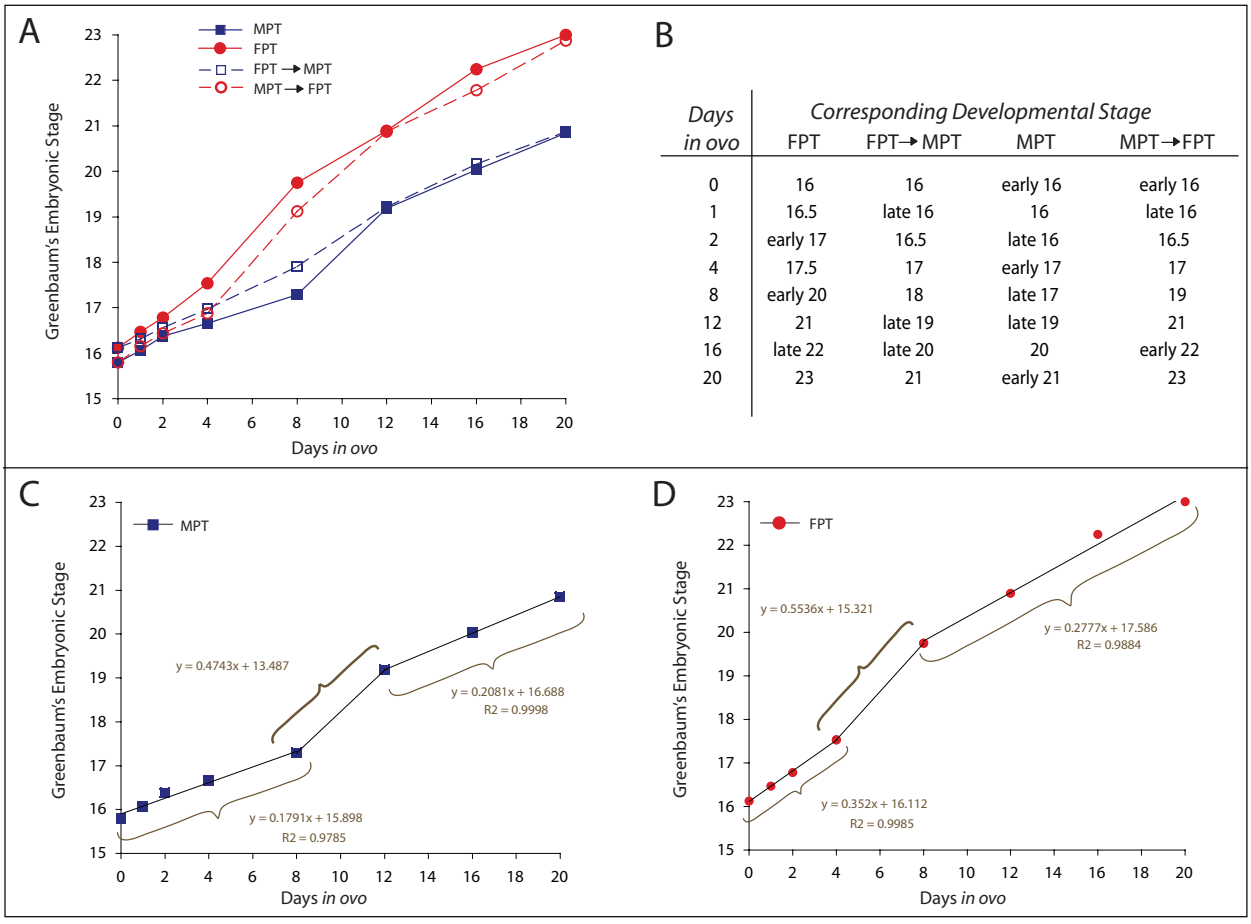

Days in ovo	*Corresponding Developmental Stage*			
	FPT	FPT→MPT	MPT	MPT→FPT
0	16	16	early 16	early 16
1	16.5	late 16	16	late 16
2	early 17	16.5	late 16	16.5
4	17.5	17	early 17	17
8	early 20	18	late 17	19
12	21	late 19	late 19	21
16	late 22	late 20	20	early 22
20	23	21	early 21	23

Figure 16. Effect of phenol red in culture medium on gonadal gene expression.
Gonads were dissected from embryos at Greenbaum's stage 16 (= Day 0) and cultured *in vitro* for up to 16 days in either (A) phenol red-free Leibovitz's L15 culture medium supplemented with charcoal-stripped fetal bovine serum (FBS) or (B) Leibovitz's L-15 containing phenol red supplemented with unstripped FBS. Following culture, gonads were preserved for qPCR analysis. Right y-axes correspond to uncalibrated relative transcript abundance normalized to *PP1* expression, and left y-axes represent normalized values calibrated to the lowest expression point within each gene (n = 3-6 gonads per data point).

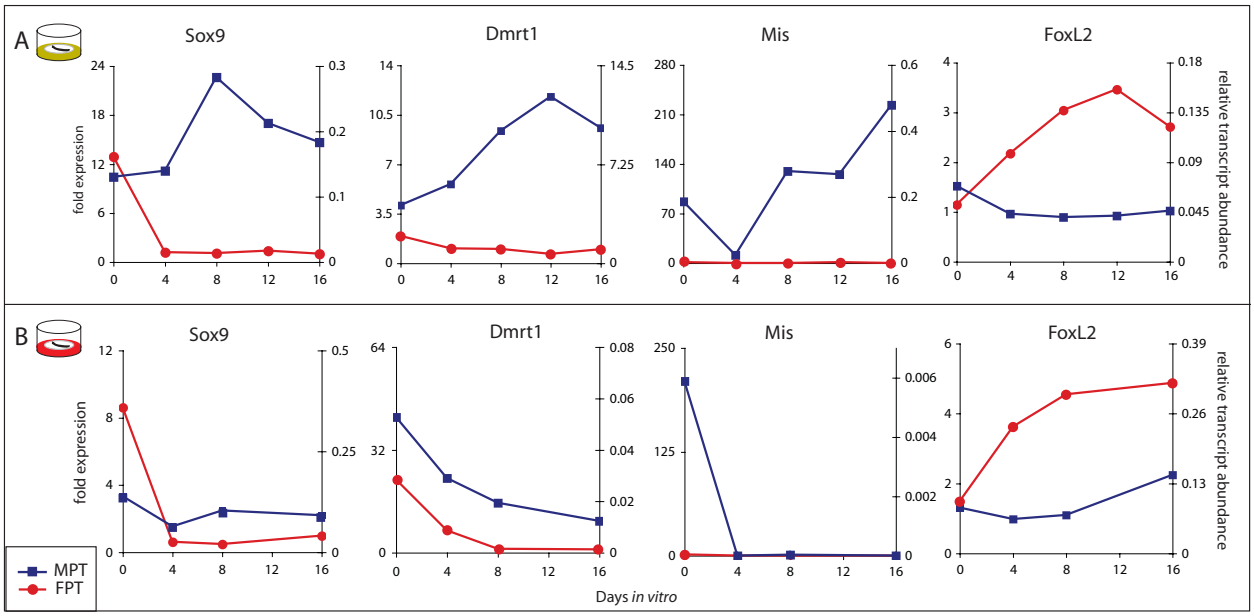

Figure 17. Morphological characteristics of gonad development *in ovo* and *in vitro*.
(A) Developmental progression of embryos incubating *in ovo* at MPT or FPT was monitored. At Greenbaum's embryonic stage 16 (= Day 0), some eggs remained at constant temperatures (i and iii) while others were shifted to the opposite temperature (ii and iv). Following up to 20 days further *in ovo* incubation, embryos were sacrificed and gonads preserved for standard hematoxylin and eosin (H&E) staining. (B) Developmental progression of embryos incubating *in ovo* at MPT or FPT was monitored and at Greenbaum's embryonic stage 16 (= Day 0), embyros were sacrificed and gonads dissected. Gonads from each temperature were cultured *in vitro* at either constant temperatures (v and vii) or in a shifted regime (vi and viii) for up to 20 days and preserved for H&E staining. Bar = 100um; m = medullary region, c = cortex, pgc = primordial germ cell, sc = sex cord.

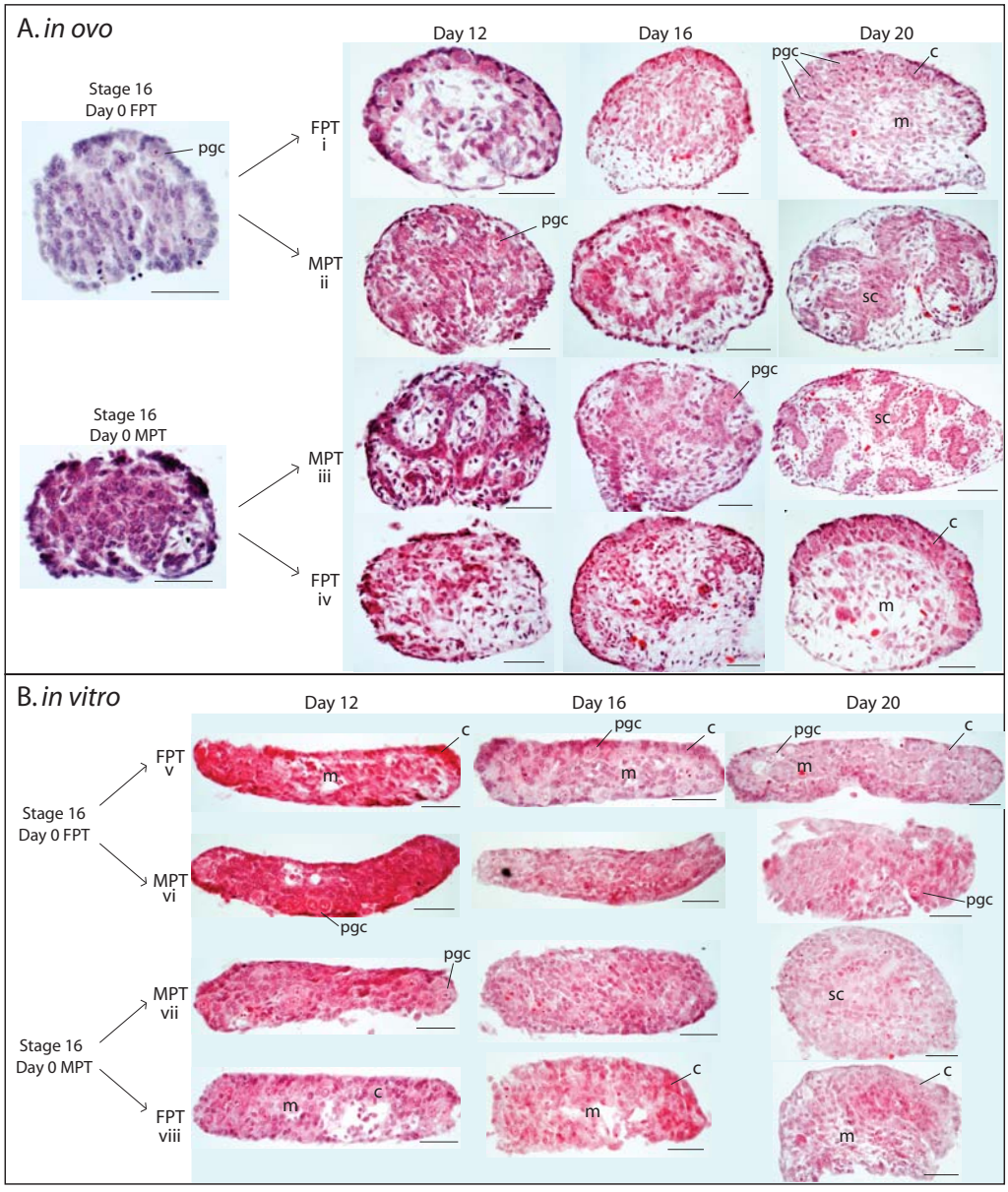

Figure 18. Gonadal expression of *Sox9* in individual turtle gonads *in ovo* and *in vitro*. Embryos developed *in ovo* until Greenbaum's stage 16 (=Day 0), at which point gonads either (A, B) continued developing *in ovo* or (C) were dissected and cultured *in vitro*. Following up to 20 days additional development, gonads were preserved individually for qPCR analysis (n = 7-10 per data point). Right y-axes correspond to relative transcript abundance normalized to constitutive *PP1* expression, and left y-axes of all graphs represent normalized values calibrated to level of *Sox9* at FPT Day 20 *in ovo*. X-axes correspond to (A) Greenbaum's developmental stage, (B) days of development in the egg, or (C) days of development in *in vitro* culture. Gene expression data in A and B is identical but plotted against two different measures of developmental time to illustrate the effect of rate of development at differing incubation temperatures. Thus, the discrepancy in data in (A) between sexes is due to the acceleration of development that occurs at higher temperatures. Statistical comparisons are all made within gene, within day or stage, between temperatures. Expression points contained within the same gray shaded box are not statistically different from each other, while points in separated boxes within one day are statistically different. Points not contained in any shaded box are not statistically different from any other point within the same day. Relationships that could not be accurately described by this shading system are indicated on the graph by a bracket and associated p-value. Asterisks indicate statistical relationships that were too complicated to be accurately described and are described in Supplementary Table 1. Statistics in (A) are identical to those shown in (B). Statistical values for all comparisons can be found in Supplementary Table 1. (D, E) *In situ* hybridization at stage 15 in both FPT and MPT embryos shows localization of *Sox9* transcript in clusters of expressing cells that surround non-expressing cells.

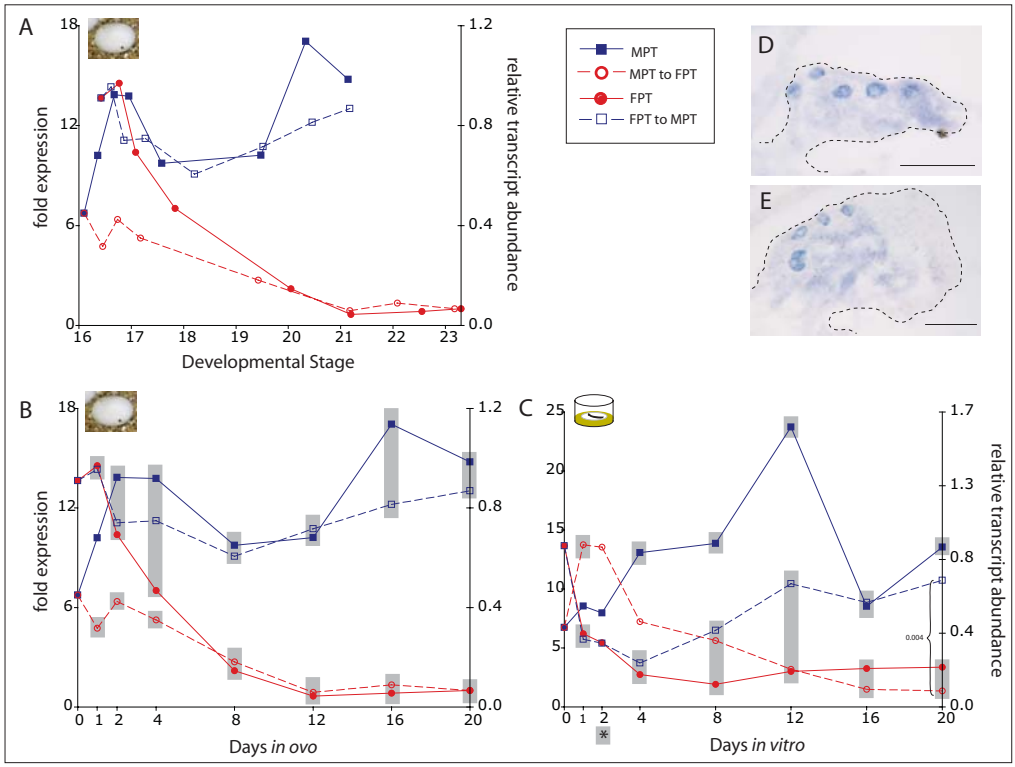

Figure 19. Gonadal expression of *Dmrt1*, *Mis*, and *FoxL2* in individual turtle gonads *in ovo* and *in vitro*.
Embryos developed *in ovo* until Greenbaum's stage 16 (=Day 0), at which point gonads either (A, C, E) continued developing *in ovo* or (B, D, E) were dissected and cultured *in vitro*. After up to 20 days additional development, gonads were preserved individually for qPCR analysis (n = 7-10 per data point). Right y-axes represent relative transcript abundance normalized to *PP1* expression, and left y-axes correspond to normalized values calibrated to expression level at (A, C) FPT Day 20 *in ovo* or (E) MPT Day 20 *in ovo*. X-axes correspond to (A, C, E) days of development in the egg or (B, D, E) days of development in *in vitro* culture. Statistical comparisons indicated by gray shaded boxes are made in the same manner as in Figure 5.

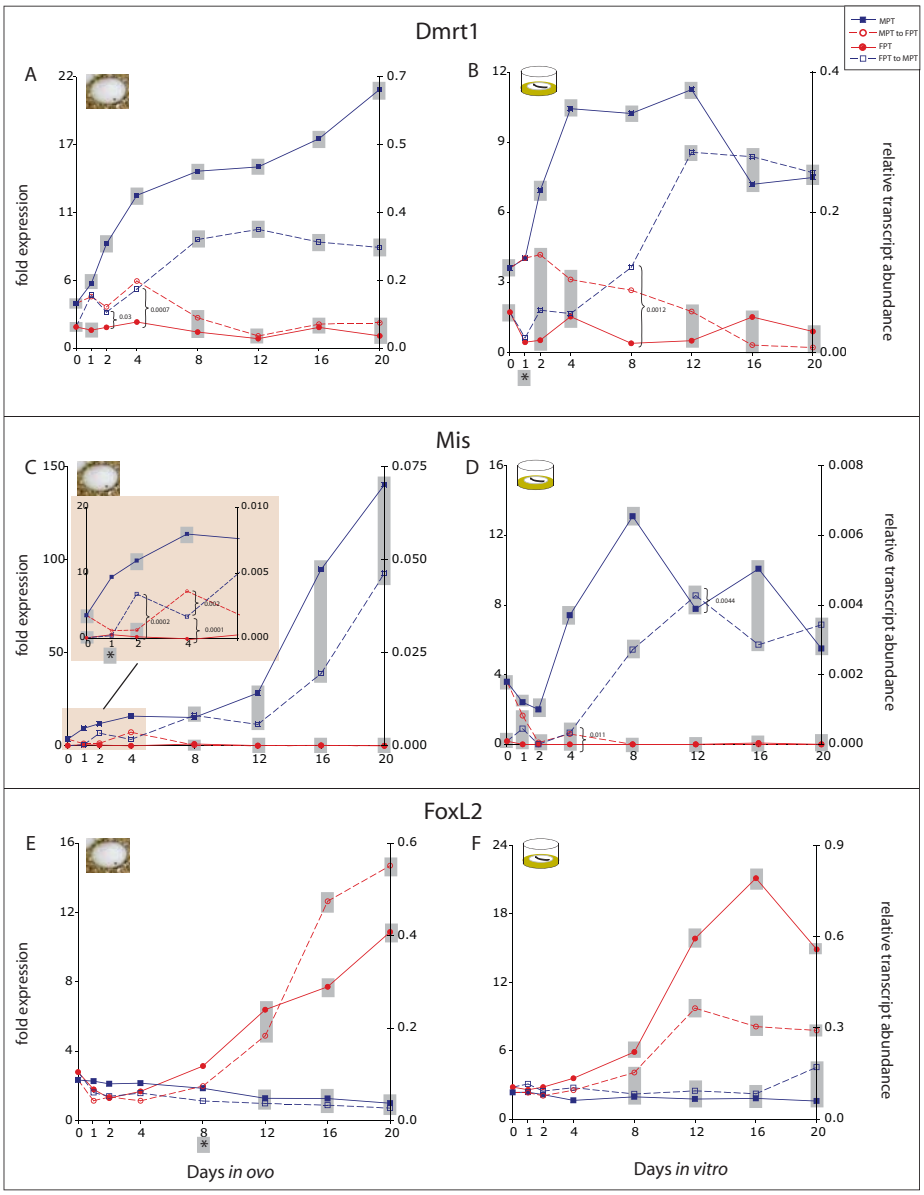

Figure 20. Individual variation in gene expression levels during *in vitro* gonad development.
Data in Figs. 5 and 6 is replotted here to show individual variation among gonads developing *in vitro*.
(A) FPT→MPT gonads were termed "responsive" if they exhibited MPT-typical patterns of gene expression for all genes examined (n= X), "nonresponsive" if they exhibited FPT-typical patterns of gene expression (n=1), and "repressed" if they exhibited decreased gene expression (n=Y). FPT average expression is plotted for comparison. (B) MPT→FPT gonads all exhibited FPT-typical patterns of gene expression and were termed "responsive". MPT average expression is plotted for comparison.

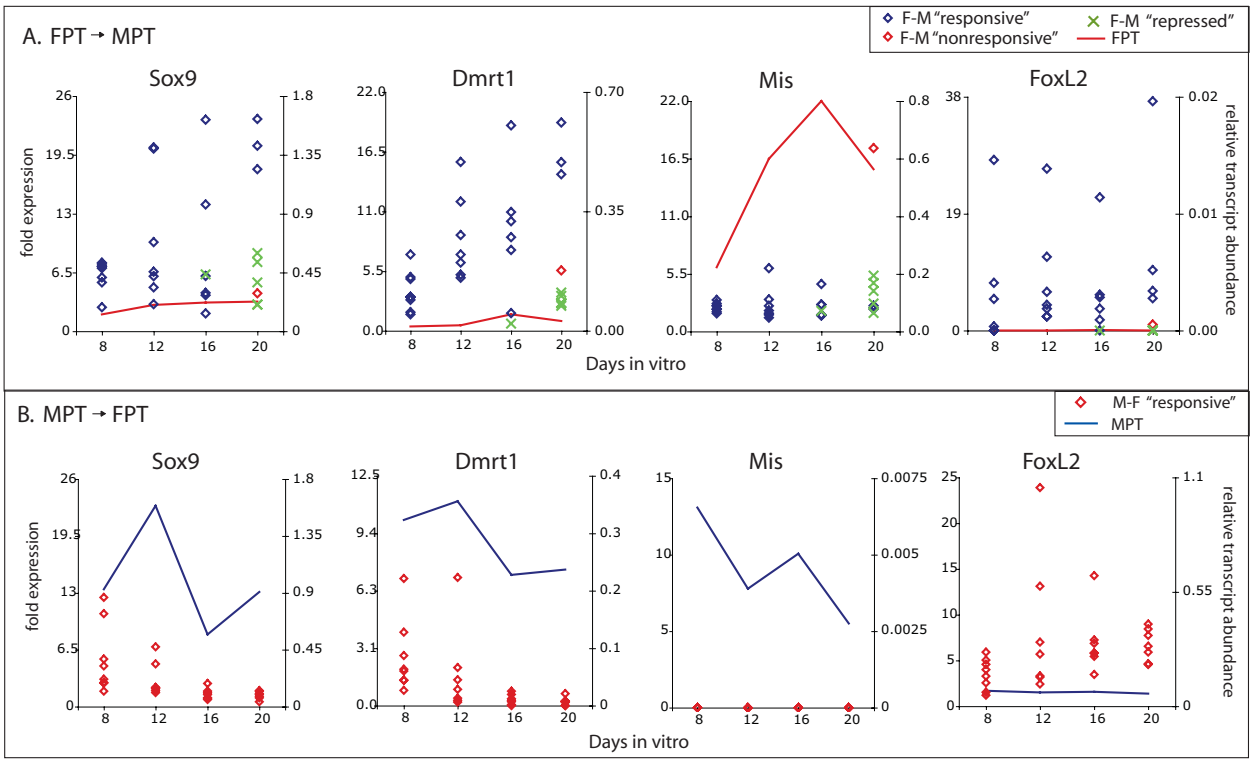

Figure 21. Misexpression of *Sox9* in gonads developing *in vitro* at female-producting temperatures.
Gonads were dissected from embryos incubating at FPT at stage 16, electroporated with a fusion construct and cultured *in vitro* at FPT for up to three days. Electroporation efficiency evaluated by GFP expression under fluorescence is shown in two typical gonads at Day 1 for (A) pCS107:GFP and (B) pCS107:GFP:Sox9. (C) Effect of plasmid electroporation on gene expression was measured by qPCR and average relative transcript abundance is plotted with standard error bars (n=12 to 20 gonads per data point).

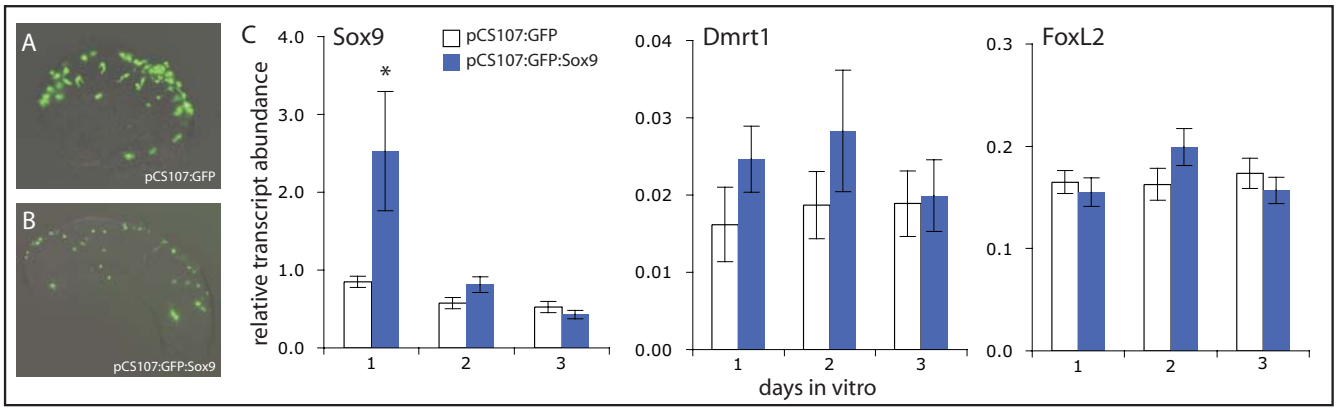

Table 5. Data from staging embryos used in analyzing rates of development in Figure 15.

Sex	Day	Stages of Individual Embryos								average	Stage
FPT	0	15.75	15.75	16	16	16.25	16.25	16.5	16.5	16.13	16
FPT	1	16.5	16.5	16.25	16.5	16.5	16.5	16.5	16.5	16.47	16.5
FPT	2	16.75	16.75	17	16.5	17	17	16.75	16.5	16.78	early 17
FPT	4	17.75	17.25	17.75	17.25	17.25	17.75	17.75		17.54	17.5
FPT	8	19.75	19.75	19.75	20	20	19.75	19.25	19.75	19.75	early 20
FPT	12	20.75	21	21	21	20.75	21	20.75		20.89	21
FPT	16	22	22.25	22.75	22.25	22.25	22.25	22		22.25	late 22
FPT	20	23	22.75	23	23	23	23.25	23		23.00	23
FPT-->MPT	1	16.25	16.5	16.25	16.25	16.5	16.25	16.25	16.25	16.31	late 16
FPT-->MPT	2	16.5	16.75	16.5	16.5	16.75	16.5	16.5	16.5	16.56	16.5
FPT-->MPT	4	17	17	17	17	17	17	17	16.75	16.97	17
FPT-->MPT	8	17.75	18	18	18	17.75	18	18	17.75	17.91	18
FPT-->MPT	12	19.75	19.75	18.75	19.75	18	20	19.75	18	19.22	late 19
FPT-->MPT	16	20.25	20.25	20	20.25	20.25	20.25	20	20	20.16	late 20
FPT-->MPT	20	20.75	20.75	21	21.25	20.75	20.75	20.75	21	20.88	21
MPT	0	15.75	15.75	16	15.75	15.75	16	16	16	15.88	early 16
MPT	1	16	16.25	16	16	16	16.25	16.25	15.75	16.06	16
MPT	2	16.5	16.5	16.25	16.25	16.5	16.25	16.25	16.5	16.38	late 16
MPT	4	17	16.5	17	16.5	16.5	16.5	16.75	16.5	16.66	early 17
MPT	8	17.75	17.25	17.75	17	17.25	17	17	17.25	17.28	late 17
MPT	12	19.25	19.25	19.25	19.75	18.75	19	19		19.18	late 19
MPT	16	19.75	20	20	20	20	20.25	20	20.25	20.03	20
MPT	20	21	21	20.75	21	21	21	20.25	20.75	20.84	early 21
MPT-->FPT	1	16	16.25	16.25	16.25	16	16	16.25	16.25	16.16	late 16
MPT-->FPT	2	16.25	16.5	16.5	16.5	16.5	16.5	16.25	16.5	16.44	16.5
MPT-->FPT	4	17	17	16.75	17	16.5	16.75	17	17	16.88	17
MPT-->FPT	8	19.75	18.25	19.25	19.25	19	19.25	19.25	19	19.13	19
MPT-->FPT	12	20.75	21	21	20.75	20.75	20.75	21	21	20.88	21
MPT-->FPT	16	21.75	21.75	21.25	22	22	22	21.75	21.75	21.78	early 22
MPT-->FPT	20	22.75	23	22.75	22.75	23	22.75	23	23	22.88	23

Table 6. Type 3 Tests of Fixed Effects

Gene, tissue	Effect	Num DF	Den DF	F Value	Pr > F
FoxL2 ovo	sex	3	210	4.65	0.0036
	day	1	210	66.85	<.0001
	day*sex	3	210	35.60	<.0001
FoxL2 vitro	sex	3	196	0.13	0.9438
	day	1	196	32.60	<.0001
	day*sex	3	196	13.22	<.0001
Sox9 ovo	sex	3	210	3.79	0.0112
	day	1	210	7.61	0.0063
	day*sex	3	210	11.56	<.0001
Sox9 vitro	sex	3	196	3.98	0.0088
	day	1	196	0.31	0.5800
	day*sex	3	196	5.99	0.0006
Dmrt1 ovo	sex	3	210	4.95	0.0024
	day	1	210	27.54	<.0001
	day*sex	3	210	25.85	<.0001
Dmrt1 vitro	sex	3	196	10.48	<.0001
	day	1	196	2.89	0.0906
	day*sex	3	196	8.40	<.0001
Mis ovo	sex	3	210	10.83	<.0001
	day	1	210	8.19	0.0046
	day*sex	3	210	22.22	<.0001
Mis vitro	sex	3	196	10.95	<.0001
	day	1	196	2.18	0.1412
	day*sex	3	196	4.09	0.0077

Table 7. Differences of Least Squares Means, adjusted by Tukey-Kramer

Gene	sex	sex	day	Estimate	Std Error	DF	T value	Pr > F	Adj P
FoxL2	FPT	MPT	0.00	-0.04982	0.03481	210	-1.43	0.1539	0.4813
ovo	F-M	FPT	1.00	0.004128	0.03559	210	0.12	0.9078	0.9994
	F-M	M-F	1.00	0.08169	0.03858	210	2.12	0.0354	0.1509
	F-M	MPT	1.00	-0.02643	0.03565	210	-0.74	0.4594	0.8803
	FPT	M-F	1.00	0.07756	0.03559	210	2.18	0.0304	0.1325
	FPT	MPT	1.00	-0.03055	0.03240	210	-0.94	0.3468	0.7817
	M-F	MPT	1.00	-0.1081	0.03565	210	-3.03	0.0027	0.0144
	F-M	FPT	2.00	-0.01430	0.03310	210	-0.43	0.6661	0.9729
	F-M	M-F	2.00	0.05150	0.03584	210	1.44	0.1521	0.4776
	F-M	MPT	2.00	-0.02559	0.03315	210	-0.77	0.4411	0.8671
	FPT	M-F	2.00	0.06580	0.03310	210	1.99	0.0481	0.1957
	FPT	MPT	2.00	-0.01129	0.03017	210	-0.37	0.7087	0.9821
	M-F	MPT	2.00	-0.07709	0.03315	210	-2.33	0.0210	0.0955
	F-M	FPT	4.00	-0.05116	0.02876	210	-1.78	0.0767	0.2863
	F-M	M-F	4.00	-0.00886	0.03095	210	-0.29	0.7750	0.9918
	F-M	MPT	4.00	-0.02391	0.02879	210	-0.83	0.4072	0.8399
	FPT	M-F	4.00	0.04230	0.02876	210	1.47	0.1428	0.4569
	FPT	MPT	4.00	0.02724	0.02642	210	1.03	0.3037	0.7314
	M-F	MPT	4.00	-0.01506	0.02879	210	-0.52	0.6016	0.9535
	F-M	FPT	8.00	-0.1249	0.02427	210	-5.15	<.0001	<.0001
	F-M	M-F	8.00	-0.1296	0.02513	210	-5.16	<.0001	<.0001
	F-M	MPT	8.00	-0.02057	0.02418	210	-0.85	0.3960	0.8302
	FPT	M-F	8.00	-0.00471	0.02427	210	-0.19	0.8463	0.9974
	FPT	MPT	8.00	0.1043	0.02329	210	4.48	<.0001	<.0001
	M-F	MPT	8.00	0.1090	0.02418	210	4.51	<.0001	<.0001
	F-M	FPT	12.00	-0.1986	0.02738	210	-7.25	<.0001	<.0001
	F-M	M-F	12.00	-0.2503	0.02721	210	-9.20	<.0001	<.0001
	F-M	MPT	12.00	-0.01722	0.02711	210	-0.64	0.5260	0.9206
	FPT	M-F	12.00	-0.05172	0.02738	210	-1.89	0.0603	0.2360
	FPT	MPT	12.00	0.1814	0.02729	210	6.65	<.0001	<.0001
	M-F	MPT	12.00	0.2331	0.02711	210	8.60	<.0001	<.0001
	F-M	FPT	16.00	-0.2723	0.03619	210	-7.52	<.0001	<.0001
	F-M	M-F	16.00	-0.3710	0.03584	210	-10.35	<.0001	<.0001
	F-M	MPT	16.00	-0.01387	0.03577	210	-0.39	0.6986	0.9801
	FPT	M-F	16.00	-0.09873	0.03619	210	-2.73	0.0069	0.0346
	FPT	MPT	16.00	0.2584	0.03612	210	7.15	<.0001	<.0001
	M-F	MPT	16.00	0.3572	0.03577	210	9.99	<.0001	<.0001
	F-M	FPT	20.00	-0.3460	0.04762	210	-7.27	<.0001	<.0001
	F-M	M-F	20.00	-0.4918	0.04757	210	-10.34	<.0001	<.0001
	F-M	MPT	20.00	-0.01052	0.04710	210	-0.22	0.8235	0.9961
	FPT	M-F	20.00	-0.1457	0.04762	210	-3.06	0.0025	0.0132
	FPT	MPT	20.00	0.3355	0.04714	210	7.12	<.0001	<.0001
	M-F	MPT	20.00	0.4812	0.04710	210	10.22	<.0001	<.0001

Gene	sex	sex	day	Estimate	Std Error	DF	T value	Pr > F	Adj P
FoxL2	vFPT	vMPT	0.00	-0.03470	0.07009	196	-0.50	0.6211	0.9601
vitro	vF-M	vFPT	1.00	0.007418	0.06546	196	0.11	0.9099	0.9995
	vF-M	vM-F	1.00	0.007260	0.06553	196	0.11	0.9119	0.9995
	vF-M	vMPT	1.00	0.008304	0.06497	196	0.13	0.8984	0.9993
	vFPT	vM-F	1.00	-0.00016	0.06576	196	-0.00	0.9981	1.0000
	vFPT	vMPT	1.00	0.000886	0.06520	196	0.01	0.9892	1.0000
	vM-F	vMPT	1.00	0.001044	0.06527	196	0.02	0.9873	1.0000
	vF-M	vFPT	2.00	-0.02466	0.06087	196	-0.41	0.6858	0.9775
	vF-M	vM-F	2.00	-0.00481	0.06091	196	-0.08	0.9372	0.9998
	vF-M	vMPT	2.00	0.01181	0.06039	196	0.20	0.8451	0.9973
	vFPT	vM-F	2.00	0.01985	0.06109	196	0.33	0.7455	0.9881
	vFPT	vMPT	2.00	0.03648	0.06057	196	0.60	0.5477	0.9313
	vM-F	vMPT	2.00	0.01662	0.06061	196	0.27	0.7842	0.9928
	vF-M	vFPT	4.00	-0.08882	0.05269	196	-1.69	0.0934	0.3340
	vF-M	vM-F	4.00	-0.02894	0.05271	196	-0.55	0.5836	0.9467
	vF-M	vMPT	4.00	0.01883	0.05225	196	0.36	0.7189	0.9839
	vFPT	vM-F	4.00	0.05988	0.05278	196	1.13	0.2579	0.6686
	vFPT	vMPT	4.00	0.1077	0.05232	196	2.06	0.0410	0.1709
	vM-F	vMPT	4.00	0.04777	0.05234	196	0.91	0.3625	0.7981
	vF-M	vFPT	8.00	-0.2171	0.04293	196	-5.06	<.0001	<.0001
	vF-M	vM-F	8.00	-0.07721	0.04300	196	-1.80	0.0741	0.2785
	vF-M	vMPT	8.00	0.03287	0.04267	196	0.77	0.4420	0.8677
	vFPT	vM-F	8.00	0.1399	0.04297	196	3.26	0.0013	0.0072
	vFPT	vMPT	8.00	0.2500	0.04264	196	5.86	<.0001	<.0001
	vM-F	vMPT	8.00	0.1101	0.04271	196	2.58	0.0107	0.0518
	vF-M	vFPT	12.00	-0.3455	0.04628	196	-7.47	<.0001	<.0001
	vF-M	vM-F	12.00	-0.1255	0.04654	196	-2.70	0.0076	0.0379
	vF-M	vMPT	12.00	0.04691	0.04629	196	1.01	0.3122	0.7418
	vFPT	vM-F	12.00	0.2200	0.04667	196	4.71	<.0001	<.0001
	vFPT	vMPT	12.00	0.3924	0.04642	196	8.45	<.0001	<.0001
	vM-F	vMPT	12.00	0.1724	0.04669	196	3.69	0.0003	0.0016
	vF-M	vFPT	16.00	-0.4738	0.06059	196	-7.82	<.0001	<.0001
	vF-M	vM-F	16.00	-0.1737	0.06108	196	-2.84	0.0049	0.0252
	vF-M	vMPT	16.00	0.06095	0.06081	196	1.00	0.3174	0.7482
	vFPT	vM-F	16.00	0.3000	0.06149	196	4.88	<.0001	<.0001
	vFPT	vMPT	16.00	0.5347	0.06122	196	8.73	<.0001	<.0001
	vM-F	vMPT	16.00	0.2347	0.06170	196	3.80	0.0002	0.0011
	vF-M	vFPT	20.00	-0.6021	0.08021	196	-7.51	<.0001	<.0001
	vF-M	vM-F	20.00	-0.2220	0.08089	196	-2.74	0.0066	0.0332
	vF-M	vMPT	20.00	0.07499	0.08052	196	0.93	0.3528	0.7881
	vFPT	vM-F	20.00	0.3801	0.08158	196	4.66	<.0001	<.0001
	vFPT	vMPT	20.00	0.6771	0.08122	196	8.34	<.0001	<.0001
	vM-F	vMPT	20.00	0.2970	0.08189	196	3.63	0.0004	0.0021

Gene	sex	sex	day	Estimate	Std Error	DF	T value	Pr > F	Adj P
Sox9	FPT	MPT	0.00	0.1320	0.1207	210	1.09	0.2756	0.6942
ovo	F-M	FPT	1.00	0.02735	0.1234	210	0.22	0.8248	0.9962
	F-M	M-F	1.00	0.4139	0.1337	210	3.10	0.0022	0.0119
	F-M	MPT	1.00	0.09381	0.1236	210	0.76	0.4487	0.8727
	FPT	M-F	1.00	0.3866	0.1234	210	3.13	0.0020	0.0106
	FPT	MPT	1.00	0.06646	0.1124	210	0.59	0.5549	0.9346
	M-F	MPT	1.00	-0.3201	0.1236	210	-2.59	0.0103	0.0500
	F-M	FPT	2.00	0.07567	0.1148	210	0.66	0.5104	0.9122
	F-M	M-F	2.00	0.4333	0.1242	210	3.49	0.0006	0.0033
	F-M	MPT	2.00	0.07660	0.1149	210	0.67	0.5059	0.9096
	FPT	M-F	2.00	0.3576	0.1148	210	3.12	0.0021	0.0112
	FPT	MPT	2.00	0.000935	0.1047	210	0.01	0.9929	1.0000
	M-F	MPT	2.00	-0.3567	0.1149	210	-3.10	0.0022	0.0116
	F-M	FPT	4.00	0.1723	0.09971	210	1.73	0.0855	0.3118
	F-M	M-F	4.00	0.4720	0.1073	210	4.40	<.0001	0.0001
	F-M	MPT	4.00	0.04218	0.09983	210	0.42	0.6731	0.9746
	FPT	M-F	4.00	0.2997	0.09971	210	3.01	0.0030	0.0156
	FPT	MPT	4.00	-0.1301	0.09164	210	-1.42	0.1572	0.4884
	M-F	MPT	4.00	-0.4299	0.09983	210	-4.31	<.0001	0.0001
	F-M	FPT	8.00	0.3656	0.08411	210	4.35	<.0001	0.0001
	F-M	M-F	8.00	0.5495	0.08710	210	6.31	<.0001	<.0001
	F-M	MPT	8.00	-0.02666	0.08383	210	-0.32	0.7508	0.9888
	FPT	M-F	8.00	0.1840	0.08411	210	2.19	0.0298	0.1302
	FPT	MPT	8.00	-0.3922	0.08072	210	-4.86	<.0001	<.0001
	M-F	MPT	8.00	-0.5762	0.08383	210	-6.87	<.0001	<.0001
	F-M	FPT	12.00	0.5588	0.09485	210	5.89	<.0001	<.0001
	F-M	M-F	12.00	0.6270	0.09431	210	6.65	<.0001	<.0001
	F-M	MPT	12.00	-0.09549	0.09397	210	-1.02	0.3107	0.7401
	FPT	M-F	12.00	0.06819	0.09485	210	0.72	0.4730	0.8895
	FPT	MPT	12.00	-0.6543	0.09451	210	-6.92	<.0001	<.0001
	M-F	MPT	12.00	-0.7225	0.09397	210	-7.69	<.0001	<.0001
	F-M	FPT	16.00	0.7521	0.1253	210	6.00	<.0001	<.0001
	F-M	M-F	16.00	0.7045	0.1242	210	5.67	<.0001	<.0001
	F-M	MPT	16.00	-0.1643	0.1240	210	-1.33	0.1865	0.5478
	FPT	M-F	16.00	-0.04759	0.1253	210	-0.38	0.7045	0.9813
	FPT	MPT	16.00	-0.9164	0.1251	210	-7.33	<.0001	<.0001
	M-F	MPT	16.00	-0.8688	0.1240	210	-7.01	<.0001	<.0001
	F-M	FPT	20.00	0.9453	0.1649	210	5.73	<.0001	<.0001
	F-M	M-F	20.00	0.7820	0.1649	210	4.74	<.0001	<.0001
	F-M	MPT	20.00	-0.2332	0.1633	210	-1.43	0.1547	0.4832
	FPT	M-F	20.00	-0.1634	0.1649	210	-0.99	0.3231	0.7550
	FPT	MPT	20.00	-1.1785	0.1633	210	-7.22	<.0001	<.0001
	M-F	MPT	20.00	-1.0152	0.1633	210	-6.22	<.0001	<.0001

Gene	sex	sex	day	Estimate	Std Error	DF	T value	Pr > F	Adj P
Sox9	vFPT	vMPT	0.00	-0.3904	0.1944	196	-2.01	0.0460	0.1884
vitro	vF-M	vFPT	1.00	0.01501	0.1820	196	0.08	0.9344	0.9998
	vF-M	vM-F	1.00	-0.4786	0.1822	196	-2.63	0.0093	0.0456
	vF-M	vMPT	1.00	-0.3995	0.1803	196	-2.22	0.0279	0.1226
	vFPT	vM-F	1.00	-0.4936	0.1827	196	-2.70	0.0075	0.0374
	vFPT	vMPT	1.00	-0.4145	0.1808	196	-2.29	0.0230	0.1034
	vM-F	vMPT	1.00	0.07906	0.1811	196	0.44	0.6629	0.9721
	vF-M	vFPT	2.00	0.04356	0.1692	196	0.26	0.7971	0.9940
	vF-M	vM-F	2.00	-0.4125	0.1694	196	-2.44	0.0158	0.0739
	vF-M	vMPT	2.00	-0.3950	0.1676	196	-2.36	0.0194	0.0890
	vFPT	vM-F	2.00	-0.4560	0.1698	196	-2.69	0.0078	0.0389
	vFPT	vMPT	2.00	-0.4386	0.1680	196	-2.61	0.0097	0.0475
	vM-F	vMPT	2.00	0.01747	0.1681	196	0.10	0.9174	0.9996
	vF-M	vFPT	4.00	0.1007	0.1465	196	0.69	0.4927	0.9018
	vF-M	vM-F	4.00	-0.2803	0.1465	196	-1.91	0.0573	0.2261
	vF-M	vMPT	4.00	-0.3860	0.1450	196	-2.66	0.0084	0.0415
	vFPT	vM-F	4.00	-0.3809	0.1467	196	-2.60	0.0101	0.0492
	vFPT	vMPT	4.00	-0.4867	0.1451	196	-3.35	0.0010	0.0053
	vM-F	vMPT	4.00	-0.1057	0.1452	196	-0.73	0.4674	0.8857
	vF-M	vFPT	8.00	0.2149	0.1193	196	1.80	0.0733	0.2760
	vF-M	vM-F	8.00	-0.01586	0.1196	196	-0.13	0.8946	0.9992
	vF-M	vMPT	8.00	-0.3680	0.1185	196	-3.11	0.0022	0.0116
	vFPT	vM-F	8.00	-0.2308	0.1195	196	-1.93	0.0548	0.2182
	vFPT	vMPT	8.00	-0.5829	0.1184	196	-4.92	<.0001	<.0001
	vM-F	vMPT	8.00	-0.3521	0.1186	196	-2.97	0.0034	0.0176
	vF-M	vFPT	12.00	0.3291	0.1286	196	2.56	0.0113	0.0544
	vF-M	vM-F	12.00	0.2485	0.1295	196	1.92	0.0565	0.2236
	vF-M	vMPT	12.00	-0.3500	0.1287	196	-2.72	0.0071	0.0356
	vFPT	vM-F	12.00	-0.08060	0.1298	196	-0.62	0.5355	0.9253
	vFPT	vMPT	12.00	-0.6791	0.1290	196	-5.26	<.0001	<.0001
	vM-F	vMPT	12.00	-0.5985	0.1299	196	-4.61	<.0001	<.0001
	vF-M	vFPT	16.00	0.4434	0.1685	196	2.63	0.0092	0.0450
	vF-M	vM-F	16.00	0.5129	0.1701	196	3.02	0.0029	0.0153
	vF-M	vMPT	16.00	-0.3319	0.1692	196	-1.96	0.0512	0.2061
	vFPT	vM-F	16.00	0.06957	0.1711	196	0.41	0.6847	0.9772
	vFPT	vMPT	16.00	-0.7753	0.1702	196	-4.56	<.0001	<.0001
	vM-F	vMPT	16.00	-0.8449	0.1718	196	-4.92	<.0001	<.0001
	vF-M	vFPT	20.00	0.5576	0.2230	196	2.50	0.0132	0.0630
	vF-M	vM-F	20.00	0.7773	0.2253	196	3.45	0.0007	0.0038
	vF-M	vMPT	20.00	-0.3139	0.2241	196	-1.40	0.1628	0.5002
	vFPT	vM-F	20.00	0.2197	0.2269	196	0.97	0.3341	0.7677
	vFPT	vMPT	20.00	-0.8715	0.2257	196	-3.86	0.0002	0.0009
	vM-F	vMPT	20.00	-1.0912	0.2280	196	-4.79	<.0001	<.0001

Gene	sex	sex	day	Estimate	Std Error	DF	T value	Pr > F	Adj P
Dmrt1	FPT	MPT	0.00	-0.1379	0.03594	210	-3.84	0.0002	0.0009
ovo	F-M	FPT	1.00	0.08670	0.03692	210	2.35	0.0198	0.0907
	F-M	M-F	1.00	0.01036	0.04024	210	0.26	0.7971	0.9940
	F-M	MPT	1.00	-0.07619	0.03708	210	-2.05	0.0411	0.1715
	FPT	M-F	1.00	-0.07634	0.03692	210	-2.07	0.0399	0.1672
	FPT	MPT	1.00	-0.1629	0.03345	210	-4.87	<.0001	<.0001
	M-F	MPT	1.00	-0.08655	0.03708	210	-2.33	0.0205	0.0936
	F-M	FPT	2.00	0.09684	0.03433	210	2.82	0.0053	0.0268
	F-M	M-F	2.00	0.02417	0.03738	210	0.65	0.5186	0.9166
	F-M	MPT	2.00	-0.09104	0.03448	210	-2.64	0.0089	0.0438
	FPT	M-F	2.00	-0.07267	0.03433	210	-2.12	0.0355	0.1512
	FPT	MPT	2.00	-0.1879	0.03115	210	-6.03	<.0001	<.0001
	M-F	MPT	2.00	-0.1152	0.03448	210	-3.34	0.0010	0.0054
	F-M	FPT	4.00	0.1171	0.02985	210	3.92	0.0001	0.0007
	F-M	M-F	4.00	0.05179	0.03228	210	1.60	0.1101	0.3783
	F-M	MPT	4.00	-0.1207	0.02995	210	-4.03	<.0001	0.0004
	FPT	M-F	4.00	-0.06532	0.02985	210	-2.19	0.0298	0.1300
	FPT	MPT	4.00	-0.2379	0.02732	210	-8.71	<.0001	<.0001
	M-F	MPT	4.00	-0.1725	0.02995	210	-5.76	<.0001	<.0001
	F-M	FPT	8.00	0.1577	0.02538	210	6.21	<.0001	<.0001
	F-M	M-F	8.00	0.1070	0.02621	210	4.08	<.0001	0.0004
	F-M	MPT	8.00	-0.1802	0.02519	210	-7.15	<.0001	<.0001
	FPT	M-F	8.00	-0.05062	0.02538	210	-1.99	0.0474	0.1935
	FPT	MPT	8.00	-0.3378	0.02433	210	-13.89	<.0001	<.0001
	M-F	MPT	8.00	-0.2872	0.02519	210	-11.40	<.0001	<.0001
	F-M	FPT	12.00	0.1982	0.02889	210	6.86	<.0001	<.0001
	F-M	M-F	12.00	0.1623	0.02838	210	5.72	<.0001	<.0001
	F-M	MPT	12.00	-0.2396	0.02827	210	-8.47	<.0001	<.0001
	FPT	M-F	12.00	-0.03592	0.02889	210	-1.24	0.2152	0.6001
	FPT	MPT	12.00	-0.4378	0.02878	210	-15.21	<.0001	<.0001
	M-F	MPT	12.00	-0.4019	0.02827	210	-14.21	<.0001	<.0001
	F-M	FPT	16.00	0.2387	0.03824	210	6.24	<.0001	<.0001
	F-M	M-F	16.00	0.2175	0.03738	210	5.82	<.0001	<.0001
	F-M	MPT	16.00	-0.2990	0.03731	210	-8.01	<.0001	<.0001
	FPT	M-F	16.00	-0.02121	0.03824	210	-0.55	0.5796	0.9452
	FPT	MPT	16.00	-0.5377	0.03817	210	-14.09	<.0001	<.0001
	M-F	MPT	16.00	-0.5165	0.03731	210	-13.85	<.0001	<.0001
	F-M	FPT	20.00	0.2793	0.05027	210	5.56	<.0001	<.0001
	F-M	M-F	20.00	0.2728	0.04962	210	5.50	<.0001	<.0001
	F-M	MPT	20.00	-0.3584	0.04911	210	-7.30	<.0001	<.0001
	FPT	M-F	20.00	-0.00651	0.05027	210	-0.13	0.8970	0.9992
	FPT	MPT	20.00	-0.6377	0.04976	210	-12.82	<.0001	<.0001
	M-F	MPT	20.00	-0.6312	0.04911	210	-12.85	<.0001	<.0001

Gene	sex	sex	day	Estimate	Std Error	DF	T value	Pr > F	Adj P
Dmrt1	vFPT	vMPT	0.00	-0.2134	0.04465	196	-4.78	<.0001	<.0001
vitro	vF-M	vFPT	1.00	0.01671	0.04242	196	0.39	0.6940	0.9792
	vF-M	vM-F	1.00	-0.09157	0.04254	196	-2.15	0.0326	0.1404
	vF-M	vMPT	1.00	-0.1989	0.04152	196	-4.79	<.0001	<.0001
	vFPT	vM-F	1.00	-0.1083	0.04255	196	-2.54	0.0117	0.0563
	vFPT	vMPT	1.00	-0.2157	0.04153	196	-5.19	<.0001	<.0001
	vM-F	vMPT	1.00	-0.1074	0.04166	196	-2.58	0.0107	0.0518
	vF-M	vFPT	2.00	0.02938	0.03945	196	0.74	0.4573	0.8788
	vF-M	vM-F	2.00	-0.07135	0.03953	196	-1.80	0.0726	0.2741
	vF-M	vMPT	2.00	-0.1885	0.03858	196	-4.89	<.0001	<.0001
	vFPT	vM-F	2.00	-0.1007	0.03953	196	-2.55	0.0116	0.0558
	vFPT	vMPT	2.00	-0.2179	0.03858	196	-5.65	<.0001	<.0001
	vM-F	vMPT	2.00	-0.1172	0.03866	196	-3.03	0.0028	0.0146
	vF-M	vFPT	4.00	0.05471	0.03416	196	1.60	0.1109	0.3802
	vF-M	vM-F	4.00	-0.03092	0.03419	196	-0.90	0.3671	0.8027
	vF-M	vMPT	4.00	-0.1677	0.03337	196	-5.03	<.0001	<.0001
	vFPT	vM-F	4.00	-0.08563	0.03418	196	-2.51	0.0130	0.0622
	vFPT	vMPT	4.00	-0.2224	0.03335	196	-6.67	<.0001	<.0001
	vM-F	vMPT	4.00	-0.1368	0.03338	196	-4.10	<.0001	0.0004
	vF-M	vFPT	8.00	0.1054	0.02784	196	3.78	0.0002	0.0012
	vF-M	vM-F	8.00	0.04996	0.02798	196	1.79	0.0757	0.2833
	vF-M	vMPT	8.00	-0.1261	0.02739	196	-4.60	<.0001	<.0001
	vFPT	vM-F	8.00	-0.05541	0.02793	196	-1.98	0.0487	0.1977
	vFPT	vMPT	8.00	-0.2315	0.02735	196	-8.46	<.0001	<.0001
	vM-F	vMPT	8.00	-0.1761	0.02749	196	-6.41	<.0001	<.0001
	vF-M	vFPT	12.00	0.1560	0.02998	196	5.21	<.0001	<.0001
	vF-M	vM-F	12.00	0.1308	0.03051	196	4.29	<.0001	0.0002
	vF-M	vMPT	12.00	-0.08449	0.03006	196	-2.81	0.0054	0.0277
	vFPT	vM-F	12.00	-0.02520	0.03046	196	-0.83	0.4091	0.8415
	vFPT	vMPT	12.00	-0.2405	0.03002	196	-8.01	<.0001	<.0001
	vM-F	vMPT	12.00	-0.2153	0.03055	196	-7.05	<.0001	<.0001
	vF-M	vFPT	16.00	0.2067	0.03921	196	5.27	<.0001	<.0001
	vF-M	vM-F	16.00	0.2117	0.04017	196	5.27	<.0001	<.0001
	vF-M	vMPT	16.00	-0.04288	0.03967	196	-1.08	0.2810	0.7016
	vFPT	vM-F	16.00	0.005010	0.04014	196	0.12	0.9008	0.9993
	vFPT	vMPT	16.00	-0.2496	0.03964	196	-6.30	<.0001	<.0001
	vM-F	vMPT	16.00	-0.2546	0.04059	196	-6.27	<.0001	<.0001
	vF-M	vFPT	20.00	0.2574	0.05187	196	4.96	<.0001	<.0001
	vF-M	vM-F	20.00	0.2926	0.05320	196	5.50	<.0001	<.0001
	vF-M	vMPT	20.00	-0.00126	0.05253	196	-0.02	0.9808	1.0000
	vFPT	vM-F	20.00	0.03522	0.05320	196	0.66	0.5087	0.9112
	vFPT	vMPT	20.00	-0.2586	0.05253	196	-4.92	<.0001	<.0001
	vM-F	vMPT	20.00	-0.2938	0.05384	196	-5.46	<.0001	<.0001

Gene	sex	sex	day	Estimate	Std Error	DF	T value	Pr > F	Adj P
Mis	FPT	MPT	0.00	-1.3547	0.2379	210	-5.69	<.0001	<.0001
ovo	F-M	FPT	1.00	0.8467	0.2440	210	3.47	0.0006	0.0035
	F-M	M-F	1.00	0.2479	0.2653	210	0.93	0.3512	0.7864
	F-M	MPT	1.00	-0.6071	0.2447	210	-2.48	0.0139	0.0658
	FPT	M-F	1.00	-0.5988	0.2440	210	-2.45	0.0149	0.0703
	FPT	MPT	1.00	-1.4538	0.2214	210	-6.57	<.0001	<.0001
	M-F	MPT	1.00	-0.8550	0.2447	210	-3.49	0.0006	0.0032
	F-M	FPT	2.00	0.9720	0.2268	210	4.28	<.0001	0.0002
	F-M	M-F	2.00	0.4228	0.2464	210	1.72	0.0877	0.3182
	F-M	MPT	2.00	-0.5810	0.2276	210	-2.55	0.0114	0.0550
	FPT	M-F	2.00	-0.5492	0.2268	210	-2.42	0.0163	0.0762
	FPT	MPT	2.00	-1.5530	0.2062	210	-7.53	<.0001	<.0001
	M-F	MPT	2.00	-1.0037	0.2276	210	-4.41	<.0001	<.0001
	F-M	FPT	4.00	1.2226	0.1972	210	6.20	<.0001	<.0001
	F-M	M-F	4.00	0.7726	0.2128	210	3.63	0.0004	0.0020
	F-M	MPT	4.00	-0.5286	0.1977	210	-2.67	0.0081	0.0400
	FPT	M-F	4.00	-0.4500	0.1972	210	-2.28	0.0235	0.1054
	FPT	MPT	4.00	-1.7512	0.1807	210	-9.69	<.0001	<.0001
	M-F	MPT	4.00	-1.3012	0.1977	210	-6.58	<.0001	<.0001
	F-M	FPT	8.00	1.7239	0.1672	210	10.31	<.0001	<.0001
	F-M	M-F	8.00	1.4722	0.1728	210	8.52	<.0001	<.0001
	F-M	MPT	8.00	-0.4239	0.1661	210	-2.55	0.0114	0.0552
	FPT	M-F	8.00	-0.2517	0.1672	210	-1.51	0.1337	0.4361
	FPT	MPT	8.00	-2.1478	0.1603	210	-13.40	<.0001	<.0001
	M-F	MPT	8.00	-1.8961	0.1661	210	-11.41	<.0001	<.0001
	F-M	FPT	12.00	2.2252	0.1896	210	11.73	<.0001	<.0001
	F-M	M-F	12.00	2.1719	0.1871	210	11.61	<.0001	<.0001
	F-M	MPT	12.00	-0.3192	0.1864	210	-1.71	0.0883	0.3199
	FPT	M-F	12.00	-0.05329	0.1896	210	-0.28	0.7790	0.9922
	FPT	MPT	12.00	-2.5443	0.1890	210	-13.47	<.0001	<.0001
	M-F	MPT	12.00	-2.4910	0.1864	210	-13.36	<.0001	<.0001
	F-M	FPT	16.00	2.7264	0.2509	210	10.87	<.0001	<.0001
	F-M	M-F	16.00	2.8715	0.2464	210	11.65	<.0001	<.0001
	F-M	MPT	16.00	-0.2144	0.2460	210	-0.87	0.3843	0.8194
	FPT	M-F	16.00	0.1451	0.2509	210	0.58	0.5636	0.9385
	FPT	MPT	16.00	-2.9409	0.2504	210	-11.75	<.0001	<.0001
	M-F	MPT	16.00	-3.0860	0.2460	210	-12.55	<.0001	<.0001
	F-M	FPT	20.00	3.2277	0.3299	210	9.78	<.0001	<.0001
	F-M	M-F	20.00	3.5712	0.3272	210	10.92	<.0001	<.0001
	F-M	MPT	20.00	-0.1097	0.3238	210	-0.34	0.7351	0.9866
	FPT	M-F	20.00	0.3435	0.3299	210	1.04	0.2990	0.7255
	FPT	MPT	20.00	-3.3374	0.3266	210	-10.22	<.0001	<.0001
	M-F	MPT	20.00	-3.6809	0.3238	210	-11.37	<.0001	<.0001

Gene	sex	sex	day	Estimate	Std Error	DF	T value	Pr > F	Adj P
Mis	vFPT	vMPT	0.00	-1.7614	0.3220	196	-5.47	<.0001	<.0001
vitro	vF-M	vFPT	1.00	0.5765	0.3053	196	1.89	0.0604	0.2363
	vF-M	vM-F	1.00	0.08996	0.3061	196	0.29	0.7691	0.9911
	vF-M	vMPT	1.00	-1.2049	0.2994	196	-4.02	<.0001	0.0005
	vFPT	vM-F	1.00	-0.4866	0.3062	196	-1.59	0.1137	0.3873
	vFPT	vMPT	1.00	-1.7814	0.2995	196	-5.95	<.0001	<.0001
	vM-F	vMPT	1.00	-1.2948	0.3004	196	-4.31	<.0001	0.0002
	vF-M	vFPT	2.00	0.6391	0.2839	196	2.25	0.0255	0.1133
	vF-M	vM-F	2.00	0.1906	0.2845	196	0.67	0.5035	0.9082
	vF-M	vMPT	2.00	-1.1623	0.2782	196	-4.18	<.0001	0.0003
	vFPT	vM-F	2.00	-0.4485	0.2845	196	-1.58	0.1165	0.3945
	vFPT	vMPT	2.00	-1.8014	0.2782	196	-6.47	<.0001	<.0001
	vM-F	vMPT	2.00	-1.3529	0.2788	196	-4.85	<.0001	<.0001
	vF-M	vFPT	4.00	0.7643	0.2458	196	3.11	0.0022	0.0115
	vF-M	vM-F	4.00	0.3920	0.2460	196	1.59	0.1127	0.3848
	vF-M	vMPT	4.00	-1.0770	0.2406	196	-4.48	<.0001	<.0001
	vFPT	vM-F	4.00	-0.3723	0.2459	196	-1.51	0.1317	0.4312
	vFPT	vMPT	4.00	-1.8414	0.2405	196	-7.66	<.0001	<.0001
	vM-F	vMPT	4.00	-1.4690	0.2407	196	-6.10	<.0001	<.0001
	vF-M	vFPT	8.00	1.0147	0.2003	196	5.07	<.0001	<.0001
	vF-M	vM-F	8.00	0.7947	0.2012	196	3.95	0.0001	0.0006
	vF-M	vMPT	8.00	-0.9066	0.1974	196	-4.59	<.0001	<.0001
	vFPT	vM-F	8.00	-0.2200	0.2009	196	-1.09	0.2749	0.6931
	vFPT	vMPT	8.00	-1.9213	0.1971	196	-9.75	<.0001	<.0001
	vM-F	vMPT	8.00	-1.7013	0.1980	196	-8.59	<.0001	<.0001
	vF-M	vFPT	12.00	1.2651	0.2157	196	5.86	<.0001	<.0001
	vF-M	vM-F	12.00	1.1974	0.2192	196	5.46	<.0001	<.0001
	vF-M	vMPT	12.00	-0.7361	0.2163	196	-3.40	0.0008	0.0044
	vFPT	vM-F	12.00	-0.06766	0.2190	196	-0.31	0.7577	0.9897
	vFPT	vMPT	12.00	-2.0012	0.2161	196	-9.26	<.0001	<.0001
	vM-F	vMPT	12.00	-1.9335	0.2195	196	-8.81	<.0001	<.0001
	vF-M	vFPT	16.00	1.5154	0.2823	196	5.37	<.0001	<.0001
	vF-M	vM-F	16.00	1.6001	0.2885	196	5.55	<.0001	<.0001
	vF-M	vMPT	16.00	-0.5656	0.2852	196	-1.98	0.0488	0.1979
	vFPT	vM-F	16.00	0.08467	0.2886	196	0.29	0.7695	0.9912
	vFPT	vMPT	16.00	-2.0811	0.2853	196	-7.29	<.0001	<.0001
	vM-F	vMPT	16.00	-2.1657	0.2915	196	-7.43	<.0001	<.0001
	vF-M	vFPT	20.00	1.7658	0.3735	196	4.73	<.0001	<.0001
	vF-M	vM-F	20.00	2.0028	0.3822	196	5.24	<.0001	<.0001
	vF-M	vMPT	20.00	-0.3952	0.3777	196	-1.05	0.2968	0.7225
	vFPT	vM-F	20.00	0.2370	0.3825	196	0.62	0.5363	0.9257
	vFPT	vMPT	20.00	-2.1610	0.3781	196	-5.71	<.0001	<.0001
	vM-F	vMPT	20.00	-2.3980	0.3867	196	-6.20	<.0001	<.0001

CHAPTER FIVE

Analysis of candidate genes involved in temperature-dependent sex determination*

The process of sex determination can generally be categorized into two modes. Many vertebrates exhibit genotypic sex determination (GSD), in which a genetic factor determines the sexual fate of the initially bipotential gonad, as is the case in mammals via *Sry*. In other vertebrates, environmental factors dictate sexual fate. One example of this is temperature-dependent sex determination (TSD), in which the incubation temperature of the egg during the middle third of embryonic development determines the future sex of the embryo. All crocodilians and many turtles and lizards exhibit TSD. It was unclear if components of the molecular network underlying gonad development had been retained between organisms with GSD and TSD, and further, if their functions were conserved or novel roles had evolved.

To determine possible involvement in the molecular network underlying gonadogenesis in an organism with TSD, we cloned and examined the expression of seven candidate genes in the red-eared slider turtle, *Trachemys scripta*. The development of the mammalian testis has been well-studied, and requires the action of *Dmrt1*, *Mis* and *Sox9*, among other factors (see Brennan & Capel 2004). The vertebrate ovary has been shown to require *FoxL2* and *Rspo1*, and finally, *Dax1* and *Wnt4* play a role in mammalian gonadogenesis in both sexes. In organisms with TSD, genes involved in early phases of sex determination in the bipotential gonad are expected to be expressed in a dimorphic manner before or early in the TSP, genes involved in commitment of the gonad to a final sex would be dimorphic near the close of the TSP, and finally genes integral to downstream gonadal differentiation should be expressed dimorphically after the TSP. To clarify their location in the temperature-dependent sex-determining molecular network, we

* Portions of this chapter appear in Shoemaker & Crews, 2009.

examined the expression of these seven factors in the slider turtle at constant temperatures as well as in response to sex-reversing temperature shifts. We have demonstrated that they are all involved in TSD at various points of gonadogenesis.

The data presented in this dissertation is reviewed here in comparison with information available from other TSD species. Various species have been used in molecular studies of TSD, and the timing of the TSP window is different across species. In the discussion that follows, particular stages are detailed so that comparisons across species can be made. The reader is referred to Table 1 for further clarification, and to place these stages within the various steps of gonad development. True species-specific differences in expression patterns are found in some of the following studies. However, it is likely that the differences in techniques utilized to assay expression, the tissues used, the varying staging criteria and the actual stages examined also contribute to variation seen within the data. Interpreting the differences in these results continues to be a challenge in piecing together the molecular network underlying TSD.

Testicular development

Hypothesis I postulated that the transcription factors *Sox9* and *Dmrt1* and the hormone *Mis* are involved in the formation of a testis and/or the repression of an ovary at a male-producing temperature. Furthermore, Hypothesis IV proposed that while *Mis* expression may be maintained by *Sox9*, the initial upregulation of *Mis* in the developing testis is modulated by some other upstream factor. Finally, Hypothesis V aimed to test if *Dmrt1* plays an upstream role in testicular development and might directly sense male-producing temperature, similar to a suggested master sex-determining role in other species. These hypotheses were investigated by examining the expression of these three factors in gonads throughout the sex-determining period at both constant temperatures as well as in response to sex-reversing temperature shifts. These studies included *in situ* hybridization data to examine localization of transcripts as well as real-time PCR to examine quantitative levels of expression. Furthermore, expression of these genes in gonads developing in culture was studied to determine patterns in isolated gonad tissue. The following discussion places the findings of our studies within the context of other organisms with TSD, and evaluates these three hypotheses.

Sox9

The ability of *Sox9* to "replace" the action of *Sry* in mammals made it obvious to examine to determine if it plays a critical role upstream in testis development in TSD organisms as well. In the slider turtle, initial expression analyses of *Sox9* in AKG complexes showed monomorphic expression in both sexes throughout gonadogenesis (stages 15, 17, 20) (Spotila et al. 1998, Kettlewell et al. 2000). However, data presented here reveals that this lack of sex-specificity is likely due to the inclusion of the strong *Sox9* expression observed in dorsal metanephric tissue present in the AKG (Fig. 2). qPCR analysis on isolated gonads reveals *Sox9* transcripts at both MPT and FPT early in the TSP (stages 16-17), followed by significantly higher expression of *Sox9* at MPT at the close of the TSP and through differentiation (Fig. 22, see also Figs. 2, 8, 18). *In situ* hybridization localizes *Sox9* transcripts early in the TSP in clusters of expressing cells surrounding non-expressing cells in gonads at both temperatures (stage 15, Fig. 18). Later, transcripts become specifically localized in the MPT gonad in somatic preSertoli cells of developing sex cords and become diffuse at FPT (Fig. 2). Temperature shift experiments show strong, sustained upregulation in FPT→MPT gonads and repression in MPT→FPT gonads, indicating that *Sox9* is temperature responsive throughout the entire period of gonadogenesis. Taken together, these data strongly implicate a role for *Sox9* in the developing testis of the slider turtle, validating Hypothesis I.

Two other species of turtles and the leopard gecko show similar *Sox9* expression patterns: expression is detectable in both sexes early in gonad development and then becomes restricted to the developing testis either at the end of the TSP or during differentiation. In slight contrast, expression in the alligator gonad is undetectable in either sex early in development, and then is upregulated in the developing testis after sex has been committed.

An elegant set of studies in the Olive Ridley sea turtle, *Lepidochelys olivacea*, also demonstrates the expression patterns and temperature-response of *Sox9* in the developing gonad (Moreno-Mendoza et al. 1999, 2001, Torres-Maldonado et al. 2001). In this species, the TSP lasts for eight days during development, corresponding to stages 20-23 at MPT and to stages 24-27 at FPT (Merchant-Larios et al. 1997). Expression analyses by RT-PCR demonstrate *Sox9* is present

in early developing gonads at both MPT and FPT (stages 23-25) and is later retained at MPT but is undetectable at FPT (stages 26, 27) (Torres-Maldonado et al. 2001, 2002). MPT→FPT gonads exhibit downregulation of *Sox9* expression by 12 days post-shift (Torres-Maldonado et al. 2001). Sox9 protein is detected in a similar pattern; early in development, Sox9 is found in primitive sex cords in both MPT and FPT gonads (stages 22, 24) and is then restricted to MPT (stage 26) (Moreno-Mendoza et al. 1999). Furthermore, when gonads are grown *in vivo* or cultured *in vitro* and exposed to sex-reversing temperature shifts in either direction (MPT→FPT and FPT→MPT), Sox9 protein levels change in response (decrease and increase, respectively) (Moreno-Mendoza et al. 2001).

In the snapping turtle, *Chelydra serpentina*, *Sox9* is expressed at MPT throughout gonadogenesis and is downregulated in response to a shift to FPT (Rhen et al. 2007). Similarly, in the leopard gecko, *Eublepharis macularius*, *Sox9* is detected by whole mount *in situ* hybridization during the TSP in both MPT and FPT gonads (stage 36) and is then restricted to MPT gonads at the end of the TSP (stages 37, 40, Valleley et al. 2001). In contrast, *Sox9* transcripts in the American alligator are not detected in either sex early in the TSP (stages 20-23); expression is upregulated at MPT at the end of the TSP and during testis differentiation (stages 24-27, Western et al. 1999a). Coincidentally, the tissue sources used within this study varied; early in development the gonad is unable to be removed cleanly from underlying tissue and therefore gonad-adrenal-mesonephros (GAM, equivalent to AKG) must be analyzed (stages 20-23), while isolated gonad is only possible later in development (stages 24-27). At MPT, *Sox9* transcripts initially localize to faint expression in scattered cells (stages 23.5, 24), and subsequently to strong expression in developing sex cords (stage 25, Western et al. 1999a, 1999b).

In summary, these data suggest that *Sox9* is not involved in the initial steps of sex determination, as is seen in mammals. However, what seems more likely from the data thus far is the hypothesis that *Sox9* plays a role in the final commitment of a gonad to a testicular fate (Fig. 23). As described above, gonadal sex in organisms with TSD remains plastic until the end of the temperature-sensitive period. Dimorphic expression of genes involved in commitment to a sexual fate would not be necessary in the developing gonad until the end of the TSP when the

window of sex-reversibility is closing. From this perspective, the data from all examined species with TSD (five) are consistent with the hypothesis that *Sox9* plays a role in the commitment of the bipotential gonad to a testicular fate.

Mis

In organisms with TSD, *Mis* has been best studied in our work in the slider turtle. Expression analysis of AKG complexes and isolated gonads reveals significantly higher expression at MPT than FPT early in the bipotential gonad and continuing throughout gonadogenesis (stages 16-23) (Fig. 22, see also Figs. 3, 8, 19). *In situ* hybridization localizes transcripts to somatic cells within developing testicular sex cords (Fig. 3). In response to sex-reversing temperature shifts, FPT→MPT gonads exhibit strong, rapid upregulation of *Mis* early in the TSP, implying a necessary function in the developing testis (Fig. 19). In MPT→FPT gonads, *Mis* expression is rapidly downregulated, suggesting that the repression of a testis-specific function is critical for ovarian development. To our knowledge, the only other TSD organism in which *Mis* has been examined is the American alligator. In this species, dimorphic expression also appears early in gonad development in a few medullary cells at MPT and continues to increase throughout the TSP (stages 22-25), with no detectable specific expression at FPT (Western et al. 1999b). Taken together these data strongly suggest a role for *Mis* in either the active formation of the testis or repression of ovarian structures in the slider turtle, providing evidence for Hypothesis II (Fig. 23). Whether a role in causing the regression of Mullerian ducts has been conserved from mammalian species remains to be investigated.

Moreover, gonadal mRNA expression of *Mis* in the alligator and the slider turtle becomes upregulated in putative males prior to upregulation of *Sox9*, similar to the case in chicken (Oreal et al. 1998, Smith et al. 1999a). This suggests a divergence from the relationship seen in mammals in which *Sox9* initially upregulates *Mis* expression. Further evidence for this comes from the timing of the response of each of these genes in shifted gonads; *Mis* responds more quickly in shifts in either direction than *Sox9*, indicating that its regulation is controlled by some other mechanism. Thus we find to support Hypothesis IV, which postulated that the initial upregulation of *Mis* is not controlled by *Sox9*.

Dmrt1

Dmrt1 expression in the slider turtle in both AKG complexes and isolated gonad tissue is significantly greater at MPT than at FPT from the beginning of the temperature-sensitive period (Fig. 22, see also Figs. 4, 8, 19). *In situ* hybridization reveals cellular localization of *Dmrt1* expression in somatic cells in developing testicular sex cords (Fig. 4). Functionally, gonadal *Dmrt1* expression is rapidly upregulated in *T. scripta* FPT→MPT gonads during the TSP, suggesting a necessary function in male development (Fig. 19). Further, expression is downregulated in MPT→FPT gonads, implicating the repression of this function is required for ovarian differentiation. Our results are supported by evidence from two other species with TSD. In both alligator urogenital ridges and Olive Ridley sea turtle gonads, expression is initially detectable in both sexes, and subsequently becomes higher at MPT either during or after the TSP, respectively (Smith et al. 1999b, Torres-Maldonado et al. 2002). In summation, these data suggest the involvement of *Dmrt1* in gonadogenesis has been conserved across sex-determining mechanisms, and that it plays a role in testicular development in TSD, validating Hypothesis III. However, the specific function of Dmrt1 in the developing testis remains unknown. Due to the timing of its response to sex-reversing temperature shifts, it is unlikely that *Dmrt1* plays an initial temperature-sensing role. Thus, we find evidence in opposition to Hypothesis V, suggesting that this supposition is not true in the slider turtle. While *Dmrt1* still holds the captivating possibility of being a master sex-determining gene in several GSD species, it appears not to be directly regulated by temperature in this TSD species. However, we provide evidence that *Dmrt1* plays a critical role upstream in sex determination of the bipotential gonad (Fig. 23).

In vitro culture also provides evidence that estrogen-mimicking compounds have the ability to strongly repress the expression of all three testicular genes studied here (Fig. 16). Murdock and Wibbels also showed that exogenous application of estradiol to the eggshells of developing *T. scripta* embryos prior to the TSP inhibits *Dmrt1* expression for the duration of the TSP; the effect on other genes was not examined (Murdock & Wibbels 2006). Taken together, these data strongly implicate the involvement of *Dmrt1* in testis formation and reveal a sensitivity to both temperature and estrogen, although not necessarily a direct one. A role for estrogen in repressing

testicular factors at a female-producing temperature is likely and should be explored in future studies.

Interacting pathways

Hypothesis II of my dissertation tested whether the transcription factor *Dax1* and the signaling molecule *Wnt4* play roles in gonadogenesis in both sexes of an organism with TSD. In GSD species, these two factors function early in the bipotential gonad, and also play later testis-specific and ovarian-specific roles. Our data suggest that *Dax1* and *Wnt4* also are important for both MPT and FPT gonadogenesis in the slider turtle.

Dax1

In the slider turtle, *Dax1* is expressed in the developing gonad of embryos at both MPT and FPT. *In situ* hybridization reveals localization of *Dax1* expression in developing sex cords at MPT, in the cortex of FPT gonads, and in cells of both the Müllerian and Wolffian ducts (Fig. 6). qPCR analysis shows that *Dax1* expression levels are similar at both FPT and MPT for the duration of gonadogenesis, and decrease through time (Fig. 22, see also Fig. 7). This data is supported in three other species of turtle and the American alligator, in which gonadal *Dax1* is expressed at similar levels between the sexes. Through developmental time, this expression either decreases slightly and then dramatically (Olive Ridley sea turtle), increases slightly (alligator and painted turtle, *Chrysemys picta*), or does not change (snapping turtle) (Rhen et al. 2007, Western et al. 2000, Torres-Maldonado et al. 2002, Valenzuela 2008), and it remains to be seen what each of these timing-correlated changes mean at the functional level. The sexually-monomorphic expression pattern of *Dax1* in organisms with TSD is no surprise, as roles for *Dax1* exist in both the developing testis and ovary of mammals. However, *Dax1* expression throughout gonadogenesis lends support for Hypothesis II. Further analysis of the function of *Dax1* in TSD gonads is warranted, and due to the complexity observed in the role of *Dax1* in mammalian systems, these studies may prove more complicated than unraveling other parts of the TSD network.

Wnt4

In organisms with TSD, *Wnt4* has only been examined in the work presented here in *T. scripta*. Analysis of isolated gonad tissue reveals similar expression levels at MPT and FPT during the TSP (stages 16-19), followed by a significant increase at FPT over MPT during ovarian differentiation (stages 21, 23) (Fig. 22, see also Fig. 7). *In situ* hybridization localizes expression across the gonad of both sexes, with increased concentration of transcript in sex cords at MPT, in the cortical region at FPT, and in developing Müllerian ducts (Fig. 6). This expression during gonad development in both sexes lends support for Hypothesis III. Similar to *Sox9*, if *Wnt4* plays a role in the commitment of the bipotential gonad to a sexual fate (rather than the earlier step of sex determination), its expression should be dimorphic near the close of the TSP. Indeed, our data are consistent with a possible role of this signaling molecule in governing ovarian development at the level of sex commitment, but this requires further investigation (Fig. 23).

Ovarian development

Hypothesis III of my dissertation suggests that the transcription factor *FoxL2* and the signaling molecule *Rspo1* are involved in the formation of an ovary and/or the repression of a testis at a female-producing temperature. For a long time, *FoxL2* was one of the few genes recognized to play a critical role in the early development of the mammalian ovary. Here we show that it also plays a function in regulating female development in an organism with TSD. *Rspo1* was recently found to also play an early critical role in ovarian sex determination in mammals (Parma et al. 2006), and our work represents the first analysis of this gene in an organism with TSD. Excitingly, we find that it is likely that *Rspo1* plays a role in ovarian development in the slider turtle. Whether *Rspo1* may be directly temperature-sensitive or responds to temperature changes indirectly via another temperature-sensing molecule remains to be investigated.

FoxL2

In TSD organisms, *FoxL2* was first described in the slider turtle; expression is found in AKG complexes at both temperatures early in the TSP (stage 15), and later becomes enhanced at FPT (stages 17, 20, Loffler et al. 2003). Our subsequent analysis by qPCR on isolated gonads gave slightly different results: expression is similar at MPT and FPT early in the TSP (stages 16-17),

and does not become significantly greater at FPT until the end of the TSP (stages 19-23) (Fig. 22, see also Figs. 7, 19). *In situ* hybridization further localized *FoxL2* transcript to cells in the developing ovarian cortex (Fig. 6). In response to sex-reversing temperature shifts, *FoxL2* expression increases at the appropriate time in MPT→FPT gonads to levels significantly greater than MPT expression (Fig. 19). Further, expression remains low in FPT→MPT gonads for the duration of gonadogenesis. This data is supported by work in the snapping turtle, in which gonadal expression of *FoxL2* was also found to increase in response to a MPT→FPT shift (Rhen et al. 2007). These data confirm the temperature-responsivity of *FoxL2* and suggest an active role in ovarian development in the slider turtle, evidence of Hypothesis III. The function of *FoxL2* in the gonads of organisms with TSD remains to be investigated.

Rspo1

We examined the latest addition to the cast of critical sex determination factors in *T. scripta*. In isolated gonad tissue, expression of *Rspo1* is significantly higher at FPT than at MPT early in the TSP and continues to become increasingly disparate between the sexes throughout gonadogenesis (stages 17-23, Fig. 22, see also Fig. 9). Furthermore, when embryos are shifted from FPT to MPT early in the TSP, expression of *Rspo1* in the gonad is rapidly downregulated, consistent with the hypothesis that repression of an ovarian-specific function is necessary for testicular development. This exciting result constitutes one of the earliest significant dimorphisms in expression level of an ovary-specific factor in organisms with TSD. It implicates a role for *Rspo1* in ovarian development, as well as a responsivity to temperature, supporting Hypothesis III (Fig. 23). Further investigation of *Rspo1* as a critical candidate ovarian sex-determining gene is a fruitful avenue of future research.

Analyzing function in a non-traditional model system

As have been detailed above, descriptive studies analyzing mRNA expression patterns have been the most practically feasible place to begin investigating the involvement of candidate genes in temperature-dependent sex determination. However, clearly these studies have only taken our understanding so far. We would do well to heed a lesson from *Drosophila* sex determination: presence of transcript doesn't necessarily mean a functional transcript, that the transcript is

spliced consistently in different cellular environments, or that protein spliceoforms are functionally equivalent (see Sanchez 2008). Thus, interpretation of expression data, while clearly worthwhile and critical to laying the foundation of future studies, must all be taken with a proverbial grain of salt.

The final two hypotheses of this dissertation concerned the optimization and use of an *in vitro* culture system to address the lack of functional studies within the field. Hypothesis VI postulated that the development of whole gonads in an *in vitro* organ culture system mimics *in ovo* development, and that isolated gonadal tissue retains the ability to sense and respond to changes in environmental temperature, indicating an endogenous temperature-sensor. Furthermore, Hypothesis VII stated that molecular manipulation of explant gonads in culture allows previously unavailable functional experiments that are essential to elucidating the molecular network underlying TSD.

Here we demonstrate the optimization of an *in vitro* culture system in which gonad explants develop for up to three weeks. We show that according to gene expression data, these gonads mimic normal *in ovo* development for a minimum of 8 days and a maximum of 20 days, depending on the marker examined (Figs. 18, 19). Further, we provide evidence that a fusion GFP:Sox9 construct can be introduced into gonadal cells by electroporation and is misexpressed in a mosaic fashion throughout the gonad. *Sox9* expression in these gonads is significantly increased, and causes a slight, non-significant increase in *Dmrt1* expression (Fig. 21). While we are unable to determine from these data if *Sox9* has the ability to regulate *Dmrt1* expression, the link between these two factors suggested by our results is quite interesting, as it would represent a novel role for *Sox9* not observed in organisms with GSD. The *in vitro* culture system provides an essential tool to assess this as well as other possible interactions between components of the molecular network underlying sex determination.

The *in vitro* culture system opens the door to a myriad of functional assays in the developing slider turtle gonad. What is required next are analyses of protein expression, localization, and most importantly, function, if we are to truly understand the hierarchical cascade of gene action

underlying TSD, and any evolutionary relationship of these actions with GSD. The experiments described in Chapter 4 begin to move analyses in this nontraditional model system away from descriptive studies and into functional analyses. Overexpression and knockdown techniques can be optimized for the application to *in vitro* gonads, opening the door for understanding both the sufficiency and necessity of these molecules in the development of the temperature-determined gonad. These creative applications of techniques used routinely in model systems must continue if we are to actually understand the roles of known candidate molecules or, most excitingly, uncover the direct targets of temperature in the developing gonad.

Understanding expression data from studies of organisms with TSD within a broader context has resulted in a discussion of the level of conservation and divergence in molecular expression and function, cellular behaviors, and tissue development across sex-determining mechanisms. Unfortunately, we can't fully assess the relative importance of conserved or novel roles of common molecular players until we have better techniques to elucidate their function. For certain there will be some conservation and some divergence as we expand studies of the molecular mechanisms of sex determination into nontraditional model systems. How much of each and what meaning we can derive from them remains to be seen. Regardless, these studies lend insight into the evolution of molecular action, and at a broader level, the evolution of developmental pathways.

Figure 22. Expression of various candidate sex-determining genes in gonads of the slider turtle, *Trachemys scripta*.

(A, C, E) Expression data is reproduced from qPCR study in which each value is the average of n=3 samples, where one sample represents expression in a pooled group of 20-30 gonads from 10-20 individual turtle embryos (Data redrawn from Shoemaker et al. 2007b, Smith et al. 2008). Asterisks indicate statistically significant difference *within gene within stage between MPT and FPT* at the alpha=0.05 level. Gene of interest expression was normalized to *PP1*, a house-keeping gene whose expression does not change with sex or stage. X-axis represents developmental stage (Greenbaum 2002); Y-axis is either (A, C) fold difference in expression between MPT and FPT or (B) log-transformed fold difference in expression between MPT and FPT. For example, stage 23 *FoxL2* expression at FPT is nearly 11 times MPT expression. Line at 1.0 indicates equal expression between MPT and FPT; bars that fall below 1.0 have greater expression in the gonad of numerator sex, while bars above 1.0 have greater expression in gonad of the denominator sex. (C) Because expression of *Mis* at FPT is so low as to reach the limit of detectability (essentially equal to 0.0), fold expression values at MPT become inappropriately inflated and are therefore plotted as log-transformed data. A value of 1.0 on log y-axis corresponds to a value of 10.0 on previous non-log y-axes. (B, D, F) Whole mount *in situ* hybridization localizes gene expression patterns within turtle gonads from embryos at various stages (Data from Shoemaker et al. 2007a, 2007b).

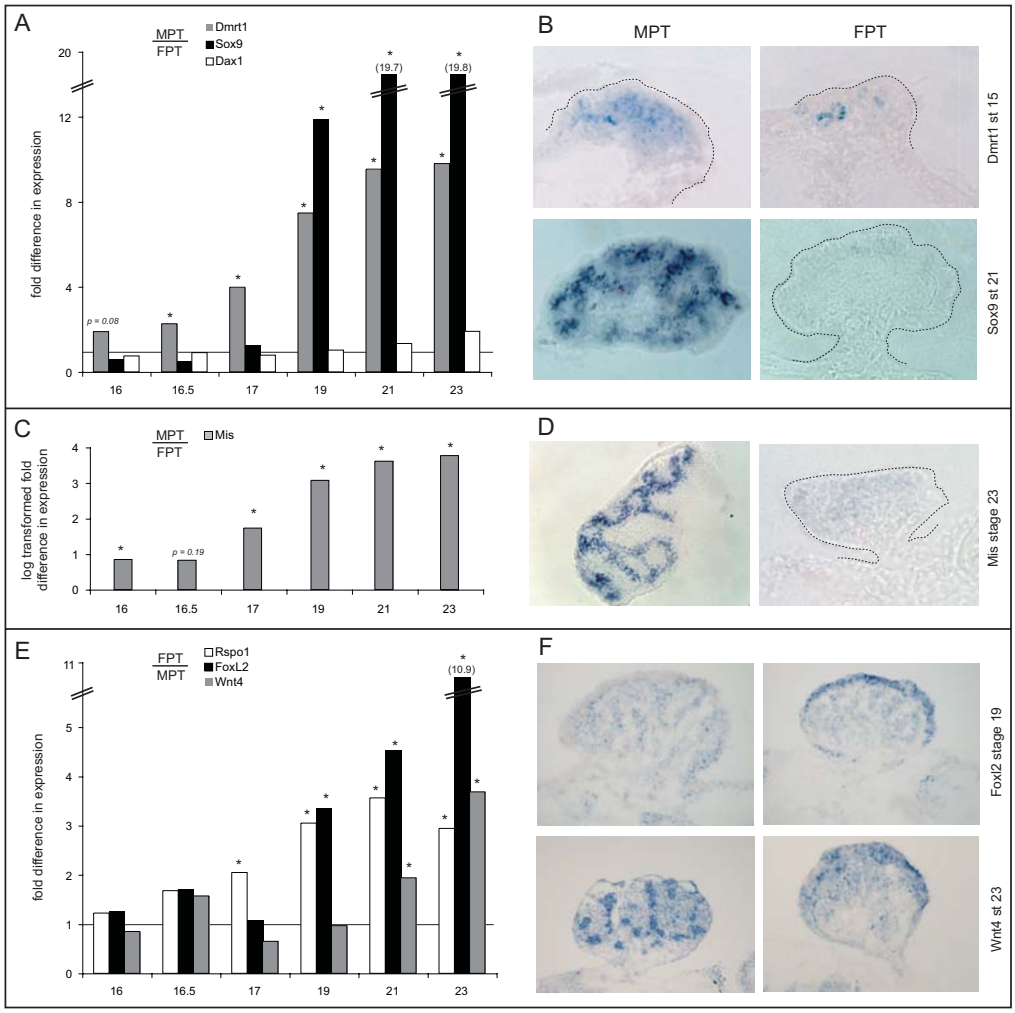

Figure 23. Simplified model of molecular network underlying sex determination in both mammal and slider turtle.
Candidate genes explored in this dissertation are compared between organisms with TSD and GSD. Genes in turtle network are placed in a temporal hierarchy as elucidated by sexually dimorphic patterns of gene expression in the red-eared slider turtle gonad. Solid arrows indicate direct relationships, while dashed arrows indicated indirect or undescribed relationships. The temperature-sensitive period (TSP) is divided into two parts: sex determination, during which *Dmrt1* and *Rspo1* appear to function, and sex commitment, during which *Sox9* and *FoxL2* appear to play a role.

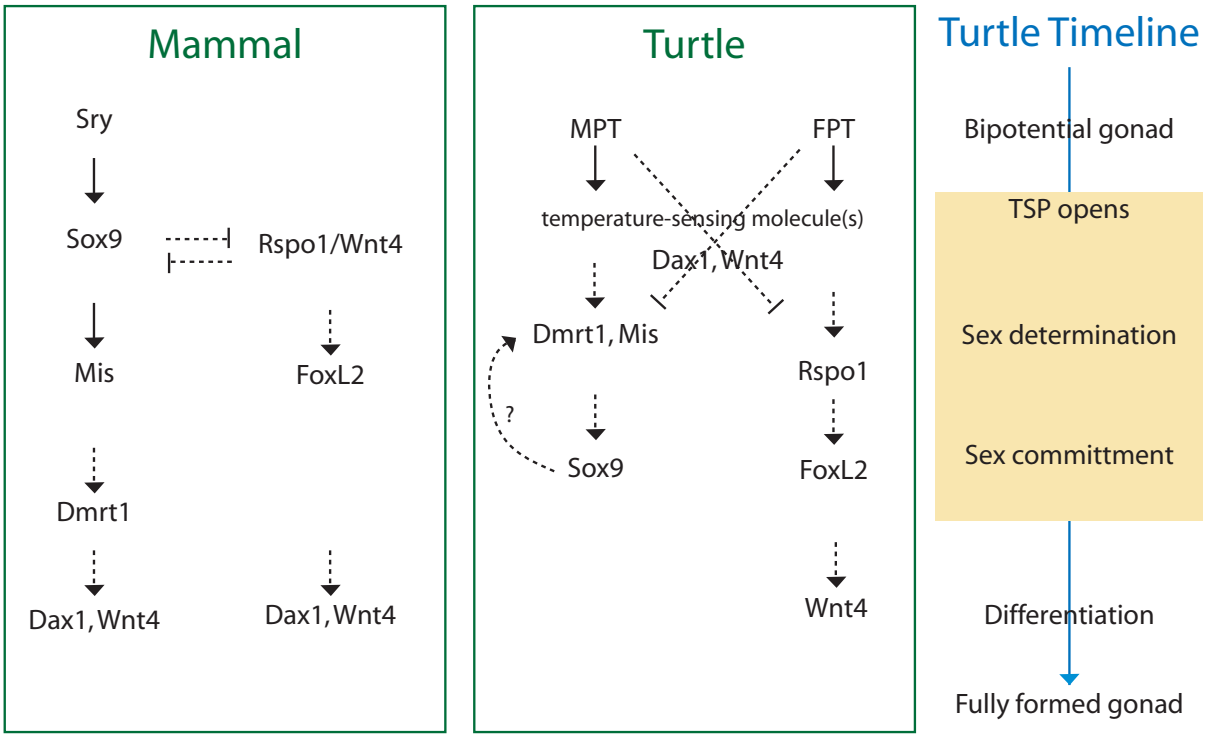

References

Allard S, Adin P, Gouedard L, di Clemente N, Josso N, Orgebin-Crist M, Picard J, Zavier F. Molecular mechanisms of hormone-mediated Müllerian duct regression: involvement of B-catenin. Dev 2000;127: 3349-3360.

Andrews JE, Smith CA, Sinclair AH. Sites of *estrogen receptor* and *aromatase* expression in the chicken embryo. Gen Comp Endo 1997;108:182-90.

Arango NA, Lovell-Badge R, Behringer RR. Targeted mutagenesis of the endogenous mouse *Mis* gene promoter: *in vivo* definition of genetic pathways of vertebrate sexual development. Cell 1999;99:409-19.

Armstrong JF, Pritchard-Jones K, Bickmore WA, Hastie ND, Bard JB. The expression of the Wilms' tumour gene, WT1, in the developing mammalian embryo. Mech Dev 1993;40:85–97.

Bardoni B, Zanaria E, Guioli S, Floridia G, Worley KC, Tonini G, Ferrante E, Chiumello G, McCabe E and Fraccaro M A dosage sensitive locus at chromosome Xp21 is involved in male to female sex reversal. Nature Genet 1994;7:497–501.

Baron D, Cocquet J, Xia X, Fellous M, Guiguen Y, Veitia RA. An evolutionary and functional analysis of *FoxL2* in rainbow trout gonad differentiation J Mol Endo 2004;33: 705-715

Barrionuevo F, Bagheri-Fam S, Klattig J, Kist R, Taketo MM, Englert C, Scherer G. Homozygous inactivation of *Sox9* causes complete XY sex reversal in mice. Biol Repro 2006;74:195-201.

Behringer RR, Cate RL, Froelick GJ, Palmiter RD, Brinster RL. Abnormal sexual development in transgenic mice chronically expressing Müllerian inhibiting substance. Nature 1990;345:167-70.

Benayoun BA, Caburet S, Dipietromaria A, Bailly-Bechet M, Fellous M, Vaiman D, Veitia RA. The identification and characterization of a FOXL2 response element provides insights into the pathogenesis of mutant alleles. Hum Mol Gen 2008;July 16 epub ahead of print.

Bernard P, Harley VR. *Wnt4* action in gonadal development and sex determination. Int J Bioch Cell Biol 2007;39:31-43.

Berthois Y, Katzenellenbogen JA. Phenol red in tissue culture media is a weak estrogen: implications concerning the study of estrogen-responsive cells in culture. Proc Natl Acad Sci 1986;83:2496-500.

Binnerts ME, Kim KA, Bright JM, Patel SM, Tran K, Zhou M, et al. *R-Spondin1* regulates Wnt signaling by inhibiting internalization of LRP6. Proc Natl Acad Sci 2007;104:14700-5.

Bishop CE, Whitworth DJ, Qin Y, Agoulnik AI. A transgenic insertion upstream of *Sox9* is associated with dominant XX sex reversal in the mouse. Nat Gen 2000;26:490-4.

Blecher SR, Erickson RP. Genetics of sexual development: a new paradigm. Am J Med Genet A 2007;143:3054-68.

Bouma GJ, Albrecht KH, Washburn LL, Recknagel AK, Churchill GA, Eicher EM. Gonadal sex reversal in mutant *Dax1* XY mice: a failure to upregulate *Sox9* in preSertoli cells Dev 2005; 132: 3045-3054

Brennan J, Karl J, Capel B. Divergent vascular mechanisms downstream of Sry establish the arterial system in the XY gonad Dev Biol 2002;244: 418-428

Brennan J, Capel B. One tissue, two fates: molecular genetic events that underlie testis versus ovary development. Nat Rev Gen 2004;5:509-21.

Britt KL, Stanton PG, Misso M, Simpson ER, Findlay JK. The effects of estrogen on the expression of genes underlying the differentiation of somatic cells in the murine gonad. Endo 2004;145:3950-60.

Bull JJ, Vogt RC. Temperature-dependent sex determination in turtles. Sci 1979;206:1186-8.

Bull JJ. Sex determination in reptiles. Q Rev Biol 1980;55:3-21.

Bull, J.J., Wibbels, T. and Crews, D. Sex-determining potencies vary among female incubation temperatures in a turtle. J Exp Zool 1990;256: 339-341.

Burtis K, and Baker B. Drosophila *doublesex* gene controls somatic sexual differentiation by producing alternatively spliced mRNAs encoding related sex-specific polypeptides. Cell 1989;56:997-1010.

Carroll TJ, Park JS, Hayashi S, Majumdar A and AP McMahon. Wnt9b plays a central role in the regulation of mesenchymal to epithelial transitions underlying organogenesis of the mammalian urogenital system Dev Cell 2005;9: 283-292

Cederroth CR, Pitetti JL, Papaioannou MD, Nef S. Genetic programs that regulate testicular and ovarian development. Mol Cell Endo 2007;265-266:3-9.

Chaboissier MC, Kobayashi A, Vidal VIP. Functional analysis of *Sox8* and *Sox9* during sex determination in the mouse. Dev 2004;131:1891-901.

Charnier M. Action of temperature on the sex ratio in the Agama agama (Agamidae, Lacertilia) embryo. C R Seances Soc Biol W Afri 1966;160:620-2.

Chassot AA, Ranc F, Gregoire EP, Roepers-Gajadien HL, Taketo MM, Camerino G, et al. Activation of {beta}-catenin signalling by *Rspo1* controls differentiation of the mammalian ovary. Hum Mol Gen 2008;17:1264-77.

Chen CD, Welsbie DS, Tran C, Baek SH, Chen R, Vessella R, Rosenfeld MG, Sawyers CL. Molecular determinants of resistance to antiandrogen therapy. Nature Med 2004;10:33-9.

Colvin JS, Green RP, Schmahl J, Capel B, Ornitz DM. Male-to-female sex reversal in mice lacking fibroblast growth factor 9. Cell 2001;104:875-89.

Conover DO, Kynard BE. Environmental sex determination: Interaction of temperature and genotype in a fish. Science 1981;213(4507):577-9.

Crews D, Bull JJ, Wibbels T. Estrogen and sex reversal in turtles: a dose-dependent phenomenon. Gen Comp Endo 1991;81:357-64.

Crews D. The organizational concept and vertebrates without sex chromosomes. Brain Behav Evol 1993;42(4-5):202-14.

Crews D, Bergeron JM, Bull JJ, Flores D, Tousignant A, Skipper JK, Wibbels T. Temperature-dependent sex determination in reptiles: proximate mechanisms, ultimate outcomes, and practical applications Dev Gen 1994;15: 297-312

Crews D. Temperature-dependent sex determination: The interplay of steroid hormones and temperature Zool Sci 1996;13: 1-13

Crews D. Sex determination: where environment and genetics meet Evol Dev 2003;5: 50-5.

Crisponi L, Deiana M, Loi A, Chiappe F, Uda M, Amati P, Bisceglia L, Zelante L, Nagaraja R, Porcu S, Ristaldi MS, Marzella R, Rocchi M, Nicolino M, Lienhardt-Roussie A, Nivelon A, Verloes A, Schlessinger D, Gasparini P, Bonneau D, Cao A, G Pilia. The putative forkhead transcription factor FOXL2 is mutated in blepharophimosis/ptosis/epicanthus inversus syndrome. Nat Gen 2001;27:159-66.

Couse JF, Hewitt SC, Bunch DO, Sar M, Walker VR. Postnatal sex reversal of the ovaries in mice lacking estrogen receptors alpha and beta. Science 1999;286:2328-2331

De Santa Barbara P, Bonneaud N, Boizet B, Desclozeaux M, Moniot B, Sudbeck P, Scherer G, Poulat G and Berta P. Direct interaction of SRY-related protein SOX9 and Steroidogenic factor 1 regulates transcription of the human anti-Mullerian hormone gene. Mol Cell Biol 1998;18:6653-65.

De Santa Barbara P, Moniot B, Poulat F, Berta P. Expression and subcellular localization of SF1, SOX9, WT1 and AMH proteins during early human testicular development. Dev Dyn 2000;217:293-8.

Deeming DC. Prevalence of TSD in crocodilians. In: Valenzuela N, Lance VA. Temperature-dependent sex determination in vertebrates. Washington: Smithsonian Books; 2004, p33-41.

DiNapoli L, Capel B. SRY and the standoff in sex determination. Mol Endo 2008;22:1-9.

Dupont S, Dennefeld C, Krust A, Chambon P, Mark M. Expression of Sox9 in granulosa cells lacking the estrogen receptors, ERalpha and ERbeta. Dev Dyn 2003;226:103-6.

Ewert MA, Nelson CE. Sex determination in turtles: Diverse patterns and some possible adaptive values. Copeia 1991;50-69.

Ewert MA, Etchberger CR, Nelson CE. Turtle sex-determining modes and TSD patterns, and some TSD pattern correlates. In: Valenzuela N, Lance VA. Temperature-dependent sex determination in vertebrates. Washington: Smithsonian Books; 2004, p. 21-32.

Flejter W, Fergestad J, Gorski J, Varvill T, Chandrasekharappa S. A gene involved in XY sex reversal is located on chromosome 9, distal to marker D9S1779. Am J Human Gen 1998;63: 794-802.

Fleming A, Crews D. Estradiol and incubation temperature modulate regulation of *steroidogenic factor 1* in the developing gonad of the red-eared slider turtle. Endo 2001;142:1403-11.

Fleming A, Vilain E. The endless quest for sex determination genes. Clin Genet 2004;67:15-25.

Foster JW, Dominguez-Steglich, Guioli S, Kwok C, Weller P, Weissenbach J, Mansour S, Young I, Goodfellow PN, Brook J, Schafer A. Campomelic dysplasia and autosomal sex reversal caused by mutations in SRY-related gene. Nature 1994;372:525-30.

Giuili G, Shen WH, Ingraham HA. The nuclear receptor SF-1 mediates sexually dimorphic expression of Mullerian inhibiting substance, *in vivo*. Dev 1997;124:1799-807.

Godwin J. Social determination of sex in reef fishes. Sems Cell Dev Biol 2009;In press.

Govoroun MS, Pannetier M, Pailhoux E, Cocquet J, Brillard JP, Couty I, Batellier F, Cotinot C. Isolation of chicken homolog of the *FoxL2* gene and comparison of its expression patterns with those of aromatase during ovarian development Dev Dyn 2004;231: 859-870

Greenbaum E. A standardized series of embryonic stages for the emydid turtle *Trachemys scripta*. Can J Zool 2002;80:1350-70.

Gutierrez OG, Jime´ nez TF, Favila R, Moreno MN, Granados RL, Barrios FA, Dı´ az CS, Merchant LH. Acetylcholinesterase-positive innervation is present at undifferentiated stages of the sea turtle *Lepidochelys olivacea* embryo gonads: Implications for temperature-dependent sex determination. J. Comp. Neurol. 1999;410, 90-8.

Hammes A, Guo JK, Lutsch G, Leheste JR, Landrock D, Ziegler U, et al. Two splice variants of the Wilms' tumor 1 gene have distinct functions during sex determination and nephron formation. Cell 2001;106:319–29.

Hanley NA, Hagan DM, Clement-Jones M, Ball SG, Strachan T, Salas-Cortes L, McElreavey K, Lindsay S, Robson S, Bullen P, Ostrer H, Wilson DI. *Sry*, *Sox9* and *Dax1* expression patterns during human sex determination and gonadal development Mechs of Dev 2000;91:403-407

Harlow PS. Temperature-dependent sex determination in lizards. In: Valenzuela N, Lance VA. Temperature-dependent sex determination in vertebrates. Washington: Smithsonian Books; 2004, p. 42-52.

Hartkamp J, Roberts SG. The role of the Wilms' tumour-suppressor protein WT1 in apoptosis. Biochem Soc Trans 2008;36:629-31.

Hudson QJ, Smith CA, AH Sinclair. Aromatase inhibition reduces expression of *FoxL2* in the embryonic chicken ovary Dev Dyn 2005;233:1052-55.

Ikeda Y, Swain A, Weber TJ, Hentges KE, Zanaria E, Lalli E, Tamai KT, Sassone-Corsi P, Lovell-Badge R, Camerino G, Parker KL. Steroidogenic Factor 1 and Dax-1 colocalize in multiple cell lineages: potential links in endocrine development Mol Endo 1996;10:1261-72.

Ikeda Y, Takeda Y, Shikayama T, Mukai T, Hisano S, Morohashi KI. Comparative localization of *Dax-1* and *Ad4BP/Sf-1* during development of the hypothalamic-pituitary-gonadal axis suggests their closely related and distinct functions. Dev Dyn 2001; 220:363-76.

Jeays-Ward K, Hoyle C, Brennan J, Dandonneau M, Alldus G, Capel B, Swain A. Endothelial and steroidogenic cell migration are regulated by WNT4 in the developing mammalian gonad. Dev 2003;130:3663-70.

Jeays-Ward K, Dandonneau M, Swain A. Wnt4 is required for proper male as well as female sexual development. Dev Biol 2004;276(2):431-40.

Jordan BK, Mohammed M, Ching ST, Delot E, Chen X, Dewing P, Swain A, Rao PN, Elejalde BR, Vilain, E. Up-regulation of WNT4 signaling and dosage-sensitive sex reversal in humans Am J of Human Genetics 2001;68: 1102-09.

Josso, N., di Clemente, N. and Gouedard L. Anti-Müllerian hormone and its receptors. Molec Cell Endo 2001;179: 25-32.

Josso N, Picard JY, Rey R, di Clemente N. Testicular anti-Müllerian hormone: history, genetics, regulation and clinical applications. Ped Endo Rev 2006;3:347-58.

Kettlewell JR, Raymond CS, Zarkower D. Temperature-dependent expression of turtle *Dmrt1* prior to sexual differentiation. Genesis 2000;26:174-8.

Kim KA, Zhao J, Andarmani S, Kakitani M, Oshima T, Binnerts ME, et al. R-Spondin proteins: a novel link to beta-catenin activation. Cell Cycle 2006;5:23-6.

Kim Y and B Capel. Balancing the bipotential gonad between alternative organ fates: A new perspective on an old problem Dev Dyn 2006;235: 2292-2300

Kim Y, Kobayashi A, Sekido R, DiNapoli L, Brennan J, Chaboissier MC, et al. *Fgf9* and *Wnt4* act as antagonistic signals to regulate mammalian sex determination. PLoS Biol 2006;4:e187.

Klattig J, Sierig R, Kruspe D, Makki MS, Englert C. WT1-mediated gene regulation in early urogenital ridge development. Sex Dev 2007;1:238-54.

Kobayashi T, Matsuda M, Kajiura-Kobayashi H, Suzuki A, Saito N, Nakamoto M, et al. Two DM domain genes, DMY and DMRT1, involved in testicular differentiation and development in the medaka, *Oryzias latipes*. Dev Dyn 2004;231:518-26.

Kobayashi T, Kajiura-Kobayashi H, Guan G, Nagahama Y. Sexual dimorphic expression of Dmrt1 and Sox9a during gonadal differentiation and hormone-induced sex reversal in the teleost fish Nile tilapia (*Oreochromis niloticus*). Dev Dyn 2008;237:297-306.

Kreidberg JA, Sariola H, Loring JM, Maeda M, Pelletier J, Housman D, Jaenisch R. WT-1 is required for early kidney development. Cell 1993;74:679–91.

Lasala C, Carre-Eusebe D, Picard J, Rey R. Subcellular and molecular mechanisms regulating anti-Müllerian hormone gene expression in mammalian and nonmammalian species. DNA Cell Biol 2004;23:572-85.

Loffler KA, Zarkower D, Koopman P. Etiology of ovarian failure in blepharophimosis ptosis epicanthus inversus syndrome: FOXL2 is a conserved, early-acting gene in vertebrate ovarian development. Endo 2003;144:3237-43.

Ludbrook LM, Harley VR. Sex determination: a 'window' of DAX1 activity. Trends Endo Metab 2004;15:116-21.

Luo X, Ikeda Y, Parker KL. A cell-specific nuclear receptor is essential for adrenal and gonadal development and sexual differentiation. Cell 1994;77:481-90.

Martineau J, Nordqvist K, Tilmann C, Lovell-Badge R and Capel B. Male-specific cell migration into the developing gonad. Curr Biol 1997;7: 958-68.

Matsuda M, Nagahama Y, Shinomiya A, Sato T, Matsuda C, Kobayashi T, Morrey C, Shibata N, Asakawa S, Shimizu N, Hori H, Hamaguchi S, Sakaizumi M. DMY is a Y-specific DM-domain gene required for male development in the medaka fish. Nature 2002;417:559-63.

Matsuzawa-Watanabe Y, Inoue J, Semba K. Transcriptional activity of testis-determining factor SRY is modulated by the Wilms' tumor 1 gene product, WT1. Oncogene 2003;22:7900-4.

McCue MD. General effects of temperature on animal biology. In: Valenzuela N, Lance VA. Temperature-dependent sex determination in vertebrates. Washington: Smithsonian Books; 2004, p. 71-78.

McLaren A. Sex determination in mammals. Trends Genet 1988;4(6):153-7.

Meeks JJ, Crawford SE, Russell TA, Morohashi K, Weiss J and Jameson JL. *Dax1* regulates testis cord organization during gonadal differentiation. Dev 2003a;130:1029-36.

Meeks JJ, Weiss J, Jameson JL. *Dax1* is required for testis determination. Nat Genet 2003b;34:32-3.

Merchant LH, Villalpando FI, Centeno UB. Gonadal morphogenesis under controlled temperature in sea turtle *Lepidochelys olivacea*. Herpetol. Monogr. 1989;3, 43– 61.

Merchant-Larios H, Ruiz-Ramirez S, Moreno-Mendoza N, Marmolejo-Valencia A. Correlation among thermosensitive period, estradiol response, and gonad differentiation in the sea turtle *Lepidochelys olivacea*. Gen Comp Endo 1997;107:373-85.

Mizusaki H, Kawabe K, Mukai T, Ariyoshi E, Kasahara M, Yoshioka H, Swain A, Morohashi K-I. *Dax-1* gene transcription is regulated by *Wnt4* in the female developing gonad Mol Endo 2003;17: 507-19.

Moreno-Mendoza N, Harley VR, Merchant-Larios H. Differential expression of SOX9 in gonads of the sea turtle *Lepidochelys olivacea* at male- or female-promoting temperatures. J Exp Zool 1999;284:705-10.

Moreno-Mendoza N, Harley VR, Merchant-Larios H. Temperature regulates SOX9 expression in cultured gonads of *Lepidochelys olivacea*, a species with temperature sex determination. Dev Biol 2001;229:319-26.

Morrish BC, Sinclair AH. Vertebrate sex determination: many means to an end. Reprod 2002;124:447-57.

Muller P, Janovjak H, Miserez A, Dobbie, Z. Processing of gene expression data generated by quantitative real-time PCR Biotech 2002;32:1372-79.

Murdock C, Wibbels T. Expression of *Dmrt1* in a turtle with temperature-dependent sex determination. Cytogen Gen Res 2003;101:302-8.

Murdock C, Wibbels T. *Dmrt1* expression in response to estrogen treatment in a reptile with temperature-dependent sex determination. J Exp Zool B Mol Dev Evol 2006;306:134-9.

Nachtigal MW, Hirokawa Y, Enyeart-van Houten DL, Flanagan JN, Hammer GD, Ingraham HA. *Wilms' tumor 1* and *Dax1* modulate the orphan nuclear receptor SF1 in sex-specific gene expression. Cell 1998;93:445–54.

Nanda I, Kondo M, Hornung U, Asakawa S, Winkler C, Shimizu A, et al. A duplicated copy of DMRT1 in the sex-determining region of the Y chromosome of the medaka, *Oryzias latipes*. Proc Natl Acad Sci 2002;99:11778-83.

Niakan K, ERB McCabe. DAX1 origin, function and novel role. Mol Gen Metab 2005;86:70-83.

Oreal E, Pieau C, Mattei MG, Josso N, Picard JY, Carré-Eusèbe D, Magre S. Early expression of AMH in chicken embryonic gonads precedes testicular SOX9 expression. Dev Dyn 1998;212(4):522-32.

Ottolenghi C, Omari S, Garcia-Ortiz JE, Uda M, Crisponi L, Forabosco A, Pilia G, Schlessinger D. *FoxL2* is required for commitment to ovary differentiation. Hum Mol Gen 2005;14:2053-62.

Ottolenghi C, Pelosi E, Tran J, Colombino M, Douglass E, Nedorezov T, et al. Loss of *Wnt4* and *Foxl2* leads to female-to-male sex reversal extending to germ cells. Hum Mol Gen 2007;16:2795-804.

Pannetier M, Fabre S, Batista F, Kocer A, Renault L, Jolivet G, Mandon-Pepin B, Cotinot C, Veitia R, Pailhoux E. *FoxL2* activates P450 aromatase gene expression: towards a better understanding of the early steps of mammalian ovarian development. J Mol Endo 2006;36: 399-413

Parma P, Radi O, Vidal V, Chaboissier MC, Dellambra E, Valentini S, et al. *R-spondin1* is essential in sex determination, skin differentiation and malignancy. Nat Gen 2006;38:1304-9.

Parr BA, McMahon AP. Sexually dimorphic development of the mammalian reproductive tract requires Wnt7a Nature 1998;395:707-10.

Pfaffl MW. A new mathematical model for relative quantification in real-time RT-PCR Nuc Acids Res 2001;29(9): 2002-7.

Pieau C, Dorizzi M. Oestrogens and temperature-dependent sex determination in reptiles: all is in the gonads. J Endo 2004;181:367-77.

Place AR, Lance VA. The temperature-dependent sex determination drama: Same cast, different stars. In: Valenzuela N, Lance VA, editors. Temperature-dependent sex determination in vertebrates, Washington: Smithsonian Books; 2004, p. 99-110.

Quinn AE, Georges A, Sarre SD, Guarino F, Ezaz T, Graves JAM. Temperature sex reversal implies sex gene dosage in a reptile Science 2007;316:411.

Radder RS, Quinn AE, Georges A, Sarre SD, Shine R. Genetic evidence for co-occurrence of chromosomal and thermal sex-determining systems in a lizard. Biol Lett 2008;4:176-8.

Ramsey M, Crews D. Adrenal-kidney-gonad complex measurements may not predict gonad-specific changes in gene expression patterns during temperature-dependent sex determination in the red-eared slider turtle (*Trachemys scripta elegans*). J Exp Zool Ecol Genet Phys 2007a;307:463-70.

Ramsey M, Crews D. Steroid signaling system responds differently to temperature and hormone manipulation in the red-eared slider turtle (*Trachemys scripta elegans*), a reptile with temperature-dependent sex determination. Sex Dev 2007b;1:181-96.

Ramsey M, Shoemaker CM, Crews D. Gonadal expression of *Sf1* and *aromatase* during sex determination in the red-eared slider turtle (*Trachemys scripta*), a reptile with temperature-dependent sex determination. Diff 2007;75:978-91.

Ramsey M, Crews D. Steroid signaling and temperature-dependent sex determination – reviewing the evidence for early action of estrogen during ovarian determination in turtles. Sems Cell Mol Biol 2009;In press.

Raymond CS, Shamu CE, Shen M, Seifert K, Hirsch B, Hodgkin J, Zarkower D. Evidence for evolutionary conservation of sex-determining genes. Nature 1998;391:691-5.

Raymond CS, Murphy MW, O'Sullivan MG, Bardwell VJ, Zarkower D. *Dmrt1*, a gene related to worm and fly sexual regulators, is required for mammalian testis differentiation. Genes Dev 2000;14:2587-95.

Rhen T, Metzger K, Schroeder A, Woodward R. Expression of putative sex-determining genes during the thermosensitive period of gonad development in the snapping turtle, *Chelydra serpentina*. Sex Dev 2007;1:255-70.

Roberts SG. Transcriptional regulation by WT1 in development. Curr Opin Genet Dev 2005;15:542-7.

Sadovsky Y, Dorn C. Function of *steroidogenic factor 1* during development and differentiation of the reproductive system. Rev Reprod 2000;5:136-42.

Sanchez L. Sex-determining mechanisms in insects. Int J Dev Biol 2008;52(7):837-56.

Schmahl J, Kim Y, Colvin JS, Ornitz DM, Capel B. *Fgf9* induces proliferation and nuclear localization of FGFR2 in Sertoli precursors during male sex determination. Dev 2004;131:3627-36.

Schmidt D, Ovitt CE, Anlag K, Fehsenfeld S, Gredsted L, Treier AC, Treier M. The murine winged-helix transcription factor *Foxl2* is required for granulosa cell differentiation and ovary maintenance. Dev 2004;131:933–42.

Sekido R, Lovell-Badge R. Sex determination involves synergistic action of SRY and SF1 on a specific *Sox9* enhancer. Nature 2008;453:930-4.

Shen M, Hodgkin J. *mab-3*, a gene required for sex-specific yolk protein expression and a male-specific lineage in *C. elegans*. Cell 1998;54:1019–31.

Shen W, Moore C, Ikeda Y, Parker K, Ingraham H. Nuclear receptor *steroidogenic factor-1* regulates the Müllerian inhibiting substance gene: A link to the sex determination cascade. Cell 1994;77:651-61.

Shoemaker CM, Ramsey M, Queen J, Crews D. Expression of *Sox9*, *Mis*, and *Dmrt1* in the gonad of a species with temperature-dependent sex determination. Dev Dyn 2007a;236:1055-63.

Shoemaker CM, Queen J, Crews D. Response of candidate sex-determining genes to changes in temperature reveals their involvement in the molecular network underlying temperature-dependent sex determination. Mol Endo 2007b;21:2750-63.

Shoemaker CM, Crews D. Analyzing the coordinated gene network underlying temperature-dependent sex determination in reptiles. Sems Cell Mol Biol 2009;In press.

Simon P. Q-Gene: processing quantitative real-time RT-PCR data. Bioinform 2003;19:1439-40.

Smith CA, Smith MJ, Sinclair AH. Gene expression during gonadogenesis in the chicken embryo. Gene 1999a;234:395-402.

Smith CA, McClive PJ, Western PS, Reed KJ. Evolution: Conservation of a sex-determining gene. Nature 1999b;402:601-2.

Smith CA, Sinclair AH. Sex determination: insights from the chicken. Bioessays 2004;26:120-32.

Smith CA, Shoemaker CM, Roeszler KN, Queen J, Crews DP, Sinclair AH. Cloning and expression of *R-spondin1* in different vertebrates suggests a conserved role in ovarian development. BMC Dev Biol 2008;8:72-88.

Spotila LD, Spotila JR, Hall SE. Sequence and expression analysis of *Wt1* and *Sox9* in the red-eared slider turtle, *Trachemys scripta*. J Exp Zool 1998;281:417-27.

Sreenivasulu K, Ganesh S, Raman R. Evolutionarily conserved, DMRT1, encodes alternatively spliced transcripts and shows dimorphic expression during gonadal differentiation in the lizard, *Calotes versicolor*. Mech Dev 2002;119(S1):S55-64.

Swain A, Zanaria E, Hacker A, Lovell-Badge R, Camerino G. Mouse *Dax1* expression is consistent with a role in sex determination as well as adrenal and hypothalamus function. Nat Genet 1996;12:404–9.

Takada S, DiNapoli L, Capel B, Koopman P. *Sox8* is expressed at similar levels in gonads of both sexes during the sex determining period in turtles. Dev Dyn 2004;231:387-95.

Tomizuka K, Horikoshi K, Kitada R, Sugawara Y, Iba Y, Kojima A, et al. *R-spondin1* plays an essential role in ovarian development through positively regulating *Wnt-4* signaling. Hum Mol Gen 2008;17:1278-91.

Torres-Maldonado L, Moreno-Mendoza N, Landa A, Merchant-Larios H. Timing of SOX9 downregulation and female sex determination in gonads of the sea turtle *Lepidochelys olivacea*. J Exp Zool 2001;290:498-503.

Torres Maldonado LC, Landa Piedra A, Moreno-Mendoza N, Marmolejo Valencia A, Meza Martıınez A, Merchant Larios H. Expression profiles of *Dax1*, *Dmrt1*, and *Sox9* during temperature sex determination in gonads of the sea turtle *Lepidochelys olivacea*. Gen Comp Endo 2002;129:20-6.

Udar N, Yellore V, Chalukya M, Yelchits S, Silva-Garcia R, BPES Consortium, K Small. Comparative analysis of the *FoxL2* gene and characterization of mutations in BPES patients Hum Mut 2003;22: 222-228

Vainio S, Heikkilä M, Kispert A, Chin N, McMahon AP. Female development in mammals is regulated by *Wnt-4* signalling. Nature 1999;397:405-9.

Valenzuela N, Lance VA. Temperature-dependent sex determination in vertebrates. Washington: Smithsonian Books; 2004.

Valenzuela N. Evolution of the gene network underlying gonadogenesis in turtles with temperature-dependent and genotypic sex determination. Int Comp Biol 2008;48(4):476-85.

Valleley EM, Cartwright EJ, Croft NJ, Markham AF, Coletta PL. Characterisation and expression of *Sox9* in the Leopard gecko, *Eublepharis macularius*. J Exp Zool 2001;291:85-91.

Veitia RA, Nunes M, Brauner R, Doco-Fenzy M, Joanny-Flinois O, Jaubert F, et al. Deletions of distal 9p associated with 46,XY male to female sex reversal: definition of the breakpoints at 9p23.3-p24.1. Genomics 1997;41:271-4.

Vidal VPI, Chaboissier MC, de Rooij DG, Schedl A. *Sox9* induces testis development in XX transgenic mice. Nat Gen 2001;28:216-7.

Wagner T, Wirth J, Meyer J, Zabel B, Held M, Zimmer J, et al. Autosomal sex reversal and campomelic dysplasia are caused by mutations in and around the SRY-related gene SOX9. Cell 1994;79:1111-20.

Wang D-S, Kobayashi T, Zhou L-Y, Paul-Prasanth B, Ijiri S, Sakai F, Okubo K, Morohashi K, Nagahama Y. *FoxL2* upregulates aromatase gene transcription in a female-specific manner by binding to the promoter as well as interacting with Ad4 binding protein/Steroidogenic factor 1 Mol Endo 2007;21(3): 712-725

Wang, ZJ, Jeffs, B, Ito, M, Achermann, JC, Yu, RN, Hales, DB, Jameson JL. Aromatase (Cyp19) expression is upregulated by targeted disruption of *Dax1*. Proc Natl Acad Sci 2001;98:7988-93.

Welshons WV, Wolf MF, Murphy CS, Jordan VC. Estrogenic activity of phenol red. Mol Cell Endo 1988;57:169-78.

Western PS, Harry JL, Graves JAM, Sinclair AH. Temperature−dependent sex determination: Upregulation of SOX9 expression after commitment to male development. Dev Dyn 1999a; 214:171-7.

Western PS, Harry JL, Graves JAM, Sinclair AH. Temperature−dependent sex determination in the American alligator: AMH precedes SOX9 expression. Dev Dyn 1999b;216:411-9.

Western PS, Harry JL, Graves JAM, Sinclair AH. Temperature-dependent sex determination in the American alligator: expression of SF1, WT1 and DAX1 during gonadogenesis. Gene 2000;241:223-32.

Wibbels T, Bull JJ, Crews D. Chronology and morphology of temperature-dependent sex determination. J Exp Zool 1991;260:371-81.

Wibbels T, Bull JJ, Crews D. Temperature-dependent sex determination: a mechanistic approach J Exp Zool 1994; 270: 71-78

Wibbels T, Cowan J, LeBoeuf R. Temperature-dependent sex determination in the red-eared slider turtle, *Trachemys scripta*. J Exp Zool 1998;281:409-16.

Wibbels T, Wilson C, Crews D. Müllerian duct development and regression in a turtle with temperature-dependent sex determination J Herp 1999;33 (1): 149-152

Wilhelm D, Englert C. The Wilms tumor suppressor WT1 regulates early gonad development by activation of *Sf1*. Genes Dev 2002;16:1839-51.

Wilhelm D, Palmer S, Koopman P. Sex determination and gonadal development in mammals. Phys Rev 2007;87:1-28.

Yao HH, Matzuk MM, Jorgez CJ, Menke DB, Page DC, Swain A, Capel B. *Follistatin* operates downstream of *Wnt4* in mammalian ovary organogenesis. Dev Dyn 2004a;230:210-5.

Yao HH, DiNapoli L, Capel B. Cellular mechanisms of sex determination in the red-eared slider turtle, *Trachemys scripta*. Mech Dev 2004b;121:1393-401.

Yao HH, Capel B. Temperature, genes, and sex: a comparative view of sex determination in *Trachemys scripta* and *Mus musculus*. J Biochem 2005;138:5-12.

Yao, HHC. The pathway to femaleness: current knowledge on embryonic development of the ovary Mol Cell Endo 2005;230: 87-93

Yu RN, Ito M, Saunders TL, Camper SA and JL Jameson. Role of Ahch in gonadal development and gametogenesis Nat Gen 1998;20: 353

Zhao Y, Lu H, Yu H, Cheng H, Zhou R. Multiple alternative splicing in gonads of chicken DMRT1. Dev Genes Evol 2007;217:119-26

Vita

Christina May Shoemaker was born in New York City Hospital, the daughter of Rosalind and Peter Shoemaker. After graduating from Longmeadow High School, Massachusetts, she matriculated into Connecticut College. During her junior year, she received an Excellence in Organic Chemistry Award from the American Chemical Society. The following year, she earned the degree of Bachelor of Arts in Biochemistry with an American Chemical Society certification, *cum laude*. She was the sole recipient in her graduating class of the Amercian Institute of Chemist's Award for Excellence in Biochemistry. During the following years she undertook research projects in molecular biology and genetics as a research technician at Harvard University and Boston University Medical Center. She entered graduate school in the Fall of 2003 at The University of Texas at Austin.

Permanent Address: 1603 Eva Street, Austin, TX 78704

This manuscript was typed by the author.